



University of  
Zurich<sup>UZH</sup>

**UZH**  
Blockchain  
Center

---

# CAPITAL ADEQUACY RATIOS OF DECENTRALIZED FINANCE PROTOCOLS

---

MASTER THESIS

SUBMITTED IN PARTIAL FULFILLMENT OF THE REQUIREMENTS FOR  
THE DEGREE OF MASTER OF SCIENCE IN QUANTITATIVE FINANCE

AUTHOR

**YOUNGHOON KIM**

BUCHEGGSTRASSE 155, ZÜRICH

MATRICULATION NUMBER: **21-743-703**

EMAIL: [YOUNGHOON.KIM@UZH.CH](mailto:YOUNGHOON.KIM@UZH.CH)

SUPERVISOR

**PROF. DR CLAUDIO J. TESSONE**

BLOCKCHAIN & DISTRIBUTED LEDGER TECHNOLOGIES

DEPARTMENT OF INFORMATICS

UNIVERSITY OF ZURICH

DATE OF SUBMISSION: 21.09.2023

## Executive Summary

This thesis explores the application of the Basel Framework to the emerging field of Decentralized Finance (DeFi). The process of the application can be divided into three distinct phases: an introduction to the Basel Framework, a description of the code implementation, and a quantitative analysis of the collected data.

The first phase involves introducing the relevant standards and definitions from the Basel Framework to define the Capital Adequacy Ratio (CAR) of DeFi protocols. While some concepts from the framework can be directly applied to the DeFi taxonomy, others require modifications and new interpretations within the framework for proper application. The paper highlights these ambiguities in the framework while also acknowledging the limitations of this approach, aiming to assist regulators who may need to develop a similar framework.

In the second phase, the paper outlines the data collection process and provides information on external data sources. Example input files for the collection process illustrate the necessary data definitions to calculate the CAR for the protocols. The thesis makes the source code for the data collection process available online through a public repository.

In the final phase, a risk spillover analysis is conducted on the CAR data through the estimation of Vector Autoregression (VAR) and Time-Varying Parameter Vector Autoregression (TVP-VAR) models. The mathematical background for these models is introduced, and the required statistical tests for estimation are also presented. The analysis results are visualized through time series of spillover indices and corresponding graphs.

# Contents

|          |   |           |
|----------|---|-----------|
| <b>1</b> | <b>Introduction</b>                       | <b>1</b>  |
| <b>2</b> | <b>Related Works</b>                      | <b>3</b>  |
| <b>3</b> | <b>Methodology and Approaches</b>         | <b>5</b>  |
| 3.1      | The Basel Framework . . . . .             | 5         |
| 3.1.1    | Risk-based Capital Requirements . . . . . | 8         |
| 3.1.2    | Credit Risk . . . . .                     | 11        |
| 3.1.3    | Market Risk . . . . .                     | 13        |
| 3.1.4    | Operational Risk . . . . .                | 17        |
| 3.2      | Data Collection . . . . .                 | 19        |
| 3.2.1    | Data Sources . . . . .                    | 22        |
| 3.2.2    | Data Summary . . . . .                    | 27        |
| 3.3      | Risk Spillover Analysis . . . . .         | 29        |
| 3.3.1    | Spillover Index from VAR . . . . .        | 29        |
| 3.3.2    | Spillover Index from TVP-VAR . . . . .    | 31        |
| 3.3.3    | Model Estimation . . . . .                | 33        |
| <b>4</b> | <b>Results</b>                            | <b>38</b> |
| 4.1      | Capital Adequacy Ratios . . . . .         | 38        |
| 4.1.1    | RWA for Credit Risk . . . . .             | 44        |
| 4.1.2    | RWA for Market Risk . . . . .             | 45        |
| 4.1.3    | RWA for Operational Risk . . . . .        | 48        |
| 4.2      | Risk Spillover Analysis . . . . .         | 49        |
| 4.2.1    | Total Connectivity Index . . . . .        | 49        |
| 4.2.2    | Pairwise Connectivity Index . . . . .     | 51        |

|                   |  |           |
|-------------------|--|-----------|
| 4.2.3             | Net Pairwise Directional Connectedness | 54        |
| <b>5</b>          | <b>Discussions and Limitations</b>     | <b>58</b> |
| <b>6</b>          | <b>Conclusion</b>                      | <b>60</b> |
| <b>Appendices</b> |  |           |
| <b>A</b>          | <b>Additional Tables</b>               | <b>62</b> |
| A.1               | Data Summary                           | 62        |
| A.2               | Statistical Tests                      | 66        |
| <b>B</b>          | <b>Additional Figures</b>              | <b>69</b> |
| B.1               | Capital Adequacy Ratios                | 69        |

# List of Figures

|      |  |    |
|------|--|----|
| 3.1  | Typical ERC20 token transfers between two DeFi protocols . . . . .                 | 8  |
| 3.2  | Service diagram of the data collection process . . . . .                           | 19 |
| 3.3  | Entity relationship diagram of the database . . . . .                              | 20 |
| 3.4  | Screenshot of the query result from the Label Word Cloud in Etherscan . . . . .    | 23 |
| 3.5  | Screenshot of the Hacks tab in DeFiLlama . . . . .                                 | 24 |
| 3.6  | Screenshot of the Security Leaderboard in CertiK . . . . .                         | 25 |
| 3.7  | Screenshot of aUSDC transfers from Idle Finance . . . . .                          | 28 |
| 3.8  | The count distribution of the CAR data . . . . .                                   | 33 |
| 3.9  | Granger Causality between protocols, arrows denote the p-values under 5% . . . . . | 36 |
| 4.1  | CET1/RWA of 9 protocols excluding Ethereum Foundation . . . . .                    | 39 |
| 4.2  | Total Value Locked in Ethereum and Bitcoin price . . . . .                         | 40 |
| 4.3  | CAR values of 10 protocols . . . . .   | 41 |
| 4.4  | RWA values of 10 protocols . . . . .   | 43 |
| 4.5  | RWA for credit risk of Uniswap, changing the haircut ratio . . . . .               | 44 |
| 4.6  | RWA for market risk of Aave, changing the industry bucket . . . . .                | 45 |
| 4.7  | RWA for market risk of DXdao, changing the window for $\sigma$ . . . . .           | 46 |
| 4.8  | RWA for market risk of DXdao, changing the window for delta and vega . . . . .     | 47 |
| 4.9  | CET1/RWA of Compound, changing the window for hacks . . . . .                      | 48 |
| 4.10 | Overlay of TCI values from $H = 5$ to $H = 10$ . . . . .                           | 49 |
| 4.11 | TCI values from 9 protocols, excluding the Ethereum Foundation . . . . .           | 50 |
| 4.12 | PCI values between Uniswap and Compound . . . . .                                  | 51 |
| 4.13 | Graph constructed from the average PCI of the VAR model . . . . .                  | 52 |
| 4.14 | Graph constructed from the average PCI of the TVP-VAR model . . . . .              | 53 |
| 4.15 | NPDC values from Uniswap to Aave . . . . .   | 54 |

|      |  |    |
|------|--|----|
| 4.16 | Graph constructed from the average NPDC of the VAR model . . . . .       | 55 |
| 4.17 | Graph constructed from the average NPDC of the TVP-VAR model . . . . .   | 56 |
| B.1  | Total capital/RWA of 9 protocols excluding Ethereum Foundation . . . . . | 69 |
| B.2  | RWA for credit risk, changing the haircut ratio . . . . .                | 70 |
| B.3  | RWA for market risk, changing the industry bucket . . . . .              | 71 |
| B.4  | RWA for market risk, changing the window for $\sigma$ . . . . .          | 72 |
| B.5  | RWA for market risk, changing the window for delta and vega . . . . .    | 73 |
| B.6  | CET1/RWA of 10 protocols, changing the window for hacks . . . . .        | 74 |

# List of Tables

|      |  |    |
|------|--|----|
| 3.1  | Prudential classification of the cryptoassets from the Basel Framework . . . . . | 6  |
| 3.2  | My classification of the cryptoassets . . . . .                                  | 7  |
| 3.3  | Risk weights for the counterparty credit risk . . . . .                          | 12 |
| 3.4  | Risk weights for the DRC requirement . . . . .                                   | 16 |
| 3.5  | BI ranges and marginal coefficients . . . . .                                    | 18 |
| 3.6  | Financial asset classes that correspond to each ITC EEP code . . . . .           | 26 |
| 3.7  | List of protocols with non-numeric values in CAR data . . . . .                  | 28 |
| 3.8  | Basic statistics of the filtered dataset - first 5 protocols . . . . .           | 33 |
| 3.9  | Basic statistics of the filtered dataset - last 5 protocols . . . . .            | 34 |
| 3.10 | p-values for the ADF test . . . . .  | 35 |
| 3.11 | Values of AIC and BIC for different lag orders . . . . .                         | 36 |
| A.1  | Summary of the collected transfers for 33 protocols . . . . .                    | 63 |
| A.2  | Summary of the CAR data for 33 protocols . . . . .                               | 65 |
| A.3  | Test statistics for the ADF test after log-difference . . . . .                  | 66 |
| A.4  | p-values for the Granger Causality test - first 5 protocols . . . . .            | 67 |
| A.5  | p-values for the Granger Causality test - last 5 protocols . . . . .             | 68 |

# Chapter 1

## Introduction

Decentralized Finance (DeFi) is a new financial paradigm that allows individuals to access a range of financial services, including borrowing, lending, and investing, without relying on traditional financial intermediaries (Auer et al. 2023). DeFi services leverage the distributed ledger technology, or more often called as the blockchain technology, to implement these services through software programs known as smart contracts. In order to develop and maintain these automated programs, the stakeholders of a DeFi service often establish a community of developers and users, referred to as the DeFi protocol (Alonso et al. 2021).

Due to the nature of blockchain technology, all information related to the protocol activities is publicly accessible. This includes the source code of the software programs that facilitate the financial services, leading to a development environment akin to that of open-source software. In this environment, anonymous contributors can make modifications and updates to the source code online. Consequently, it becomes imperative for DeFi protocols to orchestrate the contributions of these anonymous participants to align with their objectives.

To this end, DeFi protocols often create a new form of organization referred to as a Decentralized Autonomous Organization (DAO), which seeks to aggregate the opinions of protocol participants and incentivize specific activities (Beck et al. 2018). This incentivization have given rise to thousands of ERC20 tokens, which are smart contracts designed specifically for the transfer of value, thus serving as digital currencies. A wide variety of methods exists through which DeFi protocols incentivize desired behaviors within their ecosystems, now commonly encompassed under the term Tokenomics (Cong et al. 2020). One of the most well known examples is distribution of tokens known as an “airdrop”, which typically occurs during the initial stages of a DeFi service or the Initial Coin Offering (ICO). These tokens often give voting rights for the DAO that issued the tokens, and thus referred to as “governance tokens”.

The strategies associated with tokenomics are growing increasingly complex as the cryptocurrency market matures. For instance, one can borrow an ERC20 token from a protocol to receive its governance token as a reward. Subsequently, the governance token can be staked in another protocol

---

to attain higher yields from providing liquidity to a third-party protocol. This complicated web of relationships between diverse cryptoassets and protocols can become very difficult to decipher, potentially resulting in unforeseen consequences, as exemplified by the chain of bankruptcy events triggered by the Terra breakdown in May of 2022, affecting crypto funds like Three Arrows in late June.

At the time of writing this thesis, the total market capitalization of cryptoassets has exceeded \$1 trillion, with a daily trading volume of over \$30 billion<sup>1</sup>. Furthermore, the total value of assets under the management of DeFi protocols, i.e., the Total Value Locked (TVL), is estimated to surpass \$40 billion<sup>2</sup>. Numerous traditional financial institutions are actively considering the incorporation of distributed ledger technology for the creation of new assets. Additionally, emerging regulatory jurisdictions, such as the Swiss Financial Market Supervisory Authority (FINMA), are being established to provide guidance for these institutions.

Nonetheless, we currently do not have a framework that can address the diverse financial risks stemming from these complex structures. The Basel Framework<sup>3</sup>, which serves as the primary global standard for financial supervision and risk assessment, currently does not categorize cryptoassets as financial assets. Although recent discussions on the prudential treatment of cryptoassets (BCBS et al. 2021) have resulted in the creation of a new chapter, SCO60, set to take effect from January 1, 2025, the current standards within the Basel Framework are not sufficient to address the unique risks posed by the DeFi protocols. The terminology and definitions utilized within the Basel Framework are grounded in conventional concepts related to financial assets and institutions. To effectively address counterparty risk arising from trading the cryptoassets created by a DAO, modifications to the existing framework are necessary.

To this end, this thesis aims to implement the Basel Framework for the activities of DeFi protocols. More specifically, I will calculate the Capital Adequacy Ratio (CAR) for these protocols by defining eligible capital and Risk-Weighted Assets (RWA). Given that the framework's definitions cannot be directly applied to the new entities within the DeFi landscape, I do not intend to provide precise definitions or seek to justify the calculations in my approach. Instead, the aim is to provide an illustrative overview of the overall process, highlighting the concepts from the framework that may be of interest to regulators when considering their own implementation of analogous concepts for these new financial institutions.

[Chapter 2](#) gives an introduction to the related literature. In [Chapter 3](#), I present the relevant standards from the Basel Framework, outline the data collection process, and briefly introduce the quantitative methodology used to interpret the collected data. An overview of the computed results for CAR and RWA is provided in [Section 4.1](#), followed by a quantitative analysis in [Section 4.2](#). [Chapter 5](#) is dedicated to a discussion of the limitations of my approach, and the thesis concludes with [Chapter 6](#).

---

<sup>1</sup><https://www.forbes.com/digital-assets/crypto-prices/>

<sup>2</sup><https://defillama.com/>

<sup>3</sup>[https://www.bis.org/basel\\_framework/](https://www.bis.org/basel_framework/)

# Chapter 2

## Related Works

In this chapter, I introduce the relevant literature that I referred to during the course of preparing this thesis. To the best of my knowledge, no prior publications have applied the Basel Framework to DeFi protocols. Consequently, my primary sources of reference included the literature concerning risk analysis within the banking sector and papers related to the Systemization of Knowledge (SoK) in DeFi.

Starting with the seminal work of DeYoung and Roland (2001), the field of risk analysis in banking has focused on the establishment of quantitative metrics capable of representing the financial stability of the banks, alongside the identification of regressors that can explain the movement of these metrics (Stiroh 2002; Lepetit et al. 2008; Demirgürç-Kunt and Huizinga 2009). Some examples of such metrics include the volatility of operating income and interest income (Stiroh 2002), or the Z-score of the return on average equity (Lepetit et al. 2008). This line of research aimed to propose banking strategies that can reduce these risk metrics, e.g., by decreasing the proportion of non-interest incomes.

After the Global Financial Crisis of 2007-2008, scholars began to investigate the systematic risk within the banking system (Nier et al. 2007; Battiston et al. 2012; Gai and Kapadia 2010; Kolb 2011; Acemoglu et al. 2013). Most of these efforts used novel methodologies, including the analysis of graph topology (Boss et al. 2003) and the modeling of financial contagion (Kolb 2011), to incorporate higher-order effects beyond linear correlations into the analysis of financial risk.

Nevertheless, the aforementioned novel techniques were initially developed in domains and applications unrelated to finance, thus the concepts and methodologies remained relatively unfamiliar to decision-makers within the financial sector. Instead, a branch of research in econometrics that extended Vector Autoregression (VAR) models for the analysis of systematic risk was often preferred (Francis X. Diebold and Yilmaz 2008; Francis X. Diebold and Yilmaz 2011; Demirer et al. 2015). This was driven by the fact that the stress testing frameworks employed by banks often involved the estimation of VAR models for relevant participants within the system (Foglia 2008). This line of research is referred to as the Financial Connectedness, or more frequently, risk spillover analysis.

---

I use the spillover indices introduced in Francis X Diebold and Yilmaz (2012) to conduct a quantitative analysis of the data I have gathered. Originally defined for simple VAR models, these spillover indices can be extended to more complicated forecasting models with linear impulse response functions, such as the Bayesian VAR (Korobilis and Yilmaz 2018) and DCC-GARCH (Gabauer 2020) models. In this thesis, I consider the original definition using VAR models in Francis X Diebold and Yilmaz (2012), alongside the TVP-VAR model introduced in Antonakakis et al. (2020).

When considering the DeFi domain, the academia has yet to engage in discussions concerning the risk of DeFi protocols. Most of the existing research has been focusing on defining terminologies and conventions, contributing to what is referred to as the Systemization of Knowledge (SoK) regarding blockchain technologies. Noteable examples include the works of Werner et al. (2021) and Qin, Zhou, Afonin, et al. (2021), which define terminologies frequently used by the participants of DeFi, such as ERC20 tokens and transactions. Additionally, Bartoletti et al. (2020), Cousaert et al. (2021) and Xu and Feng (2022) introduce fundamental concepts and formulas within specific subdomains of DeFi, e.g., lending pools and yield aggregators.

The existing literature on the risk analysis of DeFi can be broadly categorized into two groups: the first group focuses on potential attack vectors of malicious agents (Gudgeon et al. 2020; Qin, Zhou, Livshits, et al. 2020; Wu et al. 2021; Tolmach et al. 2021), while the second group measures the risk of cryptoassets as a novel means of investment (Borri 2018; Liu and Tsvyinski 2018; Cong et al. 2020; Alonso et al. 2021).

From the publications in the first group, some of the most relevant works to the topic of this thesis include Perez et al. (2020), which illustrates liquidations and leveraging spirals within lending protocols, and Klages-Mundt et al. (2020), which provides insights into the capital structure of stablecoins.

From the works that belong to the second group I share some of the works that employ spillover analysis: Corbet et al. (2017) calculates the spillover indices of cryptocurrency markets using the DCC-GARCH model. Yi et al. (2018) constructs a large network of cryptoassets using the LASSO-VAR model. As a more recent example using the spillover analysis, Naeem et al. (2021) examines the impact of COVID-19 on the cryptocurrency market through the quantile VAR model. However, it is worth noting that these studies focus on asset prices rather than the capital structure of the protocols.

I collect blockchain data and infer the connectivity between the protocols in this thesis, thus I also share relevant research that applies graph analysis to blockchain data (Khan 2022). Chen et al. (2020) created a Money Flow Graph that represents the transfer of ETH, the native token of Ethereum, between smart contracts. Somin, Gordon, et al. (2018), Somin, Altshuler, et al. (2020) and Victor and Lüders (2019) studied the transfer of ERC20 tokens as directed graphs. Among these, the work that most closely aligns with this thesis is Li et al. (2020), which generated daily snapshots of 31 individual ERC20 tokens.

# Chapter 3

## Methodology and Approaches

The aim of this thesis is to implement a risk framework for DeFi protocols that is analogous to the Basel Framework. To achieve this, I will first describe the key definitions in the Basel Framework, namely the components of the Capital Adequacy Ratio (CAR), and the necessary adjustments to these definitions in [Section 3.1](#). Then in [Section 3.2](#), I will explain how I have collected the relevant data for computing the CAR. Lastly, to illustrate how this data could be used for potential research in economics and finance, I will present a simple analysis of the data using the spillover indices of Francis X Diebold and Yilmaz ([2012](#)) in [Section 3.3](#).

Throughout this thesis, I will be referring to the standards in the Basel Framework using hyperlinks to its online homepage<sup>1</sup> instead of citing the articles directly. This approach allows me to direct readers to specific chapters within the standards, such as the following link: [RBC20](#), which is anchored to the chapter RBC20 of the standard named RBC. Furthermore, each web page denotes the last update date and the effective date for each standard.

I would like to note that the Basel Framework is subject to change; the Basel committee can always decide to supersede the previous standards. For instance, the following two links for RBC20 lead to different pages: [RBC20 \(forthcoming\)](#) and [RBC20 \(removed\)](#). I always refer to the current version of the Basel Framework, with respect to the date of submission of this thesis.

### 3.1 The Basel Framework

The Basel Framework is a set of standards published by the Basel Committee on Banking Supervision (BCBS) to assess the capital adequacy of banks. The current version of the framework consolidates the three Basel Accords: Basel I, Basel II and Basel III. To briefly summarize the relevance of each accord for this thesis, Basel I established fundamental standards for measuring credit risk and market risk; Basel II introduced the operational risk, and Basel III imposed higher capital adequacy

---

<sup>1</sup>[https://www.bis.org/basel\\_framework/index.htm](https://www.bis.org/basel_framework/index.htm)

ratio requirements while extending the scope of credit risk by standardizing counterparty risk. The mapping table in the background page of the Basel Framework<sup>2</sup> illustrates how each standard in the consolidated framework derives from previous BCBS publications.

As mentioned in the previous sections, the current Basel framework does not classify cryptoassets as financial assets. Nevertheless, there has been discussions within the BCBS regarding the prudential treatment of cryptoasset exposures(BCBS et al. 2021), detailed in a forthcoming chapter **SCO60**.

In **SCO60** the cryptoassets are categorized into two groups, each further subdivded into two subgroups, as shown in [Table 3.1](#).

| Group    | Description  |
|----------|--|
| Group 1a | Tokenized traditional assets                           |
| Group 1b | Cryptoassets with effective stabilization mechanisms   |
| Group 2a | Tokens with high market capitalization and derivatives |
| Group 2b | All other cryptoassets                                 |

**Table 3.1** – Prudential classification of the cryptoassets from the Basel Framework

Group 1 consists of tokens that have a reference asset recognized by the framework, while tokens in Group 2 lack a reference asset. For instance, the tokens in Group 1a can be redeemed for a predefined amount of cash or a commodity, e.g., 1 oz of gold. The tokens in Group 1b cannot be directly exchanged for the reference asset but are guaranteed to have a value equal to the reference asset. Group 2 is further divided into Group 2a and Group 2b based on available financial vehicles and market capitalization of the token.

The Basel Framework provides detailed guidelines on how to address each group in the calculating the Capital Adequacy Ratio (CAR). In summary, cryptoassets in Group 1 can be treated as reference assets with an additional add-on for technological infrastructure risk. The tokens in Group 2 should be assigned to a separate bucket in the aggregation of risk factors, with significantly higher weight factors in various dimensions, potentially reaching up to 1250%. This ensures that banks maintain a minimum risk-based capital equal to the value of cryptoassets, as explained in **SCO66.86**.

Therefore, it is possible to calculate Risk-Weighted Assets (RWA) and CAR while strictly adhering to the definitions outlined in **SCO60**. However, in this thesis, I do not take this approach but instead attempt to classify cryptoassets into one of the traditional financial asset classes and follow the standards of the Basel Framework applicable to these traditional assets.

---

<sup>2</sup><https://www.bis.org/baselframework/background.htm>

| Asset Class      | Group        | Description                                     |
|------------------|--------------|---|
| Cash             | Group 1b     | Stablecoins pegged to the native currency       |
| Equity           | Group 2a, 2b | Governance tokens                               |
| Index Fund       | Group 2b     | Tokens pegged to a portfolio of non-stablecoins |
| Commodity        | Group 1a     | Tokenizations of real-world commodities         |
| Foreign Currency | Group 1b     | Stablecoins pegged to non-native currencies     |
| Settlement       | Group 2b     | Utility tokens for on-chain transactions        |
| Derivative       | Group 2b     | Tokens pegged to a derivative of another token  |

**Table 3.2** – My classification of the cryptoassets

[Table 3.2](#) displays the 7 classes I used in this thesis and their mapping to the groups in the Basel Framework. For this categorization, I referred to the token classification provided by the International Token Standardization Association. Detailed information can be found in [Table 3.6](#) and the descriptions in [Subsection 3.2.1](#).

The first argument against following the guidelines given in [SCO60](#) is that the primary objective of this thesis is to demonstrate how I can implement a framework analogous to the Basel Framework, rather than to establish and validate the precise values for each DeFi protocol. The standards and definitions within the Basel Framework are continually evolving, and as a result, I anticipate changes in the specifics of the calculations over time.

However, the fundamental concepts for measuring the risk of each organization have remained largely unchanged for decades. The current version of [SCO60](#) can be viewed as an effort to align these concepts as closely as possible with the treatment of new assets. To achieve this, I decided to incorporate as many details as possible from the core concepts of the Basel Framework, necessitating the mapping of cryptoassets to traditional asset classes.

The second argument is that forthcoming standards do not allow the inclusion of cryptoassets in Common Equity Tier 1 (CET1) capital, as further described in [Subsection 3.1.1](#). Consequently, based on this definition, none of the DeFi protocols meet the minimum capital requirement for CET1. This conclusion arises from two considerations of the framework: stablecoins also carry default risks, and the governance tokens of a protocol are not recognized as equity shares of a financial firm.

This approach rests on the assumption that there are other assets that can be appropriately serve as CET1 capital. For example, in traditional finance, there is typically only one asset assumed to have zero risk, namely cash of the numéraire currency, with all other assets assumed to carry one or more risk factors. Since this analysis of DeFi protocols exclusively considers on-chain assets, I do not have access to this zero risk asset. Therefore, I had to select an alternative set of assets as the benchmark against which I can assess the risk of other assets. Further elaboration on governance tokens is provided in the next subsection, [Subsection 3.1.1](#).

In the following subsections, I will describe my modified approach using the new classification of assets as presented in [Table 3.2](#). For each concept, I will initially present the relevant definitions from the current Basel Framework. Subsequently, I will explain how I have connected these concepts to the activities of a DeFi protocol, and point out the modifications I have made due to the differences in my approach.

### 3.1.1 Risk-based Capital Requirements

To begin with, I first need to define how I can measure the eligible capital owned by a DeFi protocol. [Figure 3.1](#) provides an illustrative example of typical ERC20 token transfers occurring between two DeFi protocols. Contracts deployed or owned by different protocols are represented by different colors and shapes. White circles denote addresses that belong to one protocol, while grey squares represent addresses that belong to another.

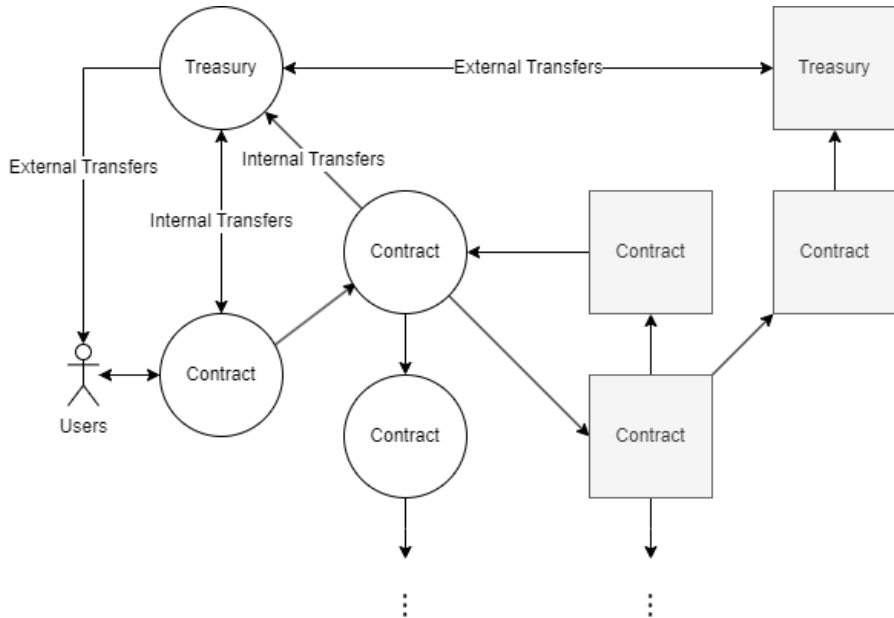


**Figure 3.1** – Typical ERC20 token transfers between two DeFi protocols

In [Figure 3.1](#), users of a DeFi protocol interact with a smart contract that serves as an interface for depositing or withdrawing cryptoassets. Subsequently, this contract invokes a chain of contracts that interact with the contracts of another DeFi protocol, and the token transfers loop back to the treasury address of the originating protocol. Most DeFi protocols create and maintain these treasury addresses, to which they redirect the fees or profit accrued from the chain of transfers. This practice enables the protocol to establish a transparent accounting system that aids stakeholders in their decision-making process.

For the Basel Framework, I define the scope of eligible capital as the sum of ERC20 tokens in the

treasury addresses of a DeFi protocol. While there may be a substantial amount of capital managed by other contracts deployed by the protocol, I consider this capital as operating assets. The services provided by these contracts should be either unwound or reduced to liquidate the assets back into the treasury. The cryptoassets in these non-treasury addresses cannot be utilized as a buffer during financial crises, so I do not include tokens from these addresses when measuring the capital of a protocol.

I would like to note that this definition does not include the native token of the Ethereum chain, i.e., ETH. I have opted not to include ETH transfers for the sake of simplicity, given that every Ethereum chain transaction involves a small amount of ETH being burned as a gas fee. I assume that the majority of the operations in the DeFi space involves ERC20 tokens. If a protocol were to transfer assets in ETH value, it would use the ERC20 version of ETH, such as the Wrapped Ethereum. This limitation in my approach has immediate consequences for the results concerning the Ethereum Foundation, as will be presented in [Chapter 4](#). I will delve further into the limitations of this thesis in [Chapter 5](#).

Furthermore, the implementation of the framework includes only a subset of the ERC20 tokens — specifically, tokens with a clear classification code for their economic purpose and a sufficient amount of price data. I elaborate further on how I have collected the data for ERC20 tokens in [Subsection 3.2.1](#).

Now I define the Capital Adequacy Ratios (CAR) for DeFi protocols based on the requirements outlined in [RBC20.1](#):

- Common Equity Tier 1 must be at least 4.5% of risk-weighted assets (RWA).
- Tier 1 capital must be at least 6% of RWA.
- Total capital must be at least 8.0% of RWA.

Throughout this thesis I focus on the first requirement concerning Common Equity Tier 1 capital, and I refer to this ratio as the CAR unless stated otherwise.

The Common Equity Tier 1 (CET1) capital comprises multiple elements, as detailed in [CAP10.6](#):

- Common shares issued by the bank that meet the criteria for classification as common shares for regulatory purposes (or the equivalent for non-joint stock companies);
- Stock surplus (share premium) resulting from the issue of instruments included Common Equity Tier 1;
- Retained earnings;
- Accumulated other comprehensive income and other disclosed reserves;

- Common shares issued by consolidated subsidiaries of the bank and held by third parties (ie minority interest) that meet the criteria for inclusion in Common Equity Tier 1 capital. See [CAP10.20](#) to [CAP10.26](#) for the relevant criteria; and
- Regulatory adjustments applied in the calculation of Common Equity Tier 1.

In this thesis, I regard governance tokens as the equivalent of common shares issued by a bank. A governance token is a token that grants ownership of the decision rights of the protocol to its holder ([Beck et al. 2018](#)). The extent of these decision rights varies among protocols, but generally token holders can participate in the voting process for events that may impact token distribution.

Governance tokens are typically distributed in the market as rewards or fees for various activities within the ecosystem. Therefore, it is of great interest to contributors of the protocol to maintain the token's value in the market, as it serves as an incentive for using the protocol's services. To achieve this, DeFi protocols often offer additional benefits to token holders, such as dividends or buybacks, which closely resemble traditional shareholder rights.

Consequently, the first and the second items in the description of CET1 from [CAP10.6](#) can be estimated by the value of the governance tokens in the treasury. As for retained earnings, income and reserves, I assume that these cash flows have been consolidated as the cash balance of the treasury. In summary, the CET1 capital of DeFi protocols is estimated by the sum of cash and governance tokens.

The Tier 1 capital is defined as the sum of CET1 and Additional Tier 1 capital, while total capital is defined as the sum of Tier 1 capital and Tier 2 capital ([CAP10.2](#)). However, the boundary between Additional Tier 1 capital and Tier 2 capital is ambiguous for DeFi protocols. Additional Tier 1 capital refers to instruments issued by the bank that are under the full discretion of the bank ([CAP10.11](#)), whereas Tier 2 capital is for loss absorption on a gone-concern basis, which includes instruments that the bank cannot directly exercise or accelerate the liquidation ([CAP10.16](#)).

The cryptoassets differ from traditional financial assets in how their values are realised. In DeFi protocols, the exercise of a token involves burning the token through the smart contract that minted it to receive the promised amount (e.g., face value or strike). Since interacting with the smart contract can be done immediately by anyone holding the token, one might argue that all cryptoassets should belong to Tier 1 capital. However, it is possible that the smart contract does not function as intended due to hacks or lack of reserves. In such cases, we could argue that every cryptoasset should belong to Tier 2 capital instead.

To avoid this source of ambiguity, I skip the criterion for Tier 1 capital and only share the results for CET1 and total capital in [Chapter 4](#). Total capital, the sum of Tier 1 capital and Tier 2 capital, is estimated by the sum of all relevant ERC20 tokens in the treasury.

The Risk-Weighted Assets (RWA) are defined as the sum of three elements, the RWA for credit risk, the RWA for market risk, and the RWA for operational risk. If the bank were to use a non-standarised approach for calculating these values, then the bank must also compare the sum with 72.5% of

the RWA computed by the standardised approach and take the maximum ([RBC20.4](#)). Through the following subsections, I describe how I tried to apply the standardised approaches for each subelement of the RWA.

### 3.1.2 Credit Risk

RWA for credit risk is calculated as the sum of the following elements, as shown in [RBC20.6](#):

- Credit RWA for banking book exposures, except the RWA listed in (2) to (6) below
- RWA for counterparty credit risk arising from banking book exposures and from trading book instruments (as specified in [CRE55](#)), except the exposures listed in (3) to (6) below, using the methods outlined in [CRE51](#).
- Credit RWA for equity investments in funds that are held in the banking book calculated using one or more of the approaches set out in [CRE60](#)
- RWA for securitisation exposures held in the banking book, calculated using one or more of the approaches set out in [CRE40](#) to [CRE45](#)
- RWA for exposures to central counterparties in the banking book and trading book, calculated using the approach set out in [CRE54](#).
- RWA for the risk posed by unsettled transactions and failed trades, where these transactions are in the banking book or trading book and are within scope of the rules set out in [CRE70](#).

It can be observed from the items above that the primary focus of the credit risk RWA is to address the risk associated with banking book exposures, rather than the instruments in the trading book. However, according to [RBC25](#) all cryptoassets can be assigned to the trading book, rendering the banking book empty. All cryptoassets lack any legal impediments against selling or hedging ([RBC25.3](#)) and they profit from short-term price movements ([RBC25.5](#)), thus classifying them all under the trading book.

The terms that remain relevant without the banking book are only the second and fifth terms: the RWA for counterparty credit risk and the RWA for exposures to central counterparties. As there are no such protocols acting as central counterparties in DeFi, the RWA for credit risk in practice becomes equivalent to the RWA for counterparty credit risk for DeFi protocols.

The standardised approach to counterparty credit risk calculates the RWA by multiplying risk weights with the Exposure At Default (EAD) of each counterparty, based on the external credit rating of the counterparties ([CRE51](#)).

For risk weights, I utilized the risk weight table for corporate exposures presented in [CRE20.43](#), which I have restated in [Table 3.3](#). I selected corporate exposures as the reference category because they had the highest risk weights for each rating, offering the most prudential treatment for the exposures.

| Credit Rating | Risk Weight |
|---------------|-------------|
| AAA to AA-    | 20%         |
| A+ to A-      | 50%         |
| BBB+ to BBB-  | 75%         |
| BB+ to BB-    | 100%        |
| Below BB-     | 150%        |

**Table 3.3** – Risk weights for the counterparty credit risk

The EAD of each counterparty is calculated as follows:

$$\text{EAD} = \alpha \cdot (\text{RC} + \text{PFE}) \quad (3.1)$$

where  $\alpha$  is an arbitrary constant currently set at 1.4. RC stands for the Replacement Cost, and PFE is the amount of Potential Future Exposure ([CRE52.1](#)).

The Replacement Cost (RC) for unmargined transactions is defined as the value of the transactions ( $V$ ) minus the haircut value of the collaterals ( $C$ ), i.e.,  $V - C$ . Since there is often no collateral for a given ERC20 token, I set  $C = 0$  for the quantitative analysis in [Section 4.2](#). I also provide the results for  $C = 0.1V$  and  $C = 0.5V$  for comparison in [Section 4.1](#).

The Potential Future Exposure (PFE) is defined as a product of a multiplier and the aggregate add-on component, where the multiplier is defined as:

$$\text{multiplier} = \min \left\{ 1; \text{Floor} + (1 - \text{Floor}) \cdot \exp \left( \frac{V - C}{2 \cdot (1 - \text{Floor}) \cdot \text{AddOn}^{\text{aggregate}}} \right) \right\} \quad (3.2)$$

where Floor is a constant set at 5% in the current framework and AddOn is the aggregate add-on component ([CRE52.23](#)).

The aggregate add-on component in [Equation 3.2](#) is defined as follows:

$$\text{AddOn}^{\text{aggregate}} = \left[ \left( \sum_{\text{entity}} \rho_{\text{entity}} \cdot \text{AddOn}^{\text{entity}} \right)^2 + \sum_{\text{entity}} (1 - (\rho_{\text{entity}})^2) \cdot (\text{AddOn}^{\text{entity}})^2 \right]^{1/2} \quad (3.3)$$

where  $\text{AddOn}^{\text{entity}}$  is the product of the effective notional ( $D$ ) and the supervisory factor ( $SF$ ) of each entity, and  $\rho_{\text{entity}}$  is a correlation parameter between the entities ([CRE52.30](#)).

For traditional financial assets with maturity and strike prices, the effective notional  $D$  must be computed through a set of formulas specific to the asset type. Since cryptoassets do not have these specifications, I assume there are no other adjustments and set  $D = V$ , i.e., the value of the transaction.

The supervisory factor  $SF$  and the correlation parameter  $\rho_{\text{entity}}$  are taken from the equity classes in

[CRE52.72](#). This choice is primarily because the supervisory factors are relatively high for equities, and it aligns with the decision to use the risk weights for corporate exposures as presented in [Table 3.3](#). Consequently, tokens classified as index funds are assigned  $SF = 20\%$  and  $\rho_{entity} = 80\%$ , while others receive  $SF = 32\%$  and  $\rho_{entity} = 50\%$ .

In this thesis, I aggregated each entity by the address of the underlying asset of a token. For example, the tokens IdleUSDTsafe and IdleUSDTbest from Idle Finance can be redeemed for the same token, USDT. I combined the exposure from these two tokens into the same entity, the address of USDT. However, I did not combine tokens with the same underlying asset but minted by different protocols, e.g. aUSDT and yvUSDT, since they belong to different counterparties. Tokens without an underlying asset are treated as separate entities.

### 3.1.3 Market Risk

RWA for market risk is calculated as the sum of the following, as shown in [RBC20.9](#):

- RWA for market risk for instruments in the trading book and for foreign exchange risk and commodities risk for exposures in the banking book
- RWA for credit valuation adjustment (CVA) risk in the banking and trading book

For DeFi protocols, I only consider the exposures in the trading book, as mentioned in [Subsection 3.1.2](#).

The standardised approach for market risk is defined in [MAR20](#), as the sum of the following three components multiplied by 12.5:

- The capital requirement under the sensitivities-based method must be calculated by aggregating three risk measures - delta, vega and curvature, as set out in [MAR21](#)
- The DRC requirement captures the jump-to-default risk for instruments subject to credit risk as set out in [MAR22.2](#). It is calibrated based on the credit risk treatment in the banking book in order to reduce the potential discrepancy in capital requirements for similar risk exposures across the bank. Some hedging recognition is allowed for similar types of exposures (corporates, sovereigns, and local governments/municipalities).
- Additionally, the Committee acknowledges that not all market risks can be captured in the standardised approach, as this might necessitate an unduly complex regime. An RRAO is thus introduced to ensure sufficient coverage of market risks for instruments specified in [MAR23.2](#). The calculation method for the RRAO is set out in [MAR23.8](#).

For the sensitivities-based method, I only consider the cryptoassets that have a specified underlying, i.e., the cryptoassets that can be classified as a derivative token. See [Table 3.6](#) and the description in [Subsection 3.2.1](#) for how I classified the ERC20 tokens.

From MAR21.8 and onward the sensitivities-based method defines how the risk factors for delta, vega, and curvature are calculated for each specific asset type. However, the framework requires one to know the function of the instrument value given the value of the underlying; for the cryptoassets there is no convention such as the Black-Scholes model for options that can derive the value process from the underlying asset. Each derivative token can have a unique optionality which requires individual modeling, e.g., the risk profiles of a liquidity position in Uniswap V2 and V3 can be very different (Aigner and Dhaliwal 2021).

In this thesis, I take a workaround to this problem by making numerical estimates for the sensitivities. I first set two constants, the window size for the estimation and another window size for estimating  $\sigma$ , the standard deviation of the underlying. For the quantitative analysis in Section 4.2 I set the first window size as 365 days and the second as 3, but I also share the results for different window sizes in Section 4.1 for comparison.

Delta is estimated by taking the rolling median over 365 days of the fraction of the differences of the underlying and the instrument, i.e., the median of  $\Delta V / \Delta S$ .  $V$  is the price of the derivative asset and  $S$  is the price of the underlying asset. I chose the median over the arithmetic mean since the median is more robust to outlier values. The estimate could be seen as a robust regression using the absolute loss  $L(x) = |x|$  instead of the squared loss  $L(x) = x^2$ .

Vega is estimated by again taking the rolling median over 365 days of the fraction of the differences of the standard deviation and the instrument, i.e., the median of  $\Delta V / \Delta \sigma$ . I estimate  $\sigma$  by the  $L^2$  norm of the log-difference, a common approach for calculating the realized volatility of prices:

$$\hat{\sigma} = \sqrt{\sum_{i=1}^T \left( \log \frac{S_i}{S_{i-1}} \right)^2} \quad (3.4)$$

where  $T$  was set to 3 in Section 4.2, and I share the results using different values for  $T$  in Section 4.1. However, this numerical estimation removes the effect of the curvature since the delta is approximated by the first-order difference. The values  $CVR_k^+$  and  $CVR_k^-$  that determine the curvature risk capital requirement are defined in MAR21.5:

$$\begin{aligned} CVR_k^+ &= - \sum_i \left\{ V_i \left( x_k^{RW(\text{Curvature})^+} \right) - V_i(x_k) - RW_k^{\text{Curvature}} \times s_{ik} \right\} \\ CVR_k^- &= - \sum_i \left\{ V_i \left( x_k^{RW(\text{Curvature})^-} \right) - V_i(x_k) + RW_k^{\text{Curvature}} \times s_{ik} \right\} \end{aligned} \quad (3.5)$$

where  $x_k$  denotes the value of the underlying,  $s_{ik}$  is the delta sensitivity of the asset  $i$  and risk factor  $k$ , and  $RW_k^{\text{Curvature}}$  is the risk weight.

In the current Basel Framework, a financial instrument can have multiple risk factors for the market risk if its value depends on multiple underlyings, such as the interest rate and credit risk spreads. I assume that the cryptoassets are always exposed only to a single underlying token value, i.e., that

the cryptoassets have a single risk factor.

Due to the way I defined the delta sensitivity  $s_{ik}$ , the terms  $\text{CVR}_k^+$  and  $\text{CVR}_k^-$  in [Equation 3.5](#) equal to zero for all assets; the market risk in this thesis thus cannot include the curvature risk and the scenario testing for the curvatures set out in [MAR21.5](#). This is one of the limitations of my approach, see [Chapter 5](#) for more discussions on the limitations.

Once we have the values for delta and vega factors, the risk capital requirement for each sensitivity factor can be calculated as follows ([MAR21.4](#)):

$$\begin{aligned}
 WS_k &= RW_k s_k \\
 K_b &= \sqrt{\max \left( 0, \sum_k WS_k^2 + \sum_k \sum_{k \neq l} \rho_{kl} WS_k WS_l \right)} \\
 \text{Requirement for Delta (Vega)} &= \sqrt{\sum_b K_b^2 + \sum_b \sum_{c \neq b} \gamma_{bc} S_b S_c} \\
 \text{where } S_b &= \sum_k WS_k \text{ for all risk factors in bucket } b
 \end{aligned} \tag{3.6}$$

where  $s_k$  is the delta (respectively vega) sensitivity for the risk factor  $k$ . Since we assumed that the cryptoassets have a single risk factor, we use this notation to instead indicate the sensitivity of an asset  $k$ . Furthermore the subscript  $b$  and  $c$  in [Equation 3.6](#) denote the different type of assets; I split the asset types according to my classification of tokens shown in [Table 3.2](#).

I refer to the risk weights for equity spot prices for the values  $RW_k$  in [MAR21.77](#). I chose the cryptoassets to be assigned as equities to give a relatively high risk weight to the exposures and to align with the previous decisions in [Subsection 3.1.2](#). In the same spirit, I chose bucket 9 in [MAR21.72](#), the small emerging market economy sector, since it had the highest risk weight. The other sector bucket, bucket 11, also has a high risk weight but does not have the correlation effect among the assets ([MAR21.80](#)); I used bucket 9 for the quantitative analysis in [Section 4.2](#), but I also share the comparison for when we use bucket 11 instead in [Section 4.1](#).

In the standardised approach for market risk, the net risk capital requirement should be calculated for three different scenarios, the “medium correlations”, “high correlations” and “low correlations” scenario, and one should take the maximum of the three ([MAR21.6](#)). For each scenario, the net risk capital requirement is defined as the sum of the capital requirement for delta, vega and curvature risk, but since we cannot compute the curvature risk, I take the sum of delta and vega requirements.

In the “medium correlations” scenario the correlation parameters  $\rho_{kl}$  and  $\gamma_{bc}$  are given from the bucket,  $\rho_{kl} = 7.5\%$  and  $\gamma_{bc} = 15\%$ . For the “high correlations” scenario the correlation parameters should be multiplied by 1.25 but capped at 100%, thus  $\rho_{kl} = 9.375\%$  and  $\gamma_{bc} = 18.75\%$ . For the “low correlations” scenario the parameters are given by the maximum of two values,  $\max(2 \times x - 100\%, 75\% - x)$  where  $x$  is the parameter in the “medium correlations” scenario. This gives

$\rho_{kl} = 5.625\%$  and  $\gamma_{bc} = 11.25\%$  for my thesis.

Apart from the capital requirement from the sensitivities-based method, the first term for the RWA for market risk has two additional components, the Default Risk Capital (DRC) requirement and the Residual Risk Add-On (RRAO).

DRC intends to capture default risk by addressing the hedging conditions of the instruments ([MAR22.1](#)). However, there is no short position for cryptoassets in DeFi. Instead, hedging is done through taking long positions in tokens that have values pegged to the downside movement of the hedging target. If I were to recognize these tokens as a short position, then the tokens that have a negative correlation also need to be assigned a partial-short position. To this end, I assume that there are no short positions available for the cryptoassets in the DeFi space.

Then the DRC can be simplified as the net balance of ERC20 tokens each multiplied by the risk weight for the protocol that minted the token. I refer to the table in [MAR22.24](#) for the risk weights, which I share in [Table 3.4](#).

| Credit Rating | Risk Weight |
|---------------|-------------|
| AAA           | 0.5%        |
| AA            | 2%          |
| A             | 3%          |
| BBB           | 6%          |
| BB            | 15%         |
| B             | 30%         |
| CCC           | 50%         |

**Table 3.4** – Risk weights for the DRC requirement

RRAO should be added to the RWA of market risk for instruments with an exotic underlying or instruments bearing other residual risks ([MAR23.2](#)). Instruments with an exotic underlying are defined as instruments that are not within the scope for the sensitivities-based method or DRC requirements in the standardised approach ([MAR23.3](#)). Since I address all cryptoassets with an underlying in the standardised approach, I only need to consider the instruments bearing other residual risks, which are defined as instruments that cannot be replicated by the combination of vanilla options ([MAR23.4](#)). I regard all cryptoassets with an underlying as instruments bearing other residual risks, and thus I add 0.1% of the gross notional amount of the exposure as the RRAO ([MAR23.8](#)).

Multiplying the sum of the capital requirements from the sensitivities-based method, DRC requirement, and the RRAO by 12.5 completes the first item for the RWA of market risk. The second item is the RWA for credit valuation adjustment (CVA) risk set out in [MAR50](#). The CVA risk reflects the adjustment of prices due to the potential default of a counterparty.

The CVA risk can be calculated by one of three methods: the basic approach, the standardised approach, or taking 100% of the bank's RWA for counterparty credit risk (RBC20.9). In this thesis, I take the last approach of using the RWA for counterparty credit risk instead of the standardised approach. The standardised approach for CVA risk is intended for banks that take active measures to hedge the CVA risk; DeFi protocols currently do not share a common standard where they can discount the value of tokens according to the default risk of each protocol.

Banks that do not hedge the CVA risk should use the basic approach for CVA risk. However, without the maturities and hedging, the calculation becomes very close to the counterparty credit risk. Since the assets under management of the DeFi protocols are below the materiality threshold (100 billion EUR, MAR50.9) I can choose to substitute the calculation for the CVA risk with the counterparty credit risk.

### 3.1.4 Operational Risk

RWA for operational risk is defined in OPE25.2 as the product of the Business Indicator Component (BIC) and the Internal Loss Multiplier (ILM), multiplied by 12.5.

BIC is calculated from the Business Indicator (BI), which is the sum of the Interest, Leases and Dividend Component (ILDC), the Services Component (SC) and the Financial Component (FC). The above three components of BI are defined as follows:

$$\begin{aligned} \text{ILDC} &= \min \left( \overline{|\text{interest income} - \text{interest expense}|}, 2.25\% \times \overline{\text{interest earning assets}} \right) \\ &\quad + \overline{\text{dividend income}} \\ \text{SC} &= \max \left( \overline{\text{other operating income}}, \overline{\text{other operating expense}} \right) \\ &\quad + \max \left( \overline{\text{fee income}}, \overline{\text{fee expense}} \right) \\ \text{FC} &= \overline{|\text{Net P&L trading book}|} + \overline{|\text{Net P&L banking book}|} \end{aligned} \tag{3.7}$$

where the bar  $\overline{(\cdot)}$  denotes the average over 3 years in OPE25.5. However, in this thesis I take the average over a single year instead since there are not many DeFi protocols that have been active for more than 3 years.

In the definition in OPE10.2, interest income is defined as “interest income from all financial assets and other interest income”, the operating income as “income from ordinary banking operations not included in other BI items but of similar nature”, whereas fee income is defined as “income received from providing advice and services.” These three sources of income/expense can be easily distinguished for banks by following their jurisdiction, which can identify each financial instrument, its creditor, and debtor.

However, for the DeFi protocols there is no central jurisdiction that can differentiate the source of income; one needs to assign each token transfer to one of these sources by observing its characteristics.

Even then, it can be challenging to assign it to a single source since a single transfer can simultaneously have the features of different assets.

As an illustration, let us assume that I borrow a token XYZ from Compound by providing another token ABC as a collateral. Then I can lend the borrowed token into Compound to receive a wrapped version of the token called cXYZ, along with COMP, the governance token of Compound. Then, I can swap cXYZ and COMP back to XYZ to pay back the original loan, and this loop of transactions theoretically should lead to a non-negative loss under the no-arbitrage condition. This net loss could be assigned as an interest expense, since Compound is known as an interest rate protocol<sup>3</sup>, but it could also be regarded as a fee expense since the loss comes from the price difference between cXYZ + COMP and XYZ.

To address this, I try to avoid searching for the financial interpretation of the transfers but instead focus on the structural difference that can be found on-chain. I completely drop the ILDC from the calculation of BI and differentiate only between the operating income/expense and the fee income/expense: the transfers that are within the ecosystem of the protocol are assigned to the fee income/expense, and that are outside are assigned to the operating income/expense.

I define the ecosystem of a protocol by a list of known addresses from the protocol; as discussed at the beginning of [Subsection 3.1.1](#), the transfers that are in the scope of the framework should either come from or go into the treasury addresses. Thus, if the address at the other end is on the list of known addresses, I classify this as an internal transfer, and if not the transfer is an external transfer, see [Figure 3.1](#) for a visual example. The internal transfers are accounted towards the fee income/expense, and the external transfers are accounted towards the operating income/expense.

For the Financial Component (FC), I only consider the profit and loss (P&L) from the trading book, as mentioned in [Subsection 3.1.2](#). The net P&L from the trading book is computed by taking the cumulative sum with a window size of 365 days (yearly), of the difference in prices multiplied by the quantity of tokens in the previous day.

Now the BIC can be calculated from the BI by dividing the BI into three buckets by its range and taking the weighted sum by the marginal coefficients shown in [Table 3.5 \(OPE25.7\)](#). Therefore, for a bank with a BI equal to €1bn the BIC would equal  $12\% \times BI$ , but as the BI exceeds €1bn, a one unit increase in BI would lead to a 0.15 increase in the BIC of the bank.

| BI Range (in €bn) | Marginal Coefficients |
|-------------------|-----------------------|
| $BI \leq 1$       | 12%                   |
| $1 < BI \leq 30$  | 15%                   |
| $BI > 30$         | 18%                   |

**Table 3.5** – BI ranges and marginal coefficients

<sup>3</sup><https://compound.finance/>

The definition of BIC requires the numéraire to be the EUR; however, in this thesis I have calculated the values for the RWA in USD for the convenience of collecting the data, as explained in [Section 3.2](#). Although there were no protocols that exceeded the first BI threshold of €1bn, I have set the thresholds for BI as the same notional amounts in USD for the implementation of this thesis.

The Internal Loss Multiplier (ILM) is defined in [OPE25.8](#) as follows:

$$\text{ILM} = \log \left( \exp(1) - 1 + \left( \frac{\text{LC}}{\text{BIC}} \right)^{0.8} \right) \quad (3.8)$$

where the Loss Component (LC) equals 15 times the average annual operational risk losses incurred over the previous 10 years.

In the current Basel Framework, banks that do not have more than five years of high-quality loss data should simply set  $\text{ILM} = 1$  ([OPE25.10](#)). However, as mentioned in [Section 3.1](#), the aim of this thesis is to illustrate how one could implement the framework for DeFi protocols rather than to define the correct values of RWA and CAR. I include the historical hacks of each DeFi protocols as the operational risk loss in the computation of ILM. Since most protocols have been active for only a couple years, I take the sum of the losses from hacks within the previous 365 days as the LC for the quantitative analysis in [Section 4.2](#). However, I also share the results from choosing different window lengths for LC in [Section 4.1](#).

## 3.2 Data Collection

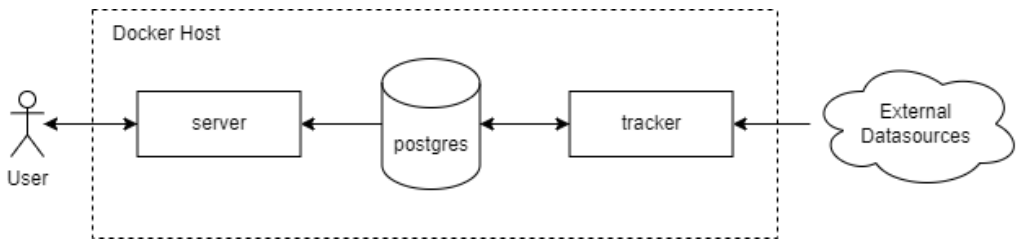


**Figure 3.2** – Service diagram of the data collection process

In this section I describe how I collected the data from DeFi protocols using the definitions from [Section 3.1](#). The source code of the services described in this section can be found in a public GitHub repository<sup>4</sup>.

The data collection process consists of three services, each containerized as a Docker service (Merkel 2014) to facilitate its use for future research. Each of the services can be built and hosted on different machines to better fit the environment of the researcher who may want to reproduce the same data. The interactions between the services, i.e., the network connections that are necessary for each service,

<sup>4</sup><https://github.com/kyhoon/defi-basel-framework>

are denoted in [Figure 3.2](#).

I used the latest image of PostgreSQL for the database, named as `postgres` in [Figure 3.2](#), and at the time of writing this thesis its latest version was 16RC1. The user can have some flexibility in choosing the relational database since I have implemented all transactions using a Python ORM called SQLAlchemy ([Bayer 2012](#)) instead of writing the SQL queries directly in the PostgreSQL dialect. The SQLAlchemy ORM is known to support multiple SQL dialects such as MySQL, Oracle, and MS-SQL. I share the entity relationship diagram of the database in [Figure 3.3](#).

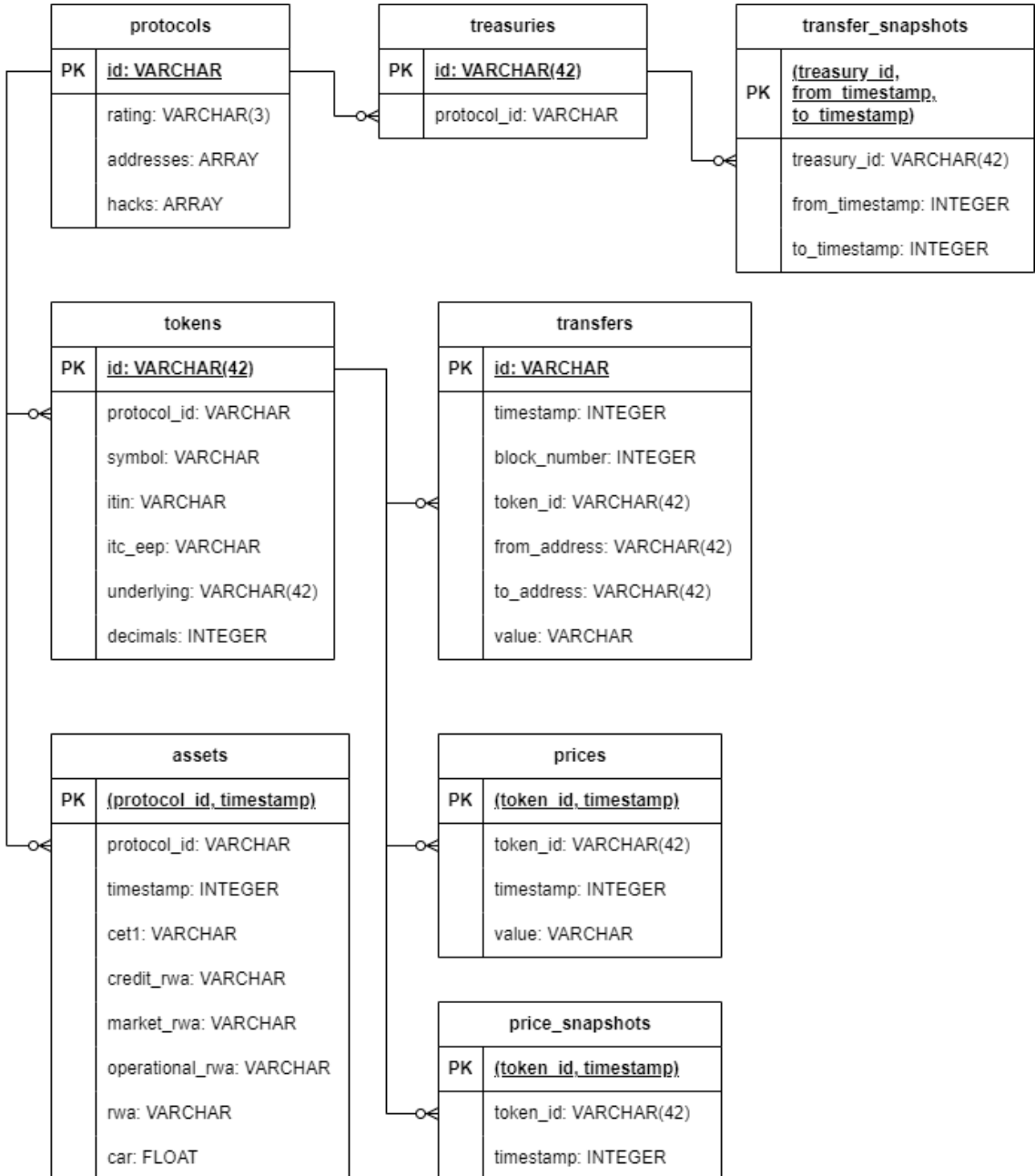


**Figure 3.3** – Entity relationship diagram of the database

The **server** service is a lightweight REST API server that acts as the point of interaction with the end user. I have implemented the server using the FastAPI framework (Ramírez 2018) for serving the API and SQLAlchemy for the interaction with the database. Users can send HTTP GET requests to the API server to obtain the collected CAR data in JSON format as shown in Listing 3.1. Please refer to the actual implementation or the documentation page of the API server to see the available methods.

---

```

1 [ 
2   {
3     "protocol": "yearn-finance",
4     "timestamp": 1613001600,
5     "cet1": "185355622.4258417578076083359",
6     "credit_rwa": "342783452.1647122986375947415",
7     "market_rwa": "692544269.4127058062715423479",
8     "operational_rwa": "615697467.8183191395452919778",
9     "rwa": "1651025189.395737244454429067"
10   }
11 ]

```

---

**Listing 3.1** – Example response from the REST API server

The **tracker** service is a data crawler that sends requests to the external data sources and calculates the values for the RWA and CAR of protocols. I implemented the **tracker** by scheduling 5 different subtasks using the APScheduler package (Grönholm 2009) in Python. The snippet of the main entrypoint of the **tracker** service can be seen in Listing 3.2.

---

```

1 scheduler = BlockingScheduler(job_defaults={"timezone": "UTC"})
2 scheduler.add_job(heartbeat, "interval", minutes=1)
3 scheduler.add_job(collect_prices, "interval", seconds=1)
4 scheduler.add_job(collect_transfers, "interval", seconds=1,
5                   max_instances=8)
6 scheduler.add_job(update_snapshots, "cron", hour=0)
7 scheduler.add_job(calculate_car, "cron", hour=1)

```

---

**Listing 3.2** – Subtasks of the tracker service

The `heartbeat()` task logs the number of collected entries for the entities shown in Figure 3.3 to check whether the service is running properly. The logging is done every minute with the verbosity set at the debugging level.

The `collect_prices()` and the `collect_transfers()` tasks send HTTP requests to public API endpoints to retrieve the prices and transfers of relevant ERC20 tokens. Both services are triggered every second to check if there is an entry in `price_snapshots` and `transfer_snapshots` shown in Figure 3.3, then consume each snapshot entry to insert a corresponding entry in `prices` and `transfers`, respectively. I discuss the public API endpoints in more detail in Subsection 3.2.1.

The `update_snapshots()` reads the static JSON files stored within the code base that describe the relevant protocols and tokens, and updates the entities `protocols` and `tokens` accordingly. Then it validates and creates the entries for `protocol_snapshots` and `token_snapshots`, ranging from the UTC timestamp called `MIN_TIMESTAMP` until the current UTC timestamp, with the interval given by the variable `INTERVAL`. The snapshot entries are placeholders for executing the subtasks `collect_prices()` and `collect_transfers()`, and are removed after each coroutine is completed. The `update_snapshots()` is triggered every day at 00:00 UTC so that the list of protocols and tokens can be updated on a daily basis.

For the results shared in this thesis, I set `MIN_TIMESTAMP` as 1534377600 (16 Aug 2018) and `INTERVAL` as 86,400 seconds (daily). Aug 16 2018 was the first date that I could retrieve the price data from the external data source DeFiLlama, which I describe in Subsection 3.2.1. I would like to note that the minimum interval for the data collection equals the block speed of the Ethereum Mainnet, which is about 12 seconds at the time of writing this thesis.

Lastly, the `calculate_car()` task performs the calculations described in Section 3.1 to populate the `assets` entity shown in Figure 3.3. It is triggered every day at 01:00 UTC, after an hour from the trigger for `update_snapshots()`, to reflect any modifications made in the JSON files of the protocols and tokens in the calculation of the RWA and CAR.

The numéraire for the computation was chosen as USD since DeFiLlama gave us the prices in USD. Thus the stablecoins that are pegged to USD were regarded as cash, and the tokens that are pegged to non-USD currencies were handled as foreign currencies, see Table 3.6 and the description in Subsection 3.2.1 for more details.

### 3.2.1 Data Sources

In this subsection, I provide more details on the external web pages and public API endpoints I used in the data collection process. Apart from the BIS, I collected data from four additional organizations: Etherscan, DeFiLlama, CertiK, and the International Token Standardization Association.

Etherscan<sup>5</sup> is a blockchain explorer that allows users to access on-chain data, such as details on transactions or smart contracts. I first used the Label Word Cloud from Etherscan to find out the addresses of known contracts from a given DeFi protocol, as shown in Figure 3.4 in an example screenshot of the feature. I included the list of addresses from the “Accounts” and “Tokens” tabs as the input for `addresses` at Line 7 of Listing 3.3, the input JSON file for each protocol.

---

<sup>5</sup><https://etherscan.io/>

The screenshot shows the Etherscan interface with the search term 'Yearn'. A table lists 20 accounts found, each with an address, name tag, balance (all 0 ETH), and transaction count. The table columns are Address, Name Tag, Balance, and Txn Count.

| Address             | Name Tag                   | Balance | Txn Count |
|---------------------|----------------------------|---------|-----------|
| 0xa069E3...eF00B5f3 | yearn: Strategy Curve YCRV | 0 ETH   | 376       |
| 0x93A62d...B1a0Efde | yearn: Treasury Vault      | 0 ETH   | 71        |
| 0x29E240...10f9f324 | yearn: yaLINK Vault        | 0 ETH   | 9,796     |
| 0x04bC0A...C4BCa9aE | yearn: yBUSD Token         | 0 ETH   | 228       |
| 0x5dbcF3...91Bca25c | yearn: yCRV Vault          | 0 ETH   | 39,325    |
| 0x975f1B...519a8DE0 | yearn: yCurve Zap In       | 0 ETH   | 291       |

**Figure 3.4** – Screenshot of the query result from the Label Word Cloud in Etherscan

```

1 {
2   "rating": "AA",
3   "treasury": [
4     "0x3d9819210A31b4961b30EF54bE2aeD79B9c9Cd3B",
5     "0x2775b1c75658Be0F640272CCb8c72ac986009e38"
6   ],
7   "addresses": [
8     "0xc3d688b66703497daa19211eedff47f25384cdc3",
9     "0x5d3a536e4d6dbd6114cc1ead35777bab948e3643"
10  ],
11  "hacks": [
12    {
13      "date": "2021-09-29",
14      "amount": 147000000
15    }
16  ]
17 }
```

**Listing 3.3** – Example JSON for protocol data

Furthermore, Etherscan provides a public API endpoint for querying the historical ERC20 token

transfers of a given address. The `collect_transfers()` task of the `tracker` service sends HTTP requests to this endpoint to collect the token transfers of the treasuries. Although it is possible to collect this data directly from the Ethereum chain by filtering the Transfer events of ERC20 tokens, I chose this method due to the faster throughput. Since the data from the Etherscan API have been pre-fetched within its infrastructure, it is much faster to collect the transfers over a wide range of blocks at once. However, this approach does not allow us to query the exact balance of an ERC20 token at a given block number, which can lead to numerical errors for some token contracts. I elaborate on this limitation in the next subsection, [Subsection 3.2.2](#).

DeFiLlama<sup>6</sup> is an open-source data platform that provides a wide variety of data related to DeFi protocols. I referred to the source code of the “adapters” in DeFiLlama<sup>7</sup> to obtain the addresses of treasuries. I chose this code repository as my reference for the treasury addresses since the source code of DeFiLlama is committed and maintained directly by the contributors of each DeFi protocol, it could give me information even for the protocols that do not host their own documentation page. The list of treasury addresses was then added to the `treasury` at [Line 3 of Listing 3.3](#).

I used the Coin Prices API from DeFiLlama to collect the historical prices in `collect_prices()`. I chose this API over the other alternatives again due to the fact that the API is maintained directly by the contributors of the DeFi protocols. The adapters of DeFiLlama can help users discover prices for the tokens that cannot be traded through an exchange but can only be swapped with another token through a smart contract.

I also used DeFiLlama for recording the previous hacks that are used for computing the Operational RWA in [Subsection 3.1.4](#). I searched for each protocol in the Hacks tab of DeFillama to check for the dates of the hacks and the amounts lost if any, see [Figure 3.5](#) for an example screenshot of the Hacks tab.

| Name             | Date                | Chains | Classification | Technique                                | Link              | Amount lost |
|------------------|---------------------|--------|----------------|--|-------------------|-------------|
| CoinEx           | 12 Sep, 2023, 00:00 |        | Infrastructure | Hot wallet hack                          | <a href="#">🔗</a> | \$55m       |
| GMBL_COMPUTER    | 6 Sep, 2023, 00:00  |        | Protocol Logic | Referral Claims Logic Exploit            | <a href="#">🔗</a> | \$0.815m    |
| Stake.com        | 4 Sep, 2023, 00:00  |        | Infrastructure | Private Key Compromised (Unknown Method) | <a href="#">🔗</a> | \$41.3m     |
| SharedStake      | 1 Sep, 2023, 00:00  |        | Protocol Logic | Ownership Override Attack                | <a href="#">🔗</a> | \$0.75m     |
| Balancer         | 27 Aug, 2023, 00:00 |        | Protocol Logic |  | <a href="#">🔗</a> | \$0.8m      |
| Magnate Finance  | 25 Aug, 2023, 00:00 |        | Rugpull        | Drained Contracts                        | <a href="#">🔗</a> | \$6.4m      |
| Harbor Protocol  | 19 Aug, 2023, 00:00 |        |                |  | <a href="#">🔗</a> |             |
| Exactly Protocol | 18 Aug, 2023, 00:00 |        | Protocol Logic | DebtManager Exploit                      | <a href="#">🔗</a> | \$7.2m      |
| RocketSwap       | 15 Aug, 2023, 00:00 |        | Infrastructure | Private Key Compromised (Brute Force)    | <a href="#">🔗</a> | \$0.865m    |
| Zunami Protocol  | 13 Aug, 2023, 00:00 |        | Ecosystem      | Price Manipulation Attack                | <a href="#">🔗</a> | \$2.1m      |
| Earning.Farm     | 9 Aug, 2023, 00:00  |        | Protocol Logic | Reentrancy                               | <a href="#">🔗</a> | \$0.54m     |
| Steadefi         | 8 Aug, 2023, 00:00  |        | Protocol Logic | Deployer Wallet Compromised              | <a href="#">🔗</a> | \$1.157m    |
| Cypher           | 7 Aug, 2023, 00:00  |        |                | Unknown                                  | <a href="#">🔗</a> | \$1.635m    |
| Uwerx            | 2 Aug, 2023, 00:00  |        | Ecosystem      | Flashloan Pool Shares Exploit            | <a href="#">🔗</a> | \$0.327m    |
| LeetSwap         | 1 Aug, 2023, 00:00  |        | Protocol Logic | Liquidity Pools Compromised              | <a href="#">🔗</a> | \$0.62m     |

**Figure 3.5** – Screenshot of the Hacks tab in DeFiLlama

<sup>6</sup><https://defillama.com/>

<sup>7</sup><https://github.com/DefiLlama/DefiLlama-Adapters>

CertiK<sup>8</sup> is a smart contract auditor and a security-focused data platform for Web3 organizations. I used CertiK Skynet, the online knowledge base of CertiK, to obtain security ratings used for computing the risk weights for the Credit RWA in Subsection 3.1.2 and the Market RWA in Subsection 3.1.3. As one can see from the screenshot in Figure 3.6, the ratings in Skynet are given analogously to the credit rating system in finance, e.g., from AAA to D. Thus in this thesis, I mapped the rating from CertiK one-to-one to that of the external credit rating system mentioned in CRE21 of the Basel Framework. I used the rating as the input for Line 2 of Listing 3.3.

| #  | Name       | Security Score | Audit | Price / 24h     | Market Cap | Ecosystem | Category    | Badge & Hono  |
|----|------------|----------------|-------|-----------------|------------|-----------|-------------|---|
| 4  | Aptos      | 94.28          | AAA   | \$5.22 ▲ 0.79%  | \$1.23B    | ■         | Infrastruct | 1     |
| 6  | Cosmos     | 94.25          | AAA   | \$6.84 ▲ 3.98%  | \$2.49B    | ■         | Infrastruct | 1     |
| 7  | XRP Ledger | 94.25          | AAA   | \$0.50 ▲ 3.19%  | \$26.39B   | ■         |             |       |
| 8  | Gala Games | 94.23          | AAA   | \$0.01 ▲ 1.07%  | \$343.38M  | ■         | Gaming      | 4     |
| 10 | PAX Gold   | 93.61          | AA    | \$1.90K ▲ 0.23% | \$472.33M  | ■         | DeFi        | 1   |

Figure 3.6 – Screenshot of the Security Leaderboard in CertiK

The International Token Standardization Association (ITSA)<sup>9</sup> aims to develop and promote market standards for the cryptoassets. ITSA assigns a unique hash to each token known as the International Token Identification Number (ITIN) and further provides each with a code based on its International Token Classification (ITC) framework. I refer to the ITC code for the Economic Purpose (EEP) to match each of the tokens to one of the traditional financial assets, see Table 3.6 for the list of the ITC EEP codes that have been mapped to each financial asset class.

<sup>8</sup><https://www.certik.com/>

<sup>9</sup><https://my.itsa.global/>

| Asset Class      | ITC EEP Codes                                 |
|------------------|---|
| Cash             | EEP21PP01USD                                  |
| Equity           | EEP22G, EEP22NT02, EEP22TU03, EEP23E, EEP23EQ |
| Index Fund       | EEP23FD                                       |
| Commodity        | EEP23A, EEP23ER                               |
| Foreign Currency | EEP21PP01CHF, EEP21PP01EUR                    |
| Settlement       | EEP22S, EEP22TU01, EEP22TU02                  |
| Derivative       | EEP23DV, EEP23DV03                            |

**Table 3.6** – Financial asset classes that correspond to each ITC EEP code

I note that not all tokens in the ITC framework had been assigned an EEP code, and I dropped the tokens that were not classified by the ITSA from the analysis. I made an exception for Wrapped Ethereum (WETH) and assigned it an EEP code of EEP22TU01, which corresponds to a Settlement contract, to include WETH in the scope of this thesis. The ITIN and the EEP code for each token can be found in the input JSON files, see [Line 4](#) and [Line 6](#) of [Listing 3.4](#) for an example.

---

```

1 {
2   "protocol": "aave",
3   "symbol": "aUSDT",
4   "itin": "G3H385VM9",
5   "decimals": 6,
6   "itc_eep": "EEP23DV",
7   "underlying": "0xdac17f958d2ee523a2206206994597c13d831ec7"
8 }
```

---

**Listing 3.4** – Example JSON for ERC20 token data

The address of the underlying token in [Line 7](#) of [Listing 3.4](#) is assigned a null value for all tokens except for derivative tokens, i.e., tokens with the EEP code of either EEP23DV or EEP23DV03. I matched the underlying token one by one by analyzing the documentation of the token, if the link is available on Etherscan.

For instance, searching for the aUSDT token on Etherscan<sup>10</sup> provides information that the token is one of the v2 contracts of Aave. From the documentation page of Aave<sup>11</sup>, I found out that the USDT stablecoin has an implementation of an “aToken” with the address that matches aUSDT. Thus, I concluded that the underlying token of aUSDT is the USDT stablecoin, as shown in [Listing 3.4](#).

<sup>10</sup><https://etherscan.io/address/0x3ed3b47dd13ec9a98b44e6204a523e766b225811>

<sup>11</sup><https://docs.aave.com/developers/v/2.0/deployed-contracts/deployed-contracts>

If the documentation was not sufficient to identify the underlying or if the token had multiple underlyings, I chose a single address following this rule of thumb: first, I tried to choose a token that belongs to a protocol that shows higher ETH usage in DeFiLlama; then I tried to choose the token that seems to have more transfers on Etherscan.

### 3.2.2 Data Summary

By the process described in the beginning of [Section 3.2](#) and [Subsection 3.2.1](#), I have collected the data for a total of 301 protocols and 349 tokens.

The protocols were taken from the intersection of the protocols that had labels in Etherscan and the protocols that had ratings in CertiK. Among the 301 protocols, I could find the treasury address for 33 protocols from DeFiLlama, and thus I have conducted the analysis using the Basel Framework for these 33 protocols in [Chapter 4](#).

The tokens were taken from the intersection of tokens that had price data in the DeFiLlama API and the tokens that had been assigned the ITC EEP codes in ITSA. Again here, I note that I manually added the Wrapped Ethereum (WETH) token and assigned it an EEP code that stands for a Settlement contract.

I could collect a total of 1,357,414 transfers using the `collect_transfers()` task. The first timestamp within the transfers was 1561995287, which translates to the UTC timezone as Jul 10 2019, and the last timestamp was 1693612595, which is Sep 01 2023. I share more details on the transfers for each of the 33 protocols that had the treasury address in the appendix, [Table A.1](#).

The number of price data I collected using the `collect_prices()` task was 505,441. The minimum timestamp I started to search for the prices, `MIN_TIMESTAMP`, was set to 1534377600 which translates to 16 Aug 2018. As mentioned earlier in [Subsection 3.2.1](#), this date was set from the earliest date I could retrieve the price data from DeFiLlama. The actual first timestamp within the prices was 17 Aug 2018, and the last timestamp was 02 Sep 2023.

Since the first date for the price data comes before the first date of the token transfers, theoretically, we should be able to calculate the USD value of the treasury balance for each day. However, as I tried to calculate the RWA and CAR by the process described in [Section 3.1](#), there were some dates missing from the `prices` entity in between the range of transfers. I used the forward filling method for the missing prices, i.e., I used the latest price before the date of the transaction to substitute for the missing price entry.

As mentioned as a limitation in [Subsection 3.2.1](#), calculating the balance from the ERC20 token transfer data from Etherscan gave numerical errors for some tokens. For instance, the balance of the Aave interest bearing USDC (aUSDC) token in an address can increase automatically as the USDC reserves in Aave accrue profit. From the screenshot shown in [Figure 3.7](#), one can see that the contract from Idle Finance could send a larger amount of aUSDC than the amount that was minted.

| Transaction Hash       | Tx Type | Method    | Age                 | From                       | To                         | Amount           | Asset                   |
|------------------------|---------|-----------|---------------------|----------------------------|----------------------------|------------------|-------------------------|
| 0xf5a804b8f6e54e53a... | ERC-20  | Withdraw  | 827 days 22 hrs ago | Idle.finance: idleUSDCY... | 0xC9f16B...036d8aA2        | 1.670487         | Aave interes... (aUSDC) |
| 0x5587c8014b6b4b66...  | ERC-20  | Rebalance | 828 days 13 hrs ago | Idle.finance: idleUSDCY... | 0xC9f16B...036d8aA2        | 32.037475        | Aave interes... (aUSDC) |
| 0x5587c8014b6b4b66...  | ERC-20  | Rebalance | 828 days 13 hrs ago | Null: 0x000...000          | Idle.finance: idleUSDCY... | 122.658623       | Aave interes... (aUSDC) |
| 0x44f5e72a30f15ad63... | ERC-20  | Rebalance | 828 days 23 hrs ago | Null: 0x000...000          | Idle.finance: idleUSDCY... | 0.000001         | Aave interes... (aUSDC) |
| 0x593bad50012942f0...  | ERC-20  | Rebalance | 829 days 4 hrs ago  | Null: 0x000...000          | Idle.finance: idleUSDCY... | 32.031987        | Aave interes... (aUSDC) |
| 0xbd4b84b6fa65091a5... | ERC-20  | Rebalance | 837 days 12 hrs ago | Idle.finance: idleUSDCY... | 0xC9f16B...036d8aA2        | 6,032,109.87091  | Aave interes... (aUSDC) |
| 0xb795b4660e67912b...  | ERC-20  | Rebalance | 837 days 21 hrs ago | Null: 0x000...000          | Idle.finance: idleUSDCY... | 6,030,969.145471 | Aave interes... (aUSDC) |

**Figure 3.7** – Screenshot of aUSDC transfers from Idle Finance

Therefore, simply taking the cumulative sum of values can lead to negative balance for some tokens such as the aUSDC. In this thesis, I take a workaround for this problem by resetting the balance to zero whenever the balance becomes negative, assuming that the protocol must have cleared out the balance of the token. However, this can potentially introduce a bias in the data and thus this still remains as one of the limitations of this thesis. I discuss further on our limitations in [Chapter 5](#).

Finally, I collected a total of 28,903 entries for the CAR data, for the 33 protocols and 349 ERC20 tokens. The timestamps follow the timestamps of the transfers and tokens, i.e., the first date for the CAR data was 10 Jul 2019 and the last date was 02 Sep 2023. None of the entries were missing from the daily interval, but there are some entries that had non-numeric values (NaN) due to division by zero. I filled the NaN values for the CAR with 0.0 since the entries with NaN had the RWA values equal to zero, meaning that the protocols were not active during that period. See [Table 3.7](#) for the list of protocols that had non-numeric values in the CAR data.

| Protocol              | Number of NaNs |
|-----------------------|----------------|
| Ethereum Name Service | 1              |
| Gitcoin               | 49             |
| Lido                  | 75             |

**Table 3.7** – List of protocols with non-numeric values in CAR data

I share more details on the CAR data for the 33 protocols that had the treasury address in the appendix, [Table A.2](#).

### 3.3 Risk Spillover Analysis

To illustrate how the data I have collected could be applied to financial research, I will share a simple analysis modeling the systematic risk of DeFi protocols. As discussed in [Chapter 2](#), there has been a large number of studies that model the systematic risk of cryptocurrencies, but there has not been much literature that focuses on the risk of DeFi protocols. Hence, my aim is to provide a simple quantitative analysis of the protocols using the most basic method, following the former studies as closely as possible.

To this end, I will follow the strand of econometrics often referred to as “Financial Connectedness” ([Francis X Diebold and Yilmaz 2015](#)). This approach allows us to compute various indices that describe the systematic risk of a complex system from the forecast error of a time series model. The decomposition of the forecast error could be applied to a wide variety of models, from the most simple models like the Vector Autoregression (VAR) to complex regime-switching models. This property makes the method suitable for the preliminary analysis of new data for which we do not know what the most appropriate model is.

In this thesis, I will apply two examples of this method, the first using the VAR ([Francis X Diebold and Yilmaz 2012](#)) and the second using a Time-Varying Parameter Vector Autoregression (TVP-VAR) ([Antonakakis et al. 2020](#)). I will briefly explain below about the core concepts of the method, the data preprocessing, and how I estimated of the parameters of the underlying model.

#### 3.3.1 Spillover Index from VAR

I first introduce the spillover indices that can be derived from a Vector Autoregression (VAR) model ([Francis X Diebold and Yilmaz 2012](#)). If a vector-valued random variable  $\mathbf{x}_t \in \mathbb{R}^n$  follows a VAR( $p$ ) model for some  $p \in \mathbb{N}$ , the elements of  $\mathbf{x}_t$  should satisfy the following system of linear equations:

$$\begin{aligned}\mathbf{x}_t &= \Phi_1 \mathbf{x}_{t-1} + \Phi_2 \mathbf{x}_{t-2} + \cdots + \Phi_p \mathbf{x}_{t-p} + \varepsilon_t \\ &= \sum_{k=1}^p \Phi_k \mathbf{x}_{t-k} + \varepsilon_t\end{aligned}\tag{3.9}$$

where  $\Phi_k \in \mathbb{R}^{n \times n}$  and  $\varepsilon_t \sim (\mathbf{0}, \Sigma)$ , meaning that the error term  $\varepsilon_t$  is independently and identically distributed with mean zero and covariance  $\Sigma$ . The positive integer  $p$  is called as the lag order of the VAR model.

[Equation 3.9](#) can be simplified as below using the lag operator  $L$ :

$$\Phi(L)\mathbf{x}_t = \varepsilon_t\tag{3.10}$$

$$\text{where } \Phi(L) = I - \Phi_1 L - \cdots - \Phi_p L^p\tag{3.11}$$

and the lag operator shifts the variable back by a single period,  $L\mathbf{x}_t = \mathbf{x}_{t-1}$ .

Using this new notation in [Equation 3.10](#), the parameters  $\Phi_k$  of the VAR model should satisfy the stationarity condition, which means that the roots in the characteristic equation of [Equation 3.11](#) should all lie outside the unit circle. Given that the VAR process is stationary, we can now transform the [Equation 3.10](#) into the Moving Average (MA) representation using  $\Psi$ :

$$\begin{aligned} \mathbf{x}_t &= \Phi^{-1}(L)\varepsilon_t = \Psi(L)\varepsilon_t \\ &= \sum_{k=0}^{\infty} \Psi_k \varepsilon_{t-k} \end{aligned} \quad (3.12)$$

$$\text{where } \Psi_k = \Phi_1 \Psi_{k-1} + \Phi_2 \Psi_{k-2} + \cdots + \Phi_p \Psi_{p-2} \quad (3.13)$$

and  $\Psi_0 = \mathbf{I} \in \mathbb{R}^{n \times n}$ ,  $\Psi_k = \mathbf{0} \in \mathbb{R}^{n \times n}$  for  $k < 0$ .

Now we consider the effect the error of the  $j$ -th element can have towards the forecast estimates of the  $i$ -th element,  $\theta_{ij}(H)$  where  $H \in \mathbb{N}$  is the length of the forecast window. Using the MA representation  $\theta_{ij}(H)$  is defined as follows:

$$\theta_{ij}(H) = \frac{\sigma_{jj}^{-1} \sum_{h=0}^{H-1} (\Psi_h \Sigma)_{ij}^2}{\sum_{h=0}^{H-1} (\Psi_h \Sigma \Psi_h')_{ii}} \quad (3.14)$$

where  $(\cdot)_{ij}$  stands for the  $(i, j)$ -th entry of a matrix, and  $\sigma_{jj}$  is the standard deviation of the  $j$ -th element of  $\varepsilon_t$ , i.e.,  $\sqrt{(\Sigma)_{jj}}$ . To compute the spillover indices we normalize  $\theta_{ij}(H)$  and denote as  $\tilde{\theta}_{ij}(H)$ :

$$\tilde{\theta}_{ij}(H) = \frac{\theta_{ij}(H)}{\sum_{j=1}^n \theta_{ij}(H)} \quad (3.15)$$

By construction,  $\sum_{j=1}^n \tilde{\theta}_{ij}(H) = 1$  and  $\sum_{i,j=1}^n \tilde{\theta}_{ij}(H) = n$ .

There are a wide variety of spillover indices one can compute using the normalized variable  $\tilde{\theta}_{ij}(H)$  ([Gabauer 2021](#)). In this thesis I will cover the following three connectedness measures: Total Connectedness Index (TCI), Pairwise Connectedness Index (PCI), and the Net Pairwise Directional Connectedness (NPDC).

The total volatility spillover index or the Total Connectedness Index (TCI) is defined as the relative share of the non-diagonal entries of  $\tilde{\theta}$ :

$$\begin{aligned} \text{TCI} &= \frac{\sum_{i \neq j}^n \tilde{\theta}_{ij}(H)}{\sum_{i,j=1}^n \tilde{\theta}_{ij}(H)} \cdot 100 \\ &= \frac{\sum_{i \neq j}^n \tilde{\theta}_{ij}(H)}{n} \cdot 100 \end{aligned} \quad (3.16)$$

The Pairwise Connectedness Index (PCI) is the bilateral version of the TCI:

$$\text{PCI}_{ij} = \text{PCI}_{ji} = 2 \cdot \frac{\tilde{\theta}_{ij}(H) + \tilde{\theta}_{ji}(H)}{\tilde{\theta}_{ii}(H) + \tilde{\theta}_{ij}(H) + \tilde{\theta}_{ji}(H) + \tilde{\theta}_{jj}(H)} \cdot 100 \quad (3.17)$$

We can also define directional measures by adding a sign in front of the variables, e.g., the Net Pairwise Directional Connectedness (NPDC) is defined as follows:

$$\text{NPDC}_{ij} = -\text{NPDC}_{ji} = \tilde{\theta}_{ji}(H) - \tilde{\theta}_{ij}(H) \quad (3.18)$$

where  $\text{NPDC}_{ij} > 0$  denotes that the  $i$ -th variable is driving the  $j$ -th variable, and vice versa.

### 3.3.2 Spillover Index from TVP-VAR

I illustrate how one can extend the above spillover indices to other VAR models, using the Time-Varying Parameter Vector Autoregression (TVP-VAR) (Antonakakis et al. 2020). If a random variable  $\mathbf{x}_t \in \mathbb{R}^n$  follows a TVP-VAR( $p$ ) model for some  $p \in \mathbb{N}$ ,  $\mathbf{x}_t$  should satisfy the equations that are very much similar to [Equation 3.9](#) but with an additional law of motion for  $\Phi$ :

$$\begin{aligned} \mathbf{x}_t &= \Phi_{1t}\mathbf{x}_{t-1} + \Phi_{2t}\mathbf{x}_{t-2} + \cdots + \Phi_{pt}\mathbf{x}_{t-p} + \varepsilon_t \\ &= \sum_{k=1}^p \Phi_{kt}\mathbf{x}_{t-k} + \varepsilon_t \\ \text{and } \Phi_{\cdot t} &= \Phi_{\cdot t-1} + \xi_t \end{aligned} \quad (3.19)$$

where  $\Phi_{kt} \in \mathbb{R}^{n \times n}$ ,  $\varepsilon_t \sim (\mathbf{0}, \Sigma_t)$ , and also  $\xi_t \sim (\mathbf{0}, \Xi_t)$ . Note that now the covariance matrices of the error terms  $\Sigma_t$  and  $\Xi_t$  are allowed to vary through time  $t$ .

In Antonakakis et al. (2020), the dynamics of the covariance matrices are given by the Kalman filter with forgetting factors. To simplify the notations for the Kalman filter updates, let us first rewrite the [Equation 3.19](#) in the companion-form:

$$\begin{aligned} \mathbf{x}_t &= \Phi_t \mathbf{z}_{t-1} + \varepsilon_t \\ \Phi_t &= \Phi_{t-1} + \xi_t, \\ \text{where } \mathbf{z}_{t-1} &= \begin{pmatrix} \mathbf{x}_{t-1} \\ \mathbf{x}_{t-2} \\ \vdots \\ \mathbf{x}_{t-p} \end{pmatrix} \quad \text{and } \Phi'_t = \begin{pmatrix} \Phi_{1t} \\ \Phi_{2t} \\ \vdots \\ \Phi_{pt} \end{pmatrix} \end{aligned} \quad (3.20)$$

where  $\mathbf{z}_{t-1} \in \mathbb{R}^{np}$  and  $\Phi_t \in \mathbb{R}^{n \times np}$ . Under this abuse of notation for  $\Phi_t$ , in this new companion-form now the parameters  $\Phi$  has subscripts for time  $t$  instead of the lag order  $p$ .

Now to perform the Kalman filter updates we first initialize the variables  $\Phi_0$ ,  $\Sigma_0$ , and  $\Sigma_0^\Phi$  from the Ordinary Least Squares (OLS) estimates of a VAR model.  $\Sigma_0^\Phi$  denotes the covariance matrix for the OLS estimator of  $\Phi_0$ . Given the values for  $\Phi_{t-1}$ ,  $\mathbf{z}_{t-1}$ , and  $\Sigma_{t-1}^\Phi$ , the prediction phase is formulated as follows:

$$\begin{aligned}\Phi_{t|t-1} &= \Phi_{t-1|t-1} \\ \varepsilon_t &= \mathbf{x}_t - \Phi_{t|t-1} \mathbf{z}_{t-1} \\ \Sigma_t &= \kappa_2 \Sigma_{t-1|t-1} + (1 - \kappa_2) \varepsilon_t' \varepsilon_t \\ \Xi_t &= (1 - \kappa_1^{-1}) \Sigma_{t-1|t-1}^\Phi \\ \Sigma_{t|t-1}^\Phi &= \Sigma_{t-1|t-1}^\Phi + \Xi_t \\ \Sigma_{t|t-1} &= \mathbf{z}_{t-1} \Sigma_{t|t-1}^\Phi \mathbf{z}_{t-1}' + \Sigma_t\end{aligned}\tag{3.21}$$

where for some variable  $X_{t-1|t-1} = X_{t-1}$ , which is again an abuse of notation to separate the variables used in the prediction phase from the variables in the update phase.  $\kappa_1, \kappa_2 \in (0, 1)$  are arbitrary decay factors used for numerical stability of the computation. In Antonakakis et al. (2020) the decay factors are set as  $\kappa_1 = 0.99$  and  $\kappa_2 = 0.96$ .

The update phase can now be expressed as follows:

$$\begin{aligned}\mathbf{K}_t &= \Sigma_{t|t-1}^\Phi \mathbf{z}_{t-1}' \Sigma_{t|t-1}^{-1} \\ \Phi_{t|t} &= \Phi_{t|t-1} + \mathbf{K}_t (\mathbf{x}_t - \Phi_{t|t-1} \mathbf{z}_{t-1}) \\ \Sigma_{t|t}^\Phi &= (\mathbf{I} - \mathbf{K}_t) \Sigma_{t|t-1}^\Phi \\ \varepsilon_{t|t} &= \mathbf{x}_t - \Phi_{t|t} \mathbf{z}_{t-1} \\ \Sigma_{t|t} &= \kappa_2 \Sigma_{t-1|t-1} + (1 - \kappa_2) \varepsilon_{t|t}' \varepsilon_{t|t}\end{aligned}\tag{3.22}$$

The term  $\mathbf{K}_t$  is often called as the Kalman gain in the literature, which explains how much the parameters should be updated from each state.

Once we have all of the values for  $\Phi_t$  and  $\varepsilon_t$ , we can formulate the MA representation of the TVP-VAR similarly to Equation 3.13:

$$\mathbf{x}_t = \sum_{k=0}^{\infty} \Psi_{kt} \varepsilon_{t-k}, \quad \Psi_{kt} = \mathbf{J}' \mathbf{M}_t^k \mathbf{J}\tag{3.23}$$

$$\text{where } \mathbf{J} = \begin{pmatrix} \mathbf{I} \\ \mathbf{0} \\ \vdots \\ \mathbf{0} \end{pmatrix} \in \mathbb{R}^{np \times n}, \quad \mathbf{M}_t = \begin{pmatrix} \Phi_t \\ \mathbf{I}_{n(p-1)} & \mathbf{0}_{n(p-1) \times n} \end{pmatrix} \in \mathbb{R}^{np \times np}\tag{3.24}$$

The calculation of the spillover indices are identical from Equation 3.14 to Equation 3.18, except that

all variables now depend on the time  $t$  since the MA terms  $\Psi_{kt}$  vary through time.

### 3.3.3 Model Estimation

To fit a VAR process to the CAR data described in Subsection 3.2.2, we first need to filter out the protocols that had insufficient data points for estimation. For instance, there was only a single data point for Paraswap and 310 points for Index Cooperative, as shown in Figure 3.8 which illustrates the count distribution of the CAR data. Including the protocols with a small number of data points in the VAR estimation would greatly reduce the available degree of freedom for the parameters.

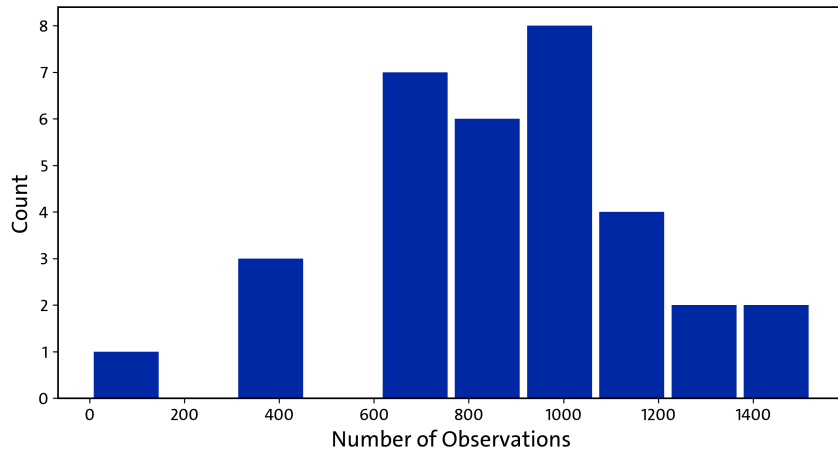


**Figure 3.8** – The count distribution of the CAR data

To this end, I have selected the top 10 protocols that had the largest number of observations, all of which had more than 1,000 data points. I share some basic statistics on this subset in Table 3.8 and Table 3.9. The floating point numbers in the tables have been rounded to four decimal places.

|          | Aave   | Compound | Cream Finance | DXdao  | Ethereum Foundation |
|----------|--------|----------|---------------|--------|---------------------|
| Count    | 1,317  | 1,490    | 1,062         | 1,525  | 1,141               |
| Mean     | 0.2649 | 0.3873   | 0.1088        | 0.2314 | 34.8940             |
| Std      | 0.2073 | 0.3213   | 0.2684        | 0.2371 | 80.0208             |
| Min      | 0.0009 | 0.0000   | 0.0000        | 0.0000 | 0.6121              |
| Q1 (25%) | 0.1133 | 0.0593   | 0.0001        | 0.0000 | 0.6652              |
| Q2 (50%) | 0.2390 | 0.3856   | 0.0029        | 0.2743 | 1.3095              |
| Q3 (75%) | 0.3729 | 0.6080   | 0.0503        | 0.3852 | 7.8277              |
| Max      | 1.2234 | 1.0358   | 1.1903        | 0.6867 | 461.9192            |

**Table 3.8** – Basic statistics of the filtered dataset - first 5 protocols

|          | Gnosis | Rook   | Synthetix | Uniswap | Yearn Finance |
|----------|--------|--------|-----------|---------|---------------|
| Count    | 1,174  | 1,026  | 1,337     | 1,081   | 1,123         |
| Mean     | 0.0343 | 0.1363 | 0.2786    | 0.4305  | 0.0743        |
| Std      | 0.0627 | 0.1081 | 0.2207    | 0.2412  | 0.0386        |
| Min      | 0.0000 | 0.0000 | 0.0000    | 0.0720  | 0.0000        |
| Q1 (25%) | 0.0072 | 0.0242 | 0.0839    | 0.2128  | 0.0519        |
| Q2 (50%) | 0.0144 | 0.1513 | 0.1759    | 0.3987  | 0.0665        |
| Q3 (75%) | 0.0333 | 0.2160 | 0.5281    | 0.5570  | 0.1001        |
| Max      | 0.6667 | 0.3840 | 0.6667    | 1.2282  | 0.8873        |

**Table 3.9** – Basic statistics of the filtered dataset - last 5 protocols

We can see that most of the CAR values fall in between 0 and 1, but the Ethereum Foundation has CAR values that are abnormally high, e.g. 461.9192. I will defer the explanation about the cause of this phenomenon to the next section; please see [Section 4.1](#) for more details. The significance of these abnormal values in this subsection is that the CAR series of Ethereum Foundation will lead to non-stationarity of the VAR model.

To guarantee the stationarity of the VAR, I perform the Augmented Dickey-Fuller (ADF) test (Dickey and Fuller [1979](#)) on the data of each protocol. The ADF test checks whether a scalar-valued time series  $y_t \in \mathbb{R}$  follows a unit root process by testing the null hypothesis  $\gamma = 0$  in the following model:

$$\Delta y_t = \alpha + \beta t + \gamma y_{t-1} + \delta_1 \Delta y_{t-1} + \cdots + \delta_{p-1} \Delta y_{t-p+1} + \varepsilon_t \quad (3.25)$$

The above can be seen as a variant of an AR( $p$ ) model where the positive integer  $p$  is the lag order of the model. If the series  $y_t$  contains a unit root then the value of  $\gamma$  will be close to zero whereas in the other case  $\gamma \ll 0$ . Thus the p-value from the ADF statistic should be small to conclude that the series does not contain a unit root, i.e., that the series is stationary.

Indeed we can see from the test results shown in [Table 3.10](#) that the CAR values of Ethereum Foundation fails to reject the null hypothesis for all given lag orders, from  $p = 1$  to  $p = 10$ . The p-values in [Table 3.10](#) are rounded to two decimal places.

| Lag Order $p$       | 1    | 2    | 3    | 4    | 5    | 6    | 7    | 8    | 9    | 10   |
|---------------------|------|------|------|------|------|------|------|------|------|------|
| Aave                | 0.00 | 0.00 | 0.00 | 0.00 | 0.00 | 0.02 | 0.02 | 0.01 | 0.00 | 0.00 |
| Compound            | 0.82 | 0.79 | 0.81 | 0.82 | 0.80 | 0.80 | 0.82 | 0.84 | 0.84 | 0.84 |
| Cream Finance       | 0.01 | 0.01 | 0.01 | 0.01 | 0.01 | 0.01 | 0.01 | 0.01 | 0.01 | 0.01 |
| DXdao               | 0.48 | 0.42 | 0.40 | 0.40 | 0.43 | 0.43 | 0.43 | 0.43 | 0.40 | 0.40 |
| Ethereum Foundation | 0.59 | 0.58 | 0.53 | 0.47 | 0.47 | 0.45 | 0.49 | 0.61 | 0.61 | 0.63 |
| Gnosis              | 0.00 | 0.00 | 0.00 | 0.00 | 0.00 | 0.00 | 0.00 | 0.00 | 0.00 | 0.00 |
| Rook                | 0.15 | 0.14 | 0.14 | 0.14 | 0.14 | 0.14 | 0.14 | 0.14 | 0.13 | 0.13 |
| Synthetix           | 0.43 | 0.47 | 0.46 | 0.44 | 0.47 | 0.45 | 0.44 | 0.42 | 0.45 | 0.45 |
| Uniswap             | 0.06 | 0.07 | 0.23 | 0.32 | 0.32 | 0.31 | 0.37 | 0.30 | 0.33 | 0.33 |
| Yearn Finance       | 0.01 | 0.01 | 0.01 | 0.03 | 0.03 | 0.03 | 0.03 | 0.03 | 0.03 | 0.04 |

**Table 3.10** – p-values for the ADF test

To handle this non-stationarity, I take the log-difference of the values:

$$\log y_t - \log y_{t-1} = \log \frac{y_t}{y_{t-1}} \approx \frac{y_t}{y_{t-1}} - 1 = \frac{y_t - y_{t-1}}{y_{t-1}} \quad (3.26)$$

where the approximation holds due to the Taylor expansion of the logarithm. The log-difference transformation is often used in financial applications since it can be interpreted as the return of an asset or the percentage change of an index.

After taking the log-difference, every protocol rejects the null hypothesis of the ADF test for all given lag orders. The p-values are all very close to zero, and they are all equal to 0.00 when rounded to two decimal places. Thus, we do not share the p-values after the transformation but instead share the ADF test statistics in the appendix; see [Table A.3](#).

Now that the data is stationary, we could fit the VAR model to this data of 10 protocols. However to make sure that none of the protocols are redundant for the estimation, I perform the Granger Causality test ([Granger 1969](#)) for each pair of protocols. The Granger Causality test for a pair of univariate time series  $x_t, y_t \in \mathbb{R}$  checks whether including the lagged values of  $x_t$  in the autoregression of  $y_t$  can decrease the variance of the error, i.e.,

$$y_t = \beta_0 + \beta_1 y_{t-1} + \cdots + \beta_p y_{t-p} + \varepsilon_t \quad (3.27)$$

$$y_t = \beta_0 + \beta_1 y_{t-1} + \cdots + \beta_p y_{t-p} + \gamma_1 x_{t-1} + \cdots + \gamma_q x_{t-q} + \varepsilon_t \quad (3.28)$$

the test checks whether the variance of  $\varepsilon_t$  in [Equation 3.28](#) is smaller than the variance in [Equation 3.27](#).

I conducted the Granger Causality test for the pairs of protocols with the maximum lag order of 10. All of the protocols appeared to have causality with at least a single protocol when using the p-value

of 5% as the significance threshold, as can be seen from Figure 3.9. I share the p-values from the test in the appendix, in Table A.4 and Table A.5.

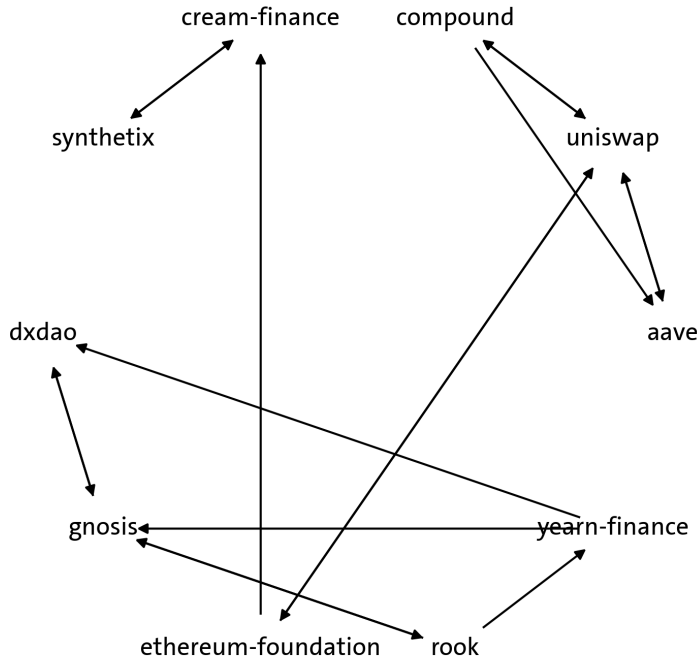


**Figure 3.9** – Granger Causality between protocols, arrows denote the p-values under 5%

We now choose the lag order  $p$  of the VAR model. I fit the VAR model for lag orders 0 to 5, where VAR(0) stands for a constant vector intercept, and compute the Akaike information criterion (AIC) and the Bayesian information criterion (BIC) from the likelihood as shown in Table 3.11. The bold face denotes the minimum value within the column, and the values in Table 3.11 have been rounded to two decimal places.

|         | AIC            | BIC            |
|---------|----------------|----------------|
| $p = 0$ | -31.06         | <b>-31.01*</b> |
| $p = 1$ | <b>-31.18*</b> | -30.65         |
| $p = 2$ | -31.10         | -30.08         |
| $p = 3$ | -31.02         | -29.51         |
| $p = 4$ | -30.91         | -28.92         |
| $p = 5$ | -30.86         | -28.38         |

**Table 3.11** – Values of AIC and BIC for different lag orders

The formula for AIC and BIC are very similar except for the penalty term:

$$\begin{aligned} \text{AIC} &= 2k - 2 \log(\hat{L}) \\ \text{BIC} &= k \log(n) - 2 \log(\hat{L}) \end{aligned} \quad (3.29)$$

where  $k$  denotes the number of parameters,  $\hat{L}$  is the maximum likelihood of the model, and  $n$  is the number of data points. Since the term for the likelihood is negative one should choose the lag order that has the minimum value for each information criterion.

Both information criteria aim to help researchers maintain a balance between maximizing the likelihood and increasing the complexity of the model. However, the difference in the penalty terms in [Equation 3.29](#) brings a subtle distinction in the interpretation of the result: AIC aims to show which model will lose the least amount of information through its representation, whereas BIC aims to show which model has the most evidence, given that the model is the true underlying model.

The result [Table 3.11](#) suggests that when following AIC, the correct lag order should be  $p = 1$ , whereas when following BIC one should choose  $p = 0$ . I choose  $p = 1$  following the AIC instead of the BIC in this thesis, since the aim of fitting a VAR model to the data is not to find out the true underlying model for the data generating process, but to provide a forecast model where the error terms can represent unforeseen shocks of the system. The result of  $p = 0$  from BIC can be interpreted as the true underlying model not being a VAR process, which is one of the limitations of this thesis. I discuss further on the limitations in [Chapter 5](#).

After fitting the VAR(1) model to the data I check that the residuals  $\varepsilon_t$  are independently distributed, by conducting a Portmanteau test ([Lütkepohl 2005](#)). This statistical test is quite loosely defined and depends heavily on the implementation of the model estimation. In this thesis I used the Statsmodels package ([Seabold and Perktold 2010](#)) in Python to estimate the VAR model and perform statistical tests. I would like to defer the description of the Portmanteau test to the documentation of the package.

The test showed a test statistic of 932.6 with a critical value of 970.9 and a p-value of 21.9%, thus unable to reject the null hypothesis. The null hypothesis of the test was that the autocorrelation of the residuals up to lag 10 is zero. Therefore, we can assume that the residuals are independent.

To calculate the spillover indices, I used the ConnectednessApproach package ([Gabauer 2022](#)) in R. To illustrate the change in the spillover indices, I fit the VAR model and the TVP-VAR model with a moving window of 200 days following [Francis X Diebold and Yilmaz \(2012\)](#) and [Antonakakis et al. \(2020\)](#). The lag order of both models is set to  $p = 1$  and the forecast horizon for the indices is set to  $H = 10$ . Nonetheless, I also share the indices computed with shorter horizons to show the sensitivity of the approach in [Section 4.2](#).

# Chapter 4

## Results

In this chapter, I share the visualizations and interpretations of the Capital Adequacy Ratios (CAR) collected by the process defined in [Chapter 3](#). In [Section 4.1](#), I provide an overview of the CAR data and share the comparisons, varying the different parameters in the definitions set out in [Section 3.1](#). In [Section 4.2](#), I share a quantitative analysis of the data using the spillover indices defined in [Section 3.3](#). Unless stated otherwise, throughout this chapter, the CAR refers to the ratio of the Common Equity Tier 1 (CET1) capital over the Risk-Weighted Assets (RWA), i.e., CET1/RWA. The numeric values that represent capital or the value of assets are expressed in USD, and the number of significant digits is 6 digits. The calculation for the RWA in [Section 3.1](#) involves floating-point arithmetic, which can have 6 significant digits in the worst case.

Also, I only consider the 10 protocols that have been selected for the estimation of VAR models in [Subsection 3.3.3](#): Aave, Compound, Cream Finance, DXdao, Ethereum Foundation, Gnosis, Rook, Synthetix, Uniswap and Yearn Finance. The number of observations for the CAR data have been truncated to 1,026 to match the minimum among the 10 protocols. The first date in the truncated dataset is 11 Nov 2020, and the last date is 02 Sep 2023.

### 4.1 Capital Adequacy Ratios

I first share an overview for CET1/RWA, the CAR defined by the first term in the requirements set out in [Subsection 3.1.1](#). According to the basel framework, banks should have at least 4.5% of the RWA as CET1 capital. [Figure 4.1](#) shows the ratio of CET1 and RWA for 9 protocols, excluding the Ethereum Foundation, where the dashed black line denotes the 4.5% threshold. I excluded the Ethereum Foundation from the overview figure due to its abnormal values; I cover this issue separately as we discuss on the individual protocols in [Figure 4.3](#).

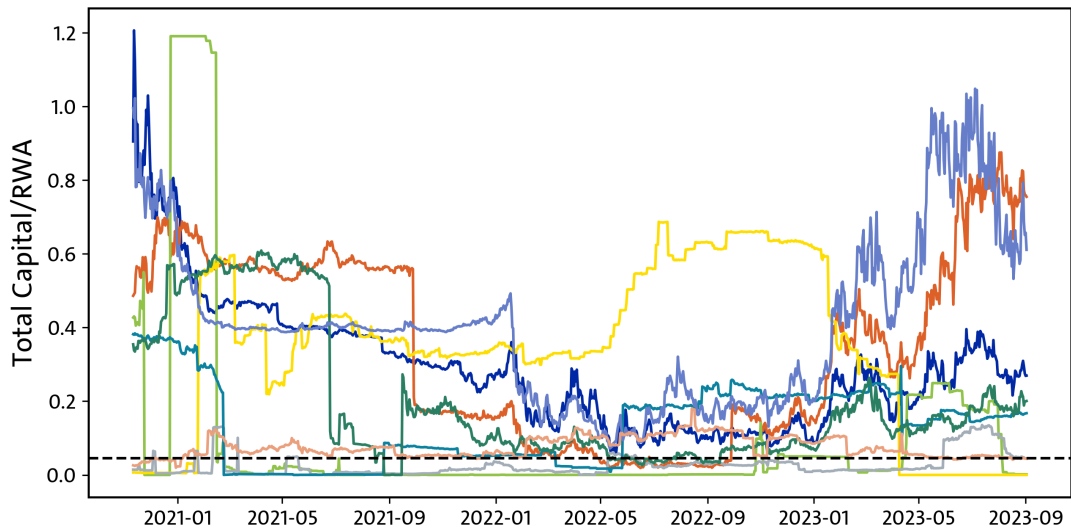


**Figure 4.1** – CET1/RWA of 9 protocols excluding Ethereum Foundation

The first interesting fact I would like to note from [Figure 4.1](#) is that most protocols show a U-shape in the ratios. One can see that the most ratios had a downward spike around late Jan 2022 and again in May 2022, then climbed back up starting from Jan 2023. These dates are related to the large movements in the Bitcoin price and the Total Value Locked (TVL) in the Ethereum blockchain. The TVL indicates the USD value of the sum of cryptoassets actively being used in DeFi protocols.

I share the daily Bitcoin price collected from Yahoo Finance<sup>1</sup> and the TVL from DeFiLlama in [Figure 4.2](#). The orange line denotes the Bitcoin price in USD, and the blue line denotes the TVL in billion USD.

<sup>1</sup><https://finance.yahoo.com/quote/BTC-USD/history/>



**Figure 4.2** – Total Value Locked in Ethereum and Bitcoin price

Figure 4.2 shows that the movement of the Bitcoin price leads the movement in the TVL, and late of Jan 2022 and May 2022 were the dates when the price of Bitcoin had significant breakdowns. The fall in Jan 2022 is regarded as due to the increase in the interest rates, and the drop in May 2022 is due to the intervention of the US Securities and Exchange Commission (SEC). These events caused the TVL to drop as well, invoking a chain of liquidations and depreciations of the collaterals within the DeFi protocols, thus decreasing the CET1 while increasing the RWA.

From Jan 2023, the Bitcoin price starts to rally up, while the TVL remains sideways. The surge in price is regarded as due to the expectation of a drop in interest rates; the TVL of the Ethereum chain did not increase as much, but instead the TVL of other blockchains, e.g., Optimism and Arbitrum, greatly increased from Jan 2023. Since the operations of the DeFi protocols on Ethereum have already been reduced throughout the latter half of 2022, this meant that the value of CET1 becomes relatively appreciated compared to the value of RWA. Therefore, the CAR of most DeFi protocols starts to increase from Jan 2023.

The shape of the time series remains the same for the overview of the CAR calculated by the total capital instead of the CET1, which I share in the appendix, Figure B.1. Thus the above interpretation could be applied on the requirement for the total capital as well. The CAR values for individual protocols shown in Figure 4.3 better illustrate the difference between the two definitions of CAR.

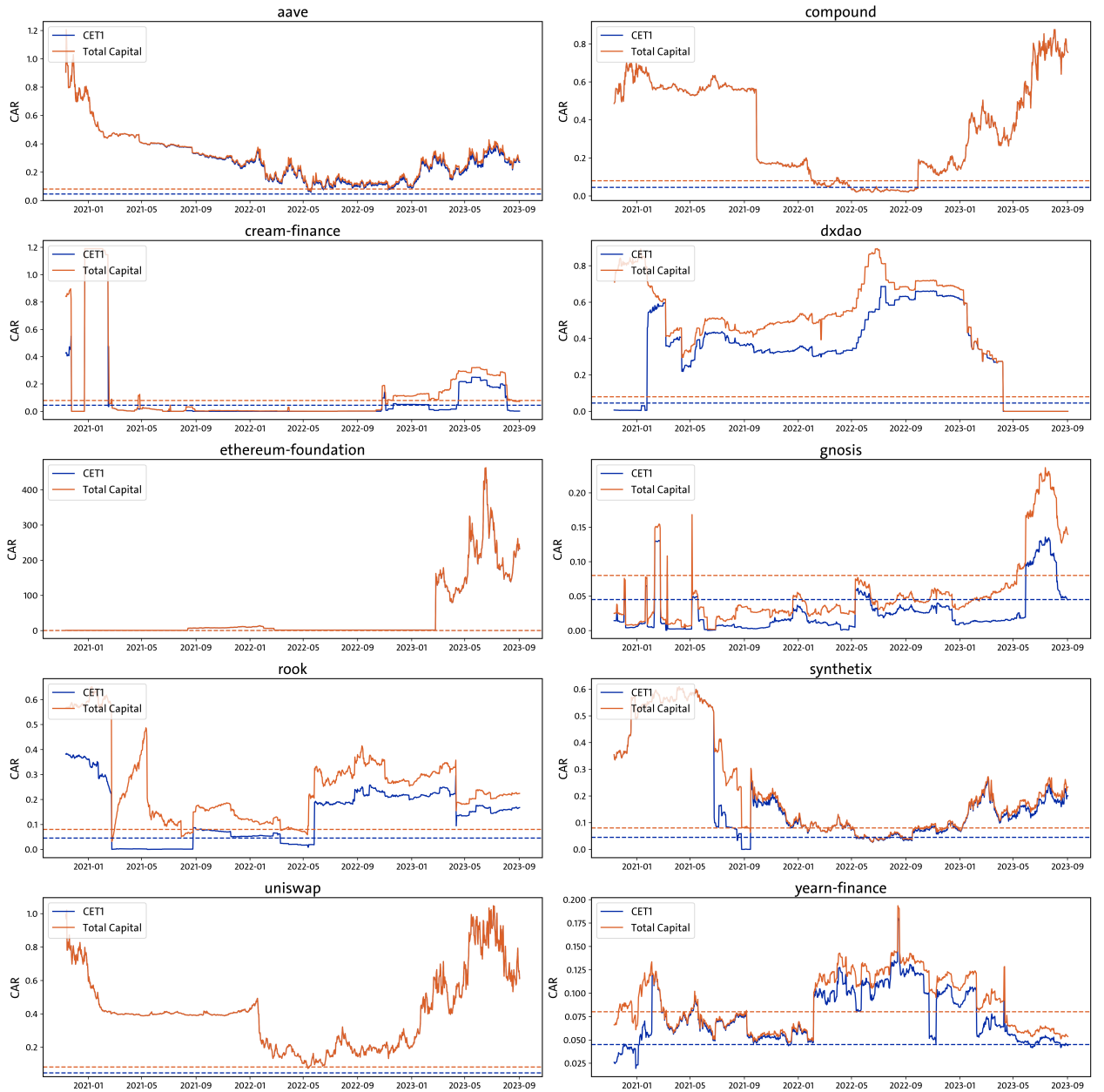


Figure 4.3 – CAR values of 10 protocols

Figure 4.3 shows the two CAR values for 10 protocols, including the Ethereum Foundation. The blue line represents the ratio CET1/RWA, and the orange line denotes total capital/RWA. It can be observed from the figure that there are some abrupt changes in the CAR for certain protocols, and most of these changes can be traced back to events in the DeFi space that caused these fluctuations. For instance, the drop in late Sep 2021 for Compound can be linked to the hack on September 29, 2021, which targeted the mathematical logic of its incentive structure. Nonetheless, I will not cover the individual events for each protocol in this thesis.

What must still be discussed, however, are the abnormal values for the Ethereum Foundation. The two CAR values defined by the CET1 and the total capital coincide, and both values rise to 400 in 2023. This is because the denominator of the CAR, the RWA, is very close to zero. As can be seen in [Figure 4.4](#), the total RWA of the Ethereum Foundation remains below \$2,000 during the entire period, and from 2023 the value drops below \$10. The Ethereum Foundation does not use the ERC20 tokens for its operations; instead, it conducts most of its transactions in ETH, the native token of the Ethereum chain. Thus, I could not capture most of the activities in the Ethereum Foundation since I did not include the ETH transfers in my framework. This is one of the limitations of my approach, I elaborate on the limitations of this thesis in [Chapter 5](#).

Another interesting observation from the figures is that there are some time periods where the CAR values remain relatively flat for some protocols. Furthermore, one can see that during these periods, there is no difference between the two CAR values shown in [Figure 4.3](#). These periods indicate when the protocols were holding only USD stablecoins in their treasury. In 2021, when many of these DeFi protocols first began to operate, stakeholders collected initial funding in USD. As the ecosystem of the protocols matured, they started to distribute the funds into the ecosystem by converting the USD stablecoins into governance tokens. This can be observed in [Figure 4.1](#), as the flat periods are mostly located in the first half of 2021.

Due to the difference in the definitions of the two CAR values, there are some protocols such as Yearn Finance that fail to satisfy one of the two requirements. This reflects the financial structure of their treasury. Protocols that fail to satisfy the CET1 condition but not the total capital requirement are those that keep only stablecoins and their governance token in the treasury. In contrast, the protocols that fail to satisfy the total capital requirement while having enough CET1 are those that operate mostly with the ERC20 tokens of other protocols.

The aim of the Basel Framework is to ensure that banks have enough going-concern capital (CET1) to cover the potential losses in a financial crisis while allowing them to incorporate some gone-concern capital for follow-up measures. As mentioned at the beginning of [Section 3.1](#), whether we should regard the cryptoassets as gone-concern capital is quite ambiguous. I believe that examining these protocols that show this discrepancy between the two CAR values could help regulators define the criteria for DeFi protocols.

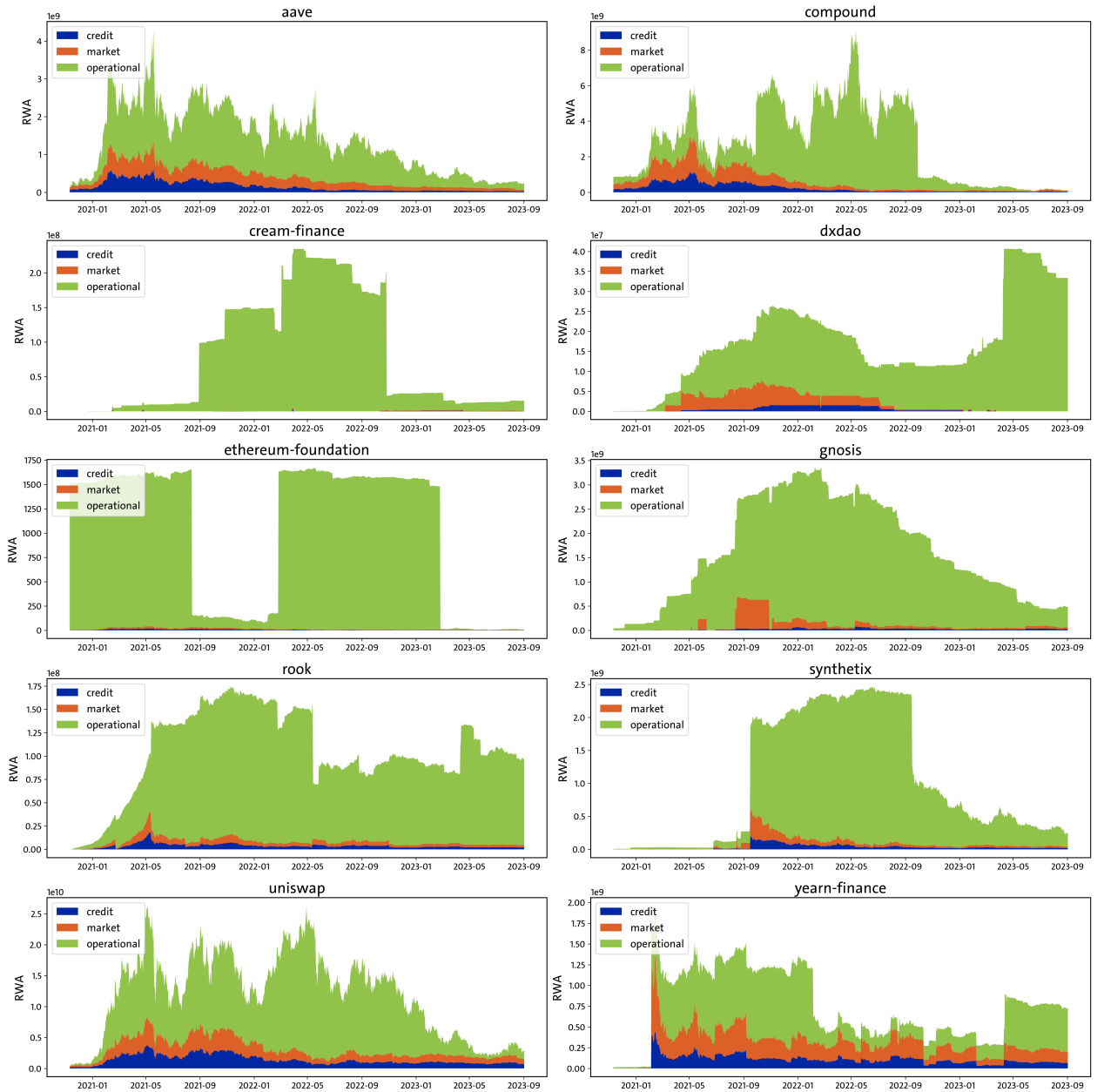


Figure 4.4 – RWA values of 10 protocols

Figure 4.4 illustrates the decomposition of RWA for the 10 protocols, where the blue area denotes the RWA for credit risk, orange area denotes the RWA for market risk, and the green area is for the operational risk. We can see that the RWA for operational risk takes up the largest portion in the RWA. The RWA for market risk is similar to the RWA for credit risk for most protocols due to how I substituted the RWA for CVA with the RWA for counterparty risk in [Subsection 3.1.3](#).

One fact to note from [Figure 4.4](#) is that for most protocols the RWA stays very low at the beginning of 2021, and when it shoots up, the extent of the increase from the credit risk and market risk differs

greatly according to the nature of the protocol. For instance, Gnosis, or more recently known as Safe, aims to develop tools and custodial services to allow users to buy cryptoassets using a credit card; for this purpose Gnosis does not need to keep ERC20 tokens from the other protocols. Whereas the protocols like Yearn Finance should hold the governance tokens from other protocols to obtain better yields from their products. This makes Yearn Finance to have a much larger portion of the RWA for credit risk and market risk compared to Gnosis.

From the following subsections I share the comparison results for when we take the alternative definitions in [Section 3.1](#). For the simplicity of the discussion I share the visualizations only from the protocols that showed a significant difference in the main text, and I share the full visualization of the 10 protocols in the appendix, [Section B.1](#).

#### 4.1.1 RWA for Credit Risk

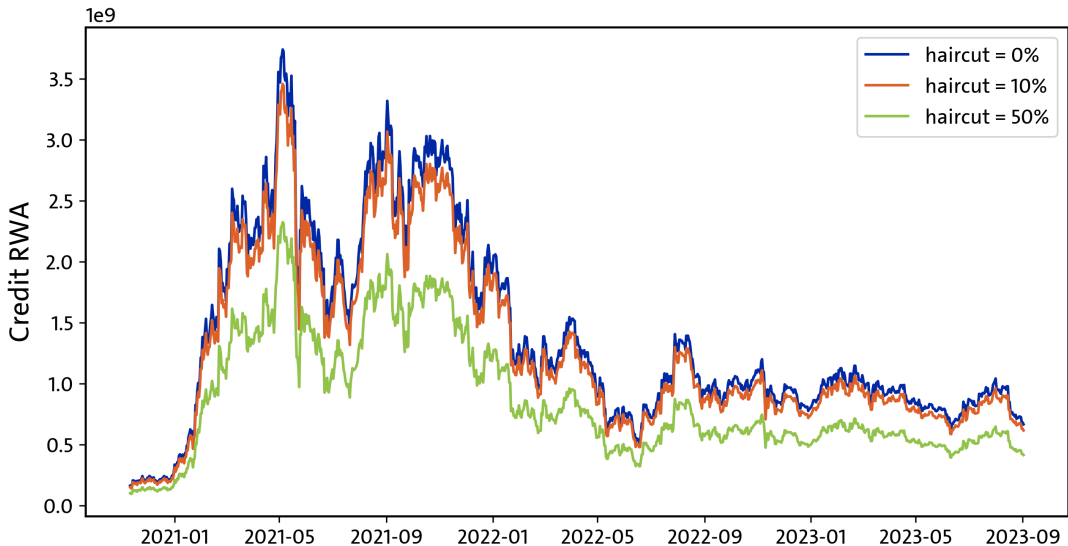


**Figure 4.5** – RWA for credit risk of Uniswap, changing the haircut ratio

[Figure 4.5](#) shows the RWA for credit risk of the protocol Uniswap. The blue line denotes the RWA calculated by the base formula, where we set the value of the haircut as 0% of the net exposure in [Subsection 3.1.2](#). The orange line denotes the RWA for setting the haircut value as 10%, and the green line is for setting it as 50% of the exposure.

The RWA vertically shifts downward as we increase the haircut value for the credit risk. The effect is almost linear to the proportion of the haircut since the coefficient for the first order term in the Taylor expansion of the exponential function in [Equation 3.2](#) is equal to 1.0. Thus allowing the DeFi protocols to have a positive haircut value would decrease the RWA for credit risk proportionately for

all protocols. See [Figure B.2](#) the comparison for all 10 protocols.

#### 4.1.2 RWA for Market Risk

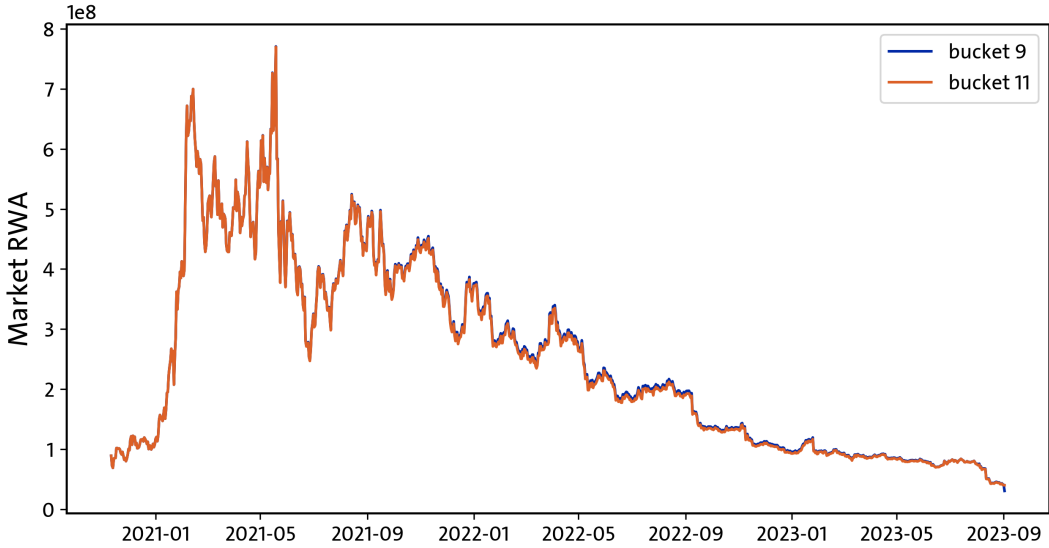


**Figure 4.6** – RWA for market risk of Aave, changing the industry bucket

[Figure 4.6](#) shows the RWA for market risk of the protocol Aave. The blue line denotes the RWA calculated by the base formula, where we set the industry bucket for equity spot rates as bucket 9 in [Subsection 3.1.3](#). The orange line denotes the case when the RWA is calculated by setting the bucket as bucket 11.

The change from bucket 9 to bucket 11 leads to the removal of the correlation parameters in the aggregation. Aave and Synthetix showed the biggest difference among the protocols but as can be seen from the figure, this did not have a significant impact on the RWA for the market risk. This means that there were not many derivative tokens of which the risk factors were highly correlated; I believe that this is because the derivative tokens recognized in my framework are mostly simple wrappers of the underlying token, i.e., have linear claims. Thus this behavior may change as we include more tokens with complicated structures. See [Figure B.3](#) for the full comparison.

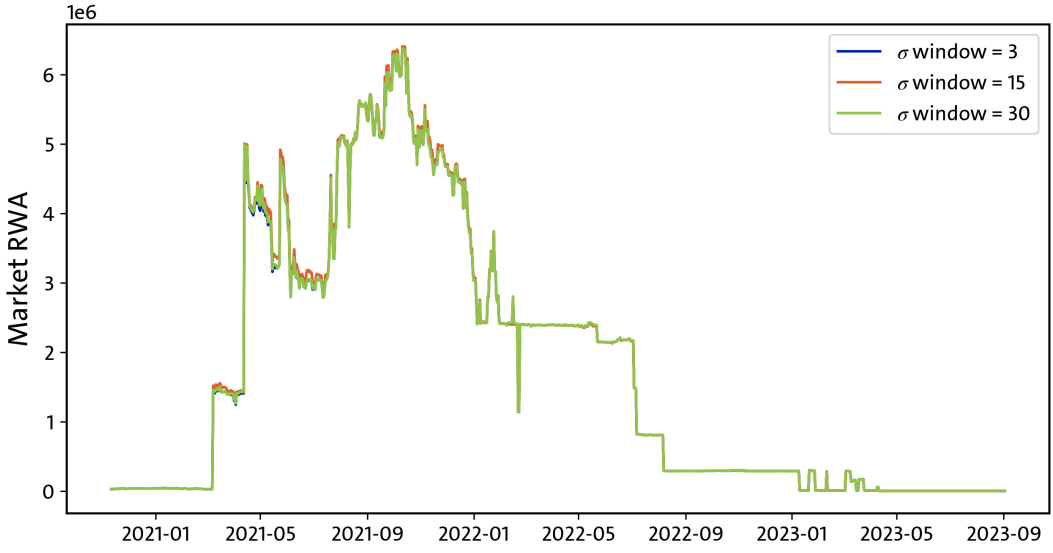


**Figure 4.7 – RWA for market risk of DXdao, changing the window for  $\sigma$**

Figure 4.7 shows the comparison for the market RWA of DXdao, changing the window for estimating  $\sigma$ . The blue line denotes the base case where the window is set to 3 in Subsection 3.1.3, orange denotes the case when the window is 15, and green is the when the window is 30.

There was no significant impact for changing this window for  $\sigma$  for all protocols, see Figure B.4 for the full visualization. I assume that this is because most protocols do not have much exposure to the vega risk factor, which requires the derivatives to have a non-linear payoff function. However we can see that some protocols do have substantial exposures to the delta risk factor in Figure 4.8.

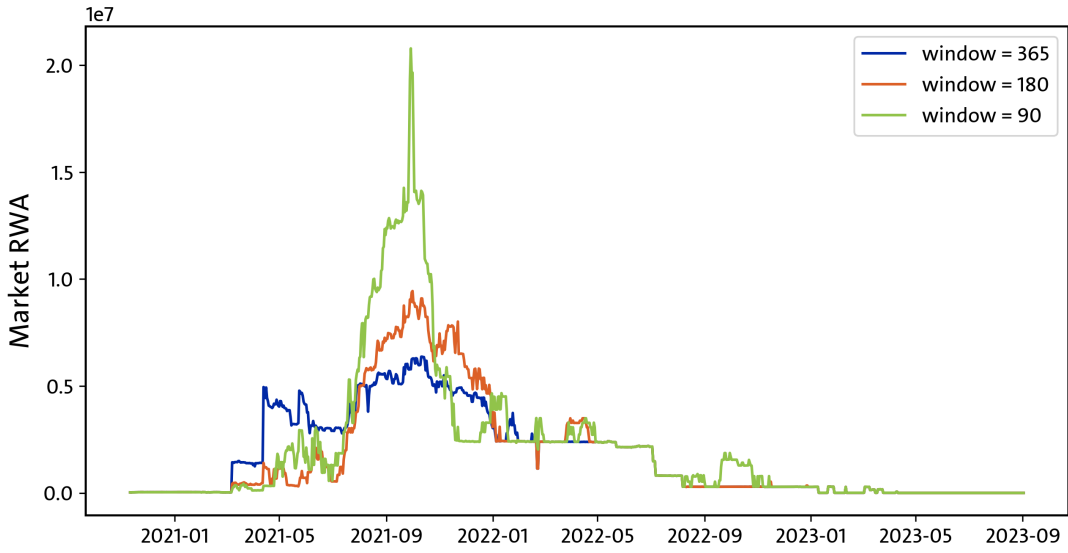


**Figure 4.8** – RWA for market risk of DXdao, changing the window for delta and vega

Figure 4.8 shows the RWA for market risk of DXdao, changing the window for estimating delta and vega. The blue line denotes the market RWA calculated from the base formula where we set the window to 365 days in Subsection 3.1.3. The orange line and the green line denote the RWA calculated by setting the window to 180 and 90 respectively.

Reducing the window size for estimating delta and vega allows the market RWA to change more rapidly, which means that the sensitivities derived from the numerical estimation can vary through time. If the payoff structure of the derivative tokens in our framework actually changed through time then reducing the window would have been preferable, however if not this would mean that the markets of the derivative and underlying lacked liquidity and the error variance of the estimation was high. In this thesis I believe that the payoff structure of the derivative token stayed the same and thus take the latter interpretation of the result. As mentioned in Subsection 3.1.3 this is a limitation that should be remedied by analyzing the smart contracts of the tokens. See Figure B.5 for the full comparison.

### 4.1.3 RWA for Operational Risk

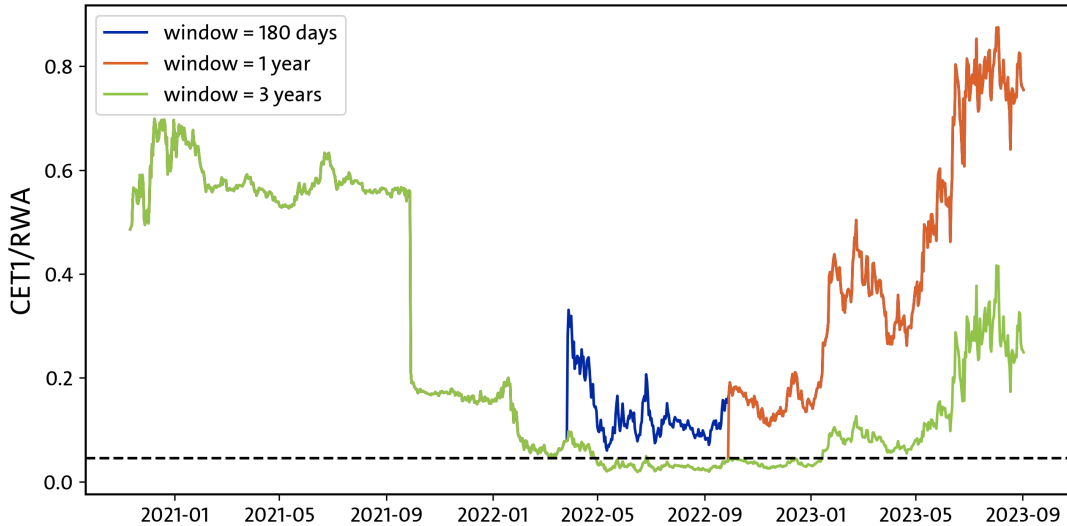


**Figure 4.9** – CET1/RWA of Compound, changing the window for hacks

Figure 4.9 shows the CAR of Compound, changing the window for including hacks in the Internal Loss Multiplier described in Subsection 3.1.4. The orange line here denotes the base case where the window is set to 1 year, blue line and green line denote the ratios for window size of 180 days and 3 years, respectively.

For protocols that experienced loss due to hacks, changing this window size can directly affect the time periods when the protocols do not meet the capital requirement criteria. Figure 4.9 shows that for Compound decreasing the window to 180 days essentially removes the period where it did not meet the capital adequacy requirements, whereas extending the window to 3 years also extended the period by about 3 months.

According to the current Basel Framework the banks that belong to the first BI range do not need to address the Internal Loss Multiplier, thus there is no need to include these events for DeFi protocols. However, if the organizations in the traditional finance would extend their market to the DeFi space and we would need to develop an analogous framework for these entities, I believe that defining this window size would have a significant impact on the intervention. See Figure B.6 for the full visualization.

## 4.2 Risk Spillover Analysis

In this section I share the risk spillover analysis of the CAR using the VAR(1) and TVP-VAR(1) model introduced in [Section 3.3](#). For the analysis and illustrations in this section I use only the base definitions in [Section 3.1](#). I share below some parameters set out in the base definition:

- We use the log-difference of CET1/RWA as the endogenous variables of the VAR model
- The haircut values are set to 0% of the exposure
- We use the bucket 9 for the aggregation in sensitivities-based method of market risk
- Window for  $\sigma$  is set to 3 days, window for delta and vega is 365 days, and the window for hacks is also 365 days

Please refer to the framework definitions in [Section 3.1](#) and the data description in [Subsection 3.3.3](#) for more details on the input data of the analysis.

### 4.2.1 Total Connectivity Index

I first show the sensitivity of the approach to the forecast horizon  $H$  by overlaying the Total Connectedness Index (TCI) computed for different values of  $H$ , from  $H = 5$  to  $H = 10$  in [Figure 4.10](#).

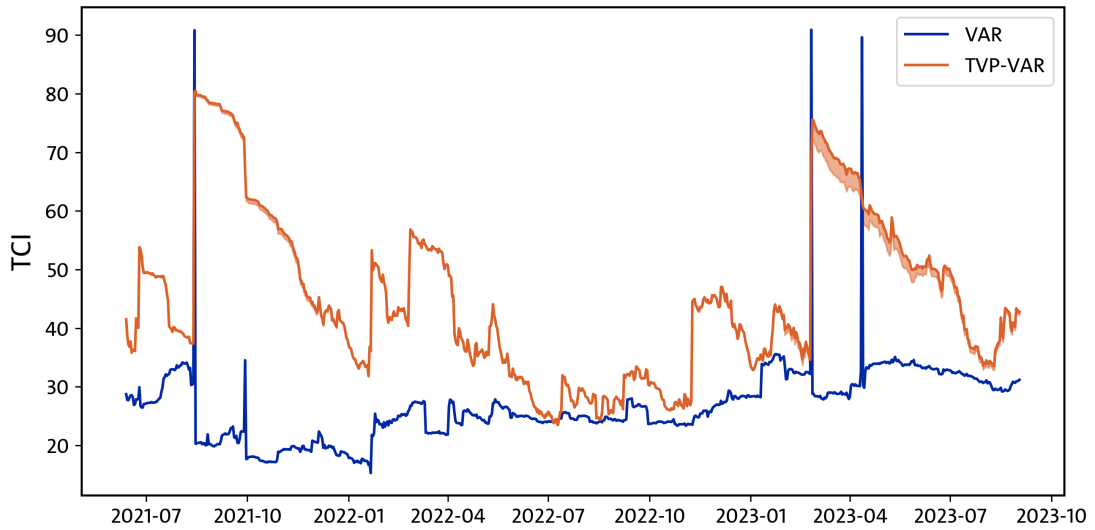


**Figure 4.10** – Overlay of TCI values from  $H = 5$  to  $H = 10$

The blue line in [Figure 4.10](#) denotes the TCI from VAR(1) computed from  $H = 10$ , and the orange line denotes the TCI from TVP-VAR(1) computed from  $H = 10$ . There are also the blue area and

the orange area in the figure that denote the range of minimum and maximum values within the different forecast horizons for the VAR(1) and TVP-VAR(1) respectively, although only a portion of the orange area is visible to the human eyes. The fact that these areas are barely visible indicates that the spillover indices from the models are robust under the different choices of  $H$ .

The three spikes in the TCI of the VAR(1) model shown by the blue line in Figure 4.10 are all connected to the abrupt changes in the CAR of protocols; the first spike at 14 Aug 2021 and the second spike at 25 Feb 2023 both stand for the drops of operational RWA from the Ethereum Foundation. However these events are not really meaningful for describing the DeFi system since as mentioned in the description for Figure 4.3, the RWA of Ethereum Foundation does not include the majority of its operations.

To give a better interpretation of the TCI, we share in Figure 4.11 the TCI values from the VAR(1) and TVP-VAR(1) models fitted from the data of 9 protocols, excluding the Ethereum Foundation. The colored lines denote the same values as Figure 4.10, but for Figure 4.11 there are no colored areas in the figure.

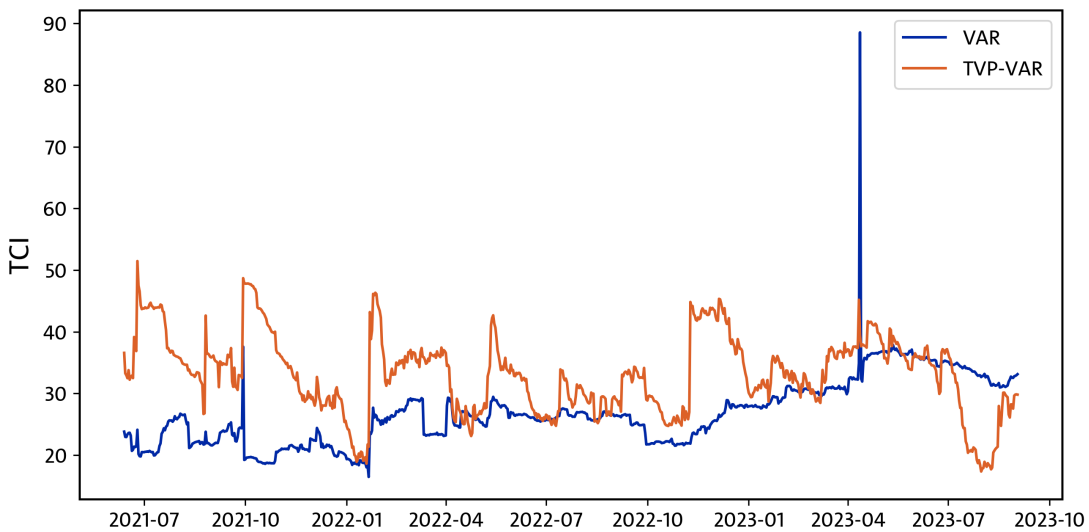


**Figure 4.11** – TCI values from 9 protocols, excluding the Ethereum Foundation

I note that the third spike from Figure 4.10 still remains in Figure 4.11, which represents the “Shanghai” upgrade of the Ethereum chain on 12 Apr 2023. This update allowed the users to withdraw the staked ETH from the chain to receive rewards, and this caused a massive redistribution of wealth in the DeFi ecosystem, which includes the 9 protocols in our analysis.

One interpretation of Figure 4.11 is that the TCI from the VAR(1) model seems to be gradually increasing. This means that the overall system is becoming more and more dependent on each participant, i.e., a financial shock on one protocol is becoming more likely to give an impact to the

other protocols.

Whereas one can see that the TCI from TVP-VAR(1) is rather showing a periodic, sideways movement. Since the variance structure of TVP-VAR varies through time unlike the VAR, a surge in the TCI for TVP-VAR can represent a regime switch; The TCI is expected to gradually flatten out by the Kalman updates unless there comes another shock that cannot be explained according to the current parameters. The small spikes in the TCI seem to repeat every 3 months, meaning that the system tends to switch its regime every quarter. The fact that the TCI has been declining until late Aug 2023 and started to climb up again implies that we will see another regime switch in this system of 9 protocols.

#### 4.2.2 Pairwise Connectivity Index

The Pairwise Connectivity Index (PCI) is defined for each pair of protocols, thus the VAR(1) and TVP-VAR(1) model fitted to 10 protocols each gives us 45 pairs for the PCI values. I will not cover each of these pairs in this thesis, and instead share an example output for the PCI between Uniswap and Compound in [Figure 4.12](#).

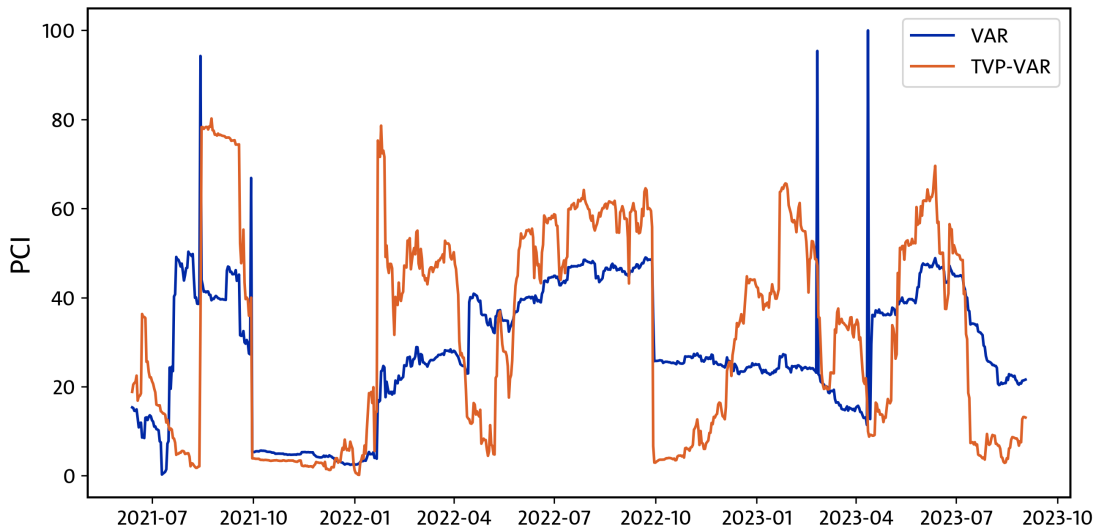


**Figure 4.12** – PCI values between Uniswap and Compound

The blue line in [Figure 4.12](#) denotes the PCI from VAR(1) and the orange line denotes the PCI from TVP-VAR(1). The interpretation for the individual PCI values could be done analogously to the interpretation for TCI as in [Subsection 4.2.1](#); I instead share a brief interpretation on the PCI by sharing the graphs constructed from the average PCI values from the VAR model and the TVP-VAR model in [Figure 4.13](#) and [Figure 4.14](#), respectively.

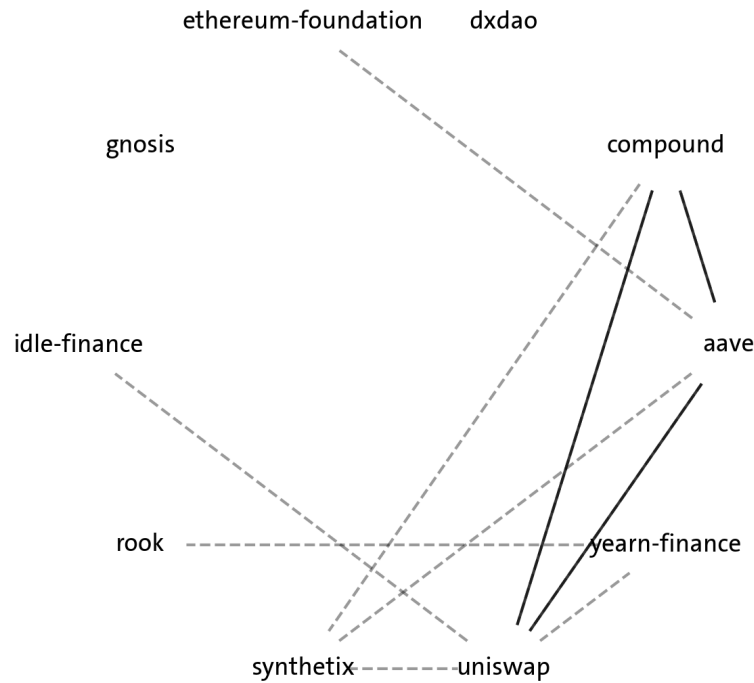


**Figure 4.13** – Graph constructed from the average PCI of the VAR model

Figure 4.13 shows the graph constructed from the average PCI of the VAR(1) model, where a solid line denotes the pair that had the average PCI above 25%, and the dashed line denotes the pair that had the average PCI above 10% but below 25%.

We can see that there is a relatively strong connection between the three biggest protocols within our 10 protocols in terms of TVL, Aave, Uniswap, and Compound. Uniswap has the highest degree in this undirected graph, which means that the activities of Uniswap has impact to the largest number of protocols within the system.

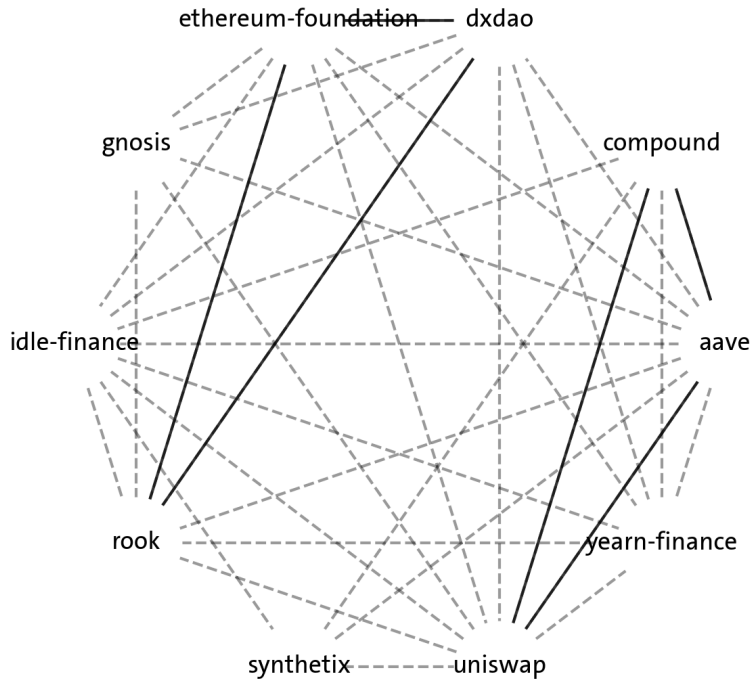


**Figure 4.14** – Graph constructed from the average PCI of the TVP-VAR model

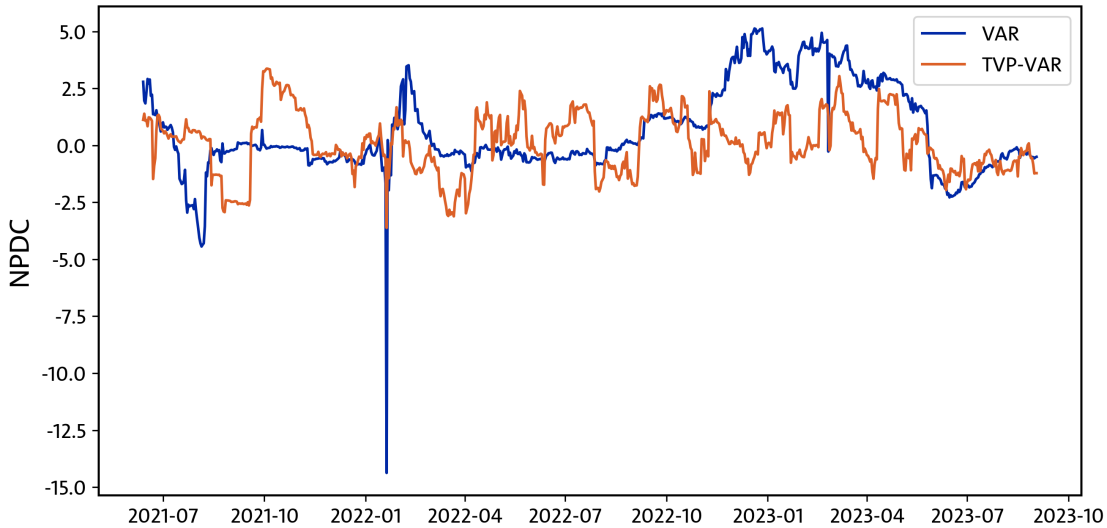
Figure 4.14 shows the graph constructed from the average PCI of the TVP-VAR(1) model, where the solid lines and the dashed lines have the same meanings as in Figure 4.13. We can see more edges compared to the graph constructed from the VAR model, due to that the TVP-VAR model can express a wider variety of relationships between the protocols.

We can find that again the triangle between the 3 protocols, Aave, Uniswap and Compound, but now also a connection between Ethereum Foundation, DXdao and Rook. The second connection comes from the movements of the RWA during the Shanghai upgrade; both DXdao and Rook had a spike in the RWA for operational risk around the upgrade, and the Ethereum Foundation had a slight movement as well. However, as we discussed in Section 4.1 the values for the Ethereum Foundation do not reflect its activities correctly, I believe that this connection is superfluous.

Both Uniswap and Aave have the highest possible degree in Figure 4.14, meaning that the activities of the two protocols gave significant impact to the other protocols in most of the regimes.

### 4.2.3 Net Pairwise Directional Connectedness

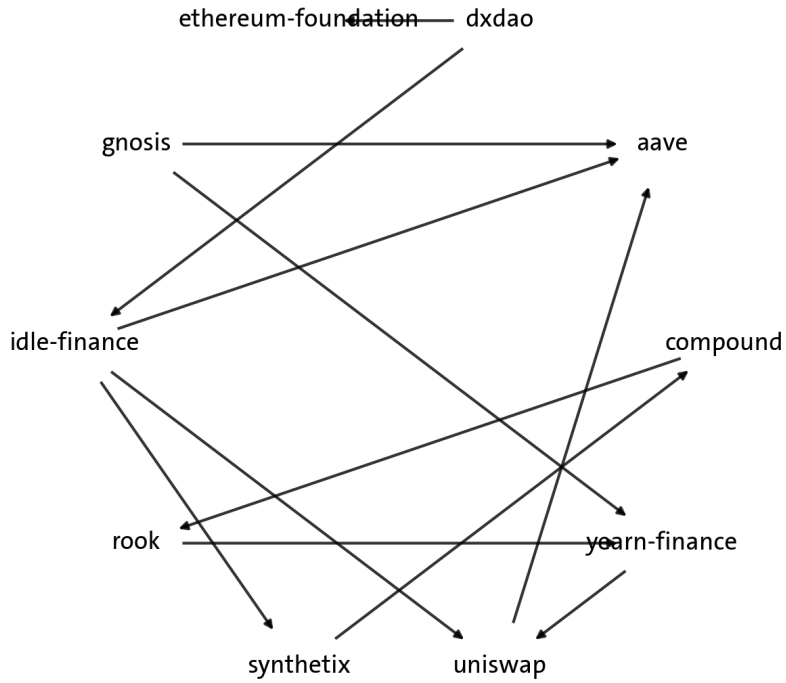
The Net Pairwise Directional Connectedness (NPDC) is also defined for each pair of protocols, the two models give us a total of 45 values of NPDC each. Thus again I just share a single example for the NPDC from the connection from Uniswap to Aave in [Figure 4.15](#).



**Figure 4.15 –** NPDC values from Uniswap to Aave

The blue line in [Figure 4.15](#) denotes the NPDC from VAR(1) and the orange line denotes the NPDC from TVP-VAR(1) model. Note that the values for the NPDC can be negative, having a positive value of NPDC from protocol A to B means that the shock in A affects B, whereas the negative value means the opposite. Thus for Uniswap and Aave shown in [Figure 4.15](#), we can interpret that the shock transmission in general goes from Uniswap towards Aave.

I again share some interpretations on the NPDC by the graph constructed from the average NPDC values from the two models in [Figure 4.16](#) and [Figure 4.17](#).



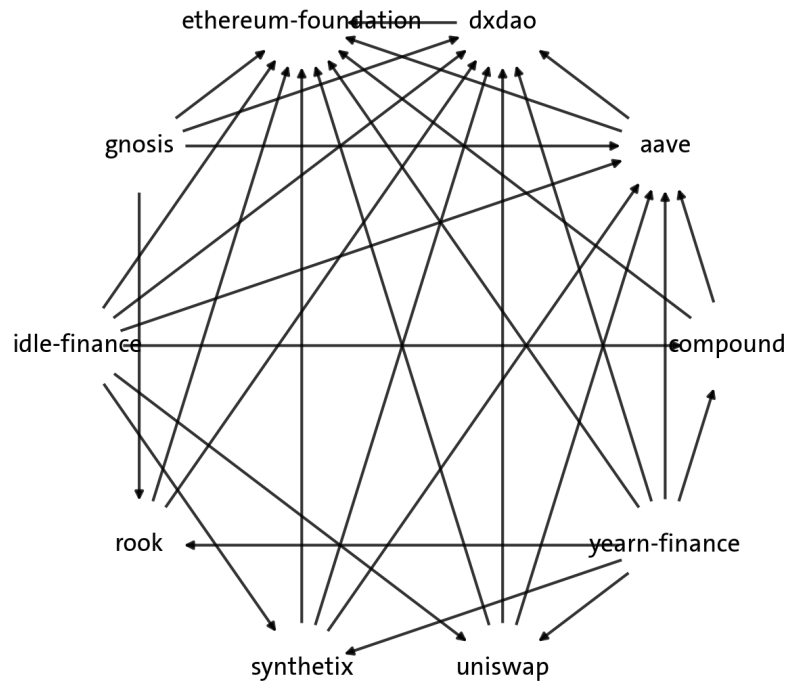
**Figure 4.16** – Graph constructed from the average NPDC of the VAR model

Figure 4.16 shows the graph constructed from the average NPDC of the VAR(1) model, the solid lines denote the pairs where the average value of NPDC was at least as high as 25% of the pair that had the maximum NPDC. The arrows denote the direction of the spillover effect captured by the NPDC, i.e., the arrow from protocol A to B denotes that the shock in A causes the shock in B more often than in the opposite direction.

However, unlike the TCI and PCI that can only have positive values, small NPDC values do not indicate a lack of connection. For instance, if the two protocols were to send signals back and forth in an alternating sequence then the average value of NPDC will be close to zero. Thus the arrows in Figure 4.16 just indicate the connections that we know the direction with certainty.

One interesting feature in Figure 4.16 is that there are only two protocols that cannot traverse the graph from, to arrive at the Uniswap node: the Ethereum Foundation and Aave. Most of the protocols have a clear channel for the transmission of shocks towards Uniswap, whereas there is none

for the two protocols. Again this does not mean that the two protocols are not correlated with the activities of Uniswap; as we discussed using the graphs constructed from the PCI shown in [Figure 4.13](#) and [Figure 4.14](#), Aave is strongly correlated with Uniswap in our data. What we can still deduce however is that the two protocols are always lagging behind the other protocols, this behavior is better illustrated in [Figure 4.17](#).



**Figure 4.17** – Graph constructed from the average NPDC of the TVP-VAR model

[Figure 4.17](#) shows the graph constructed from the average NPDC of the TVP-VAR(1) model, the solid lines denote the 25% of the maximum value. Again we see more edges in the TVP-VAR model, since the NPDC are prone to change signs more often due to the time-varying parameters.

Continuing the discussion on Aave and Ethereum Foundation, we can also see from [Figure 4.17](#) that they act as sink nodes in the system. I believe that this is because both the Ethereum Foundation and Aave put emphasis on the technical and financial security of their operations, they undergo very thorough discussions in their governance forums. The whole process of making a proposal, voting,

and redeploying the contracts for these protocols can often take more than a month. Thus they often take the role of a follower rather than the leader in the market.

In contrast, the yield aggregators like Yearn Finance and Idle Finance act as source nodes in [Figure 4.17](#). The yield aggregators actively utilize the ERC20 tokens of other protocols and build risky assets; they are exposed to a wider variety of risk factors, and thus could become the active carrier of the systematic risk if not managed properly.

# Chapter 5

## Discussions and Limitations

A criticism that can be applied to this thesis as a whole is that many critical definitions and parameters in the Basel Framework were chosen arbitrarily. For instance, the risk weights in [Subsection 3.1.2](#) and [Subsection 3.1.3](#) would need to be recalibrated if this framework were to actually be used for supervision. The industry buckets in [Subsection 3.1.3](#) would also need to be redefined, or even worse, the asset categorizations in [Table 3.2](#) might need to be reorganized to separate them from the traditional asset buckets. Although I made these arbitrary decisions to deduce the capital adequacy ratios from the framework, I believe that in reality the regulators would need to redefine many of the terminologies I have applied to the DeFi protocols.

The collected data for transfers and prices had many flaws; a generic criticism for the data is that the number of protocols and tokens are too small to represent the activities in DeFi. There are more than 17,000 DeFi protocols<sup>1</sup> and 450,000 ERC20 tokens deployed on the Ethereum chain<sup>2</sup> at the time of writing this thesis; although the number of addresses and tokens classified by the external data sources would increase through time, we may need to develop an automated, systematic way to capture the recent activities from the new protocols.

Regarding the ERC20 tokens, I failed to address the sensitivities-based method for market risk due to the lack of information on the payoff formula of the derivative tokens. For the token contracts where the underlying and the source code are known, theoretically we can derive the payoff formula by making assumptions on the value process (Heimbach et al. 2022). Although it may be difficult to derive the exact formula for each token, we would need to at least develop an approximation scheme that allows us to compute the curvature risks.

The data of ERC20 transfers between protocols do not include the native token of Ethereum, which can play a crucial role in describing the activities of the protocols. As we can see from the results in [Chapter 4](#), the data failed to capture the operations of the Ethereum Foundation and further introduced additional noise to the quantitative analysis in [Section 4.2](#). This limitation should be

---

<sup>1</sup><https://metamask.io/institutions/>

<sup>2</sup><https://bitpay.com/blog/erc-20-tokens-what-they-are-and-how-they-are-used/>

---

handled by including the ETH transfers and the gas fees into the data, such that we can also track the balance of ETH for each protocol.

Furthermore, calculating the balance from the cumulative sum of token transfers led to negative balance for certain types of tokens, e.g., the interest bearing token. I tried to mitigate this issue by resetting the balance of the token to zero whenever the balance becomes negative, which could introduce a bias to the final balance. The proper fix for this problem would be to call the `balanceOf()` method of the ERC20 tokens for each block; this means that we would need to interact directly with the chain by running a blockchain node, which would allow us to collect a wider variety of assets including the NFTs or the Soulbound tokens.

For the price data, there were some entries missing from the DeFiLlama API. For now I do not know whether this is because there were actually no activities on the market around the timestamp or the DeFiLlama API temporarily could not return the correct prices due to technical errors. To increase the resolution of the price data, we may want to incorporate other sources for the price data such as the price oracles, or develop our own software for the discovery of prices.

The quantitative analysis using the VAR model lacks support from the data. The Bayesian Information Criterion (BIC) suggests that the true model family might not come from the linear VAR models, thus we may want to introduce non-linear features such as the frequency components of the data into the model, as in Baruniék and Křehlić (2018). Moreover, we could have included more protocols into the analysis by taking sparse estimations of the VAR model, by introducing regularization terms or Bayesian priors. I leave these potential improvements for the quantitative modelling as a future work.

# Chapter 6

## Conclusion

In this thesis, I first introduced the relevant standards and definitions from the Basel Framework to define the Capital Adequacy Ratio (CAR) of DeFi protocols. The discussions on the framework showed that there are many concepts from the framework that could be directly applied to the DeFi applications, whereas there are also new components from the DeFi protocols which required modifications.

Then I shared our implementation for the data collection and the calculation of the ratios. I found that certain features that I neglected in the data collection process could be crucial to the description of the activities in DeFi. If in the future the regulators were to develop a similar service, I hope that they would consider these shortcomings in their implementations.

Finally, I provided a quantitative analysis to illustrate an application of the CAR data. The spillover indices could highlight some of the significant events in the DeFi domain, and also visualize the movement of assets between the individual protocols. Simple graph analysis on the graphs constructed from the connectedness indices could depict the risk-profile of each protocol, e.g., which other protocol it is mostly related to, and whether it gives or receives the risk to the whole system.

This thesis, to the best of my knowledge, is the first to apply the Basel Framework to DeFi protocols. I hope that this finds use for the regulators who would need to create an analogous framework for the DeFi entities, and also for the future researchers of financial risk who would want to apply a more traditional framework to analyze the novel phenomena currently occurring in the DeFi landscape.

# Appendices

# Appendix A

## Additional Tables

### A.1 Data Summary

[Table A.1](#) shows the summary of the collected ERC20 token transfer data for 33 protocols, the protocols that had a specified address or a set of addresses for the treasury. The column “Treasuries” denotes the number of treasury addresses, “Addresses” denotes the number of known addresses for the protocol including the treasury, “Transfers” denotes the number of collected transfers, and the “First Date” and “Last Date” shows the time range of the token transfers. The dates in [Table A.1](#) are presented in the UTC timezone.

| Protocol              | Treasuries | Addresses | Transfers | First Date  | Last Date   |
|-----------------------|------------|-----------|-----------|-------------|-------------|
| 1inch Network         | 1          | 19        | 4,902     | 23 Aug 2020 | 01 Sep 2023 |
| Aave                  | 4          | 73        | 667,757   | 25 Jan 2020 | 02 Sep 2023 |
| Abracadabra           | 1          | 17        | 235       | 12 Jun 2021 | 12 Jul 2023 |
| Alchemix              | 1          | 24        | 1,450     | 28 Feb 2021 | 29 Aug 2023 |
| Balancer              | 1          | 611       | 2,506     | 16 Jun 2020 | 01 Sep 2023 |
| BitDAO                | 1          | 10        | 52        | 16 Jun 2021 | 11 Aug 2023 |
| Compound              | 2          | 39        | 342,663   | 05 Aug 2019 | 01 Sep 2023 |
| Convex Finance        | 1          | 17        | 33,519    | 06 Dec 2021 | 02 Sep 2023 |
| Cream Finance         | 1          | 37        | 603       | 06 Oct 2020 | 20 Aug 2023 |
| DXdao                 | 1          | 4         | 1,145     | 01 Jul 2019 | 11 Apr 2023 |
| dYdX                  | 1          | 12        | 12        | 10 Sep 2021 | 11 Jul 2023 |
| Ethereum Foundation   | 1          | 2         | 32        | 13 Aug 2019 | 03 May 2022 |
| Ethereum Name Service | 2          | 17        | 21        | 29 Nov 2021 | 31 Jul 2023 |
| Gearbox Protocol      | 1          | 5         | 1,553     | 15 Dec 2021 | 28 Aug 2023 |
| Gitcoin               | 2          | 121       | 66        | 08 Aug 2019 | 15 Jul 2023 |
| Gnosis                | 4          | 18        | 3,187     | 16 Jun 2020 | 31 Aug 2023 |
| Idle Finance          | 6          | 42        | 26,992    | 06 Aug 2020 | 01 Sep 2023 |
| Index Cooperative     | 1          | 20        | 44        | 11 May 2021 | 26 Aug 2023 |
| Inverse Finance       | 2          | 19        | 2,882     | 09 Feb 2021 | 01 Sep 2023 |
| Lido                  | 1          | 56        | 597       | 18 Dec 2020 | 01 Sep 2023 |
| Liquity               | 2          | 10        | 257       | 16 Mar 2021 | 11 Aug 2023 |
| Maker                 | 1          | 26        | 274       | 15 Feb 2021 | 01 Sep 2023 |
| Metronome             | 2          | 5         | 11        | 18 Aug 2022 | 16 Aug 2023 |
| mStable               | 1          | 55        | 11,570    | 15 Jun 2020 | 15 May 2023 |
| Olympus DAO           | 2          | 12        | 9,793     | 29 May 2021 | 23 Aug 2023 |
| ParaSwap              | 6          | 8         | 36        | 07 May 2021 | 22 Nov 2021 |
| Ribbon Finance        | 1          | 13        | 1,234     | 03 Sep 2021 | 28 Aug 2023 |
| Rook                  | 1          | 1         | 24,413    | 09 Nov 2020 | 31 Aug 2023 |
| ShapeShift            | 1          | 2         | 1,296     | 22 Jun 2021 | 01 Sep 2023 |
| SushiSwap             | 1          | 2,276     | 223,172   | 29 Sep 2020 | 02 Sep 2023 |
| Synthetix             | 1          | 21        | 651       | 05 Jan 2020 | 01 Sep 2023 |
| Uniswap               | 3          | 8,895     | 1,215     | 15 Jun 2020 | 31 Aug 2023 |
| Yearn Finance         | 2          | 162       | 19,181    | 06 Aug 2020 | 01 Sep 2023 |

**Table A.1** – Summary of the collected transfers for 33 protocols

Table A.2 shows the summary of the CAR data computed for 33 protocols, again the protocols that

had a specified address or a set of addresses for the treasury. “Count” denotes the number of entries for the CAR of each protocol, “Min” and “Max” are the minimum and maximum values of the CAR, and the “First Date” and “Last Date” shows the time range of the computed CAR data. The values in “Min” and “Max” have been rounded to the second decimal, and INF denotes an infinite value derived from division by zero. The dates in [Table A.2](#) are in the UTC timezone.

| Protocol              | Count | Min  | Max    | First Date  | Last Date   |
|-----------------------|-------|------|--------|-------------|-------------|
| 1inch Network         | 659   | 0.64 | 6.77   | 15 Nov 2021 | 02 Sep 2023 |
| Aave                  | 1319  | 0.00 | 1.22   | 25 Jan 2020 | 02 Sep 2023 |
| Abracadabra           | 815   | 0.13 | 0.90   | 12 Jun 2021 | 02 Sep 2023 |
| Alchemix              | 919   | 0.00 | 1.23   | 28 Feb 2021 | 02 Sep 2023 |
| Balancer              | 637   | 0.09 | 0.40   | 07 Dec 2021 | 02 Sep 2023 |
| BitDAO                | 811   | 0.07 | 1.95   | 16 Jun 2021 | 02 Sep 2023 |
| Compound              | 1492  | 0.00 | 1.04   | 05 Aug 2019 | 02 Sep 2023 |
| Convex Finance        | 638   | 0.00 | 0.35   | 06 Dec 2021 | 02 Sep 2023 |
| Cream Finance         | 1064  | 0.00 | 1.19   | 06 Oct 2020 | 02 Sep 2023 |
| DXdao                 | 1527  | 0.00 | 0.69   | 01 Jul 2019 | 02 Sep 2023 |
| dYdX                  | 725   | 0.03 | 0.74   | 10 Sep 2021 | 02 Sep 2023 |
| Ethereum Foundation   | 1143  | 0.61 | 461.92 | 19 Jul 2020 | 02 Sep 2023 |
| Ethereum Name Service | 645   | 0.11 | INF    | 29 Nov 2021 | 02 Sep 2023 |
| Gearbox Protocol      | 621   | 0.00 | 0.66   | 23 Dec 2021 | 02 Sep 2023 |
| Gitcoin               | 378   | 0.42 | INF    | 23 Aug 2022 | 02 Sep 2023 |
| Gnosis                | 1176  | 0.00 | 0.67   | 16 Jun 2020 | 02 Sep 2023 |
| Idle Finance          | 1013  | 0.02 | 1.00   | 26 Nov 2020 | 02 Sep 2023 |
| Index Cooperative     | 310   | 0.00 | 12.32  | 23 May 2021 | 28 Mar 2022 |
| Inverse Finance       | 938   | 0.00 | 1.23   | 09 Feb 2021 | 02 Sep 2023 |
| Lido                  | 992   | 0.00 | INF    | 17 Dec 2020 | 02 Sep 2023 |
| Liquity               | 903   | 0.00 | 5.02   | 16 Mar 2021 | 02 Sep 2023 |
| Maker                 | 932   | 0.00 | 0.97   | 15 Feb 2021 | 02 Sep 2023 |
| Metronome             | 383   | 0.00 | 14.27  | 18 Aug 2022 | 02 Sep 2023 |
| mStable               | 903   | 0.00 | 0.67   | 16 Mar 2021 | 02 Sep 2023 |
| Olympus DAO           | 829   | 0.00 | 0.67   | 29 May 2021 | 02 Sep 2023 |
| ParaSwap              | 1     | 0.00 | 0.00   | 22 Nov 2021 | 22 Nov 2021 |
| Ribbon Finance        | 732   | 0.00 | 2.48   | 03 Sep 2021 | 02 Sep 2023 |
| Rook                  | 1028  | 0.00 | 2.98   | 11 Nov 2020 | 02 Sep 2023 |
| ShapeShift            | 805   | 0.01 | 0.67   | 22 Jun 2021 | 02 Sep 2023 |
| SushiSwap             | 1018  | 0.02 | 0.40   | 21 Nov 2020 | 02 Sep 2023 |
| Synthetix             | 1339  | 0.00 | 0.67   | 05 Jan 2020 | 02 Sep 2023 |
| Uniswap               | 1083  | 0.07 | 1.23   | 17 Sep 2020 | 02 Sep 2023 |
| Yearn Finance         | 1125  | 0.00 | 0.89   | 06 Aug 2020 | 02 Sep 2023 |

**Table A.2** – Summary of the CAR data for 33 protocols

## A.2 Statistical Tests

**Table A.3** shows the ADF test statistics after taking the log-difference on the CAR data. The values in the table are rounded to the first decimal. We can see that all of the ADF statistics are significantly smaller than zero.

| Lag Order $p$       | 1     | 2     | 3     | 4     | 5     | 6     | 7     | 8     | 9     | 10    |
|---------------------|-------|-------|-------|-------|-------|-------|-------|-------|-------|-------|
| Aave                | -25.2 | -18.3 | -17.0 | -15.0 | -12.4 | -11.4 | -11.6 | -11.7 | -10.8 | -10.5 |
| Compound            | -22.8 | -18.9 | -16.2 | -14.2 | -12.4 | -11.4 | -10.1 | -9.7  | -9.7  | -9.6  |
| Cream Finance       | -22.5 | -18.6 | -16.1 | -15.1 | -15.3 | -13.8 | -14.0 | -12.8 | -12.0 | -11.3 |
| DXdao               | -22.5 | -18.1 | -15.4 | -18.7 | -16.0 | -14.3 | -14.9 | -13.1 | -13.1 | -12.2 |
| Ethereum Foundation | -22.7 | -18.8 | -16.1 | -14.2 | -13.0 | -11.8 | -11.1 | -10.5 | -9.8  | -9.5  |
| Gnosis              | -24.3 | -23.0 | -18.4 | -16.3 | -15.1 | -13.2 | -12.1 | -11.3 | -10.6 | -9.9  |
| Rook                | -31.1 | -24.3 | -19.7 | -17.6 | -14.9 | -14.9 | -14.9 | -14.4 | -13.7 | -12.9 |
| Synthetix           | -23.0 | -18.7 | -16.6 | -14.9 | -13.7 | -12.6 | -14.1 | -14.3 | -12.6 | -11.8 |
| Uniswap             | -24.7 | -18.7 | -17.7 | -16.3 | -13.6 | -13.2 | -12.5 | -11.6 | -11.0 | -10.7 |
| Yearn Finance       | -23.6 | -19.2 | -16.9 | -14.8 | -14.2 | -13.0 | -12.2 | -11.4 | -10.9 | -10.3 |

**Table A.3** – Test statistics for the ADF test after log-difference

**Table A.4** and **Table A.5** shows the p-values for the Granger Casuality test conducted on each pair of protocols. Each entry denotes the p-value for test checking whether the protocol in the column index (x-axis) causes the protocol in the row index (y-axis). The values in the table have been rounded to four decimal places.

|                            | Aave   | Compound | Cream Finance | DXdao  | Ethereum Foundation |
|----------------------------|--------|----------|---------------|--------|---------------------|
| <b>Aave</b>                | 1.0000 | 0.0000   | 0.2316        | 0.5463 | 0.0688              |
| <b>Compound</b>            | 0.0833 | 1.0000   | 0.0503        | 0.8319 | 0.3702              |
| <b>Cream Finance</b>       | 0.2333 | 0.3409   | 1.0000        | 0.9158 | 0.0003              |
| <b>DXdao</b>               | 0.6026 | 0.8595   | 0.8334        | 1.0000 | 0.9535              |
| <b>Ethereum Foundation</b> | 0.2269 | 0.2131   | 0.4563        | 0.8702 | 1.0000              |
| <b>Gnosis</b>              | 0.5957 | 0.5494   | 0.7432        | 0.0007 | 0.9841              |
| <b>Rook</b>                | 0.7738 | 0.8776   | 0.2151        | 0.4676 | 0.9557              |
| <b>Synthetix</b>           | 0.5496 | 0.8743   | 0.0000        | 0.9715 | 0.7192              |
| <b>Uniswap</b>             | 0.0000 | 0.0069   | 0.2457        | 0.5839 | 0.0029              |
| <b>Yearn Finance</b>       | 0.4447 | 0.5504   | 0.3227        | 0.1255 | 0.4813              |

Table A.4 – p-values for the Granger Causality test - first 5 protocols

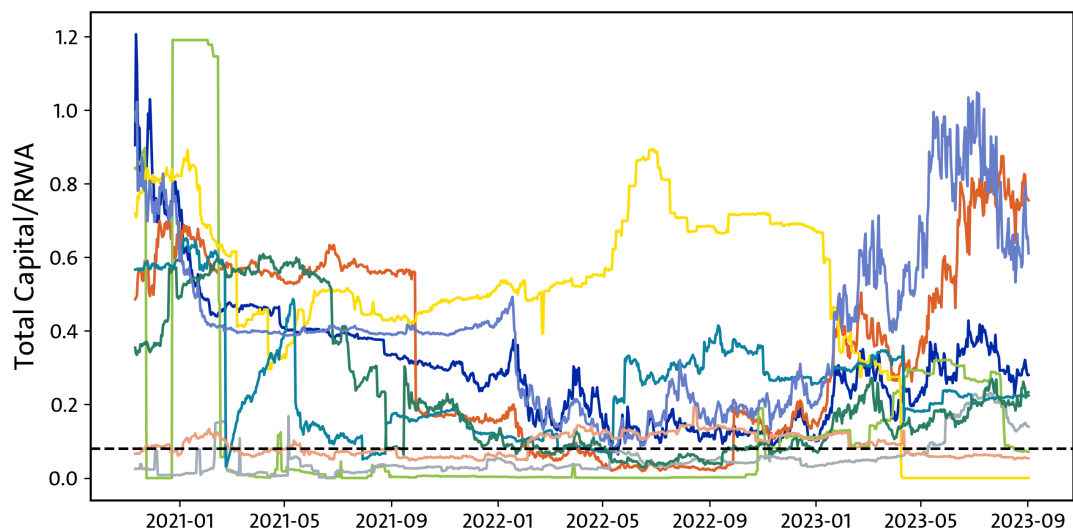
|                            | Gnosis | Rook   | Synthetix | Uniswap | Yearn Finance |
|----------------------------|--------|--------|-----------|---------|---------------|
| <b>Aave</b>                | 0.3577 | 0.8769 | 0.4580    | 0.0032  | 0.0768        |
| <b>Compound</b>            | 0.2214 | 0.7616 | 0.8413    | 0.0181  | 0.2048        |
| <b>Cream Finance</b>       | 0.6235 | 0.8619 | 0.0000    | 0.2165  | 0.8262        |
| <b>DXdao</b>               | 0.0002 | 0.6960 | 0.9951    | 0.5320  | 0.0338        |
| <b>Ethereum Foundation</b> | 0.9309 | 0.9050 | 0.9392    | 0.0085  | 0.5717        |
| <b>Gnosis</b>              | 1.0000 | 0.0334 | 0.8842    | 0.9181  | 0.0472        |
| <b>Rook</b>                | 0.0000 | 1.0000 | 0.2411    | 0.9824  | 0.1127        |
| <b>Synthetix</b>           | 0.9651 | 0.8942 | 1.0000    | 0.8052  | 0.3847        |
| <b>Uniswap</b>             | 0.8509 | 0.8278 | 0.4111    | 1.0000  | 0.1097        |
| <b>Yearn Finance</b>       | 0.4202 | 0.0014 | 0.5425    | 0.3593  | 1.0000        |

Table A.5 – p-values for the Granger Causality test - last 5 protocols

## Appendix B

### Additional Figures

#### B.1 Capital Adequacy Ratios



**Figure B.1** – Total capital/RWA of 9 protocols excluding Ethereum Foundation

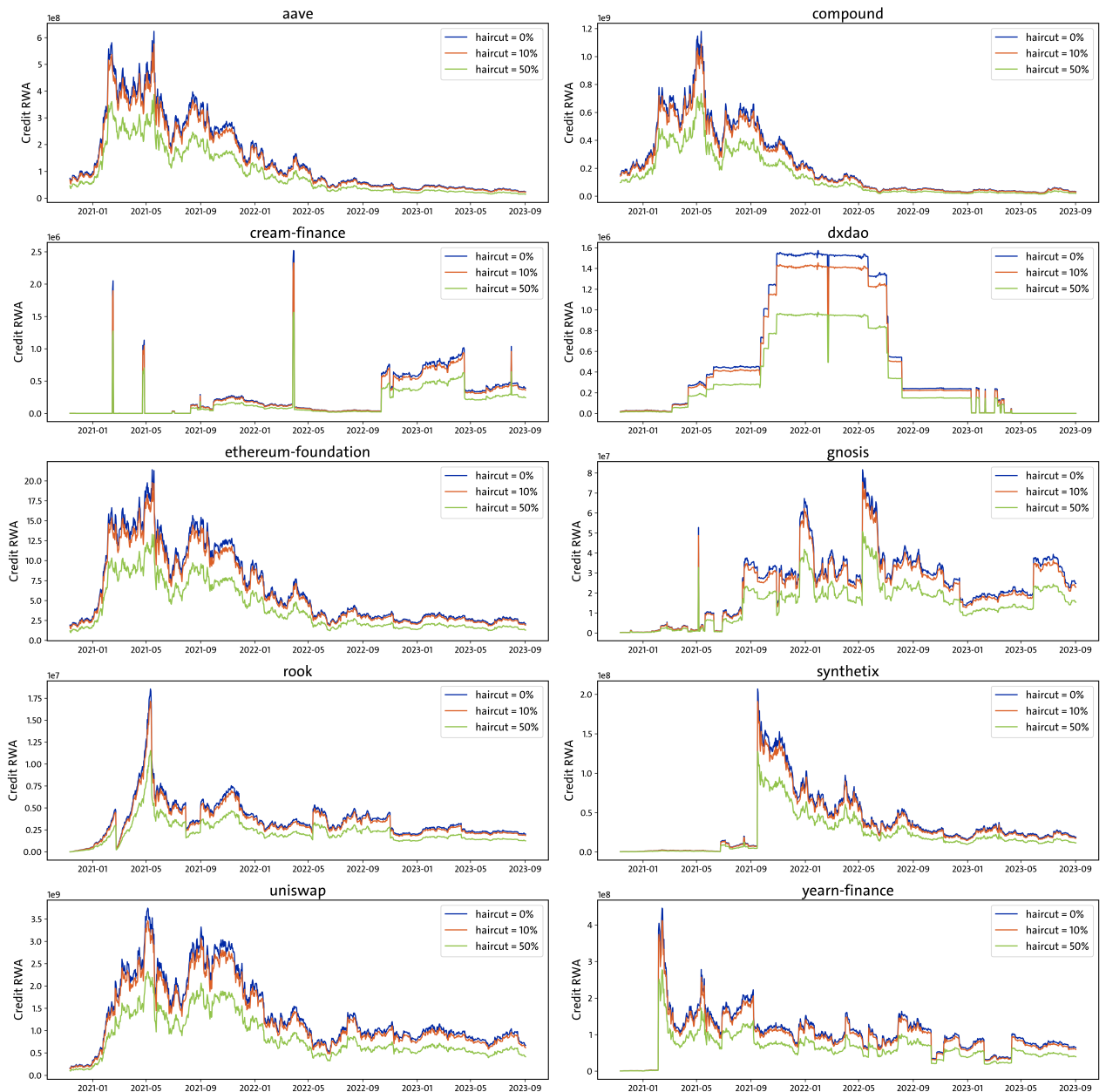


Figure B.2 – RWA for credit risk, changing the haircut ratio

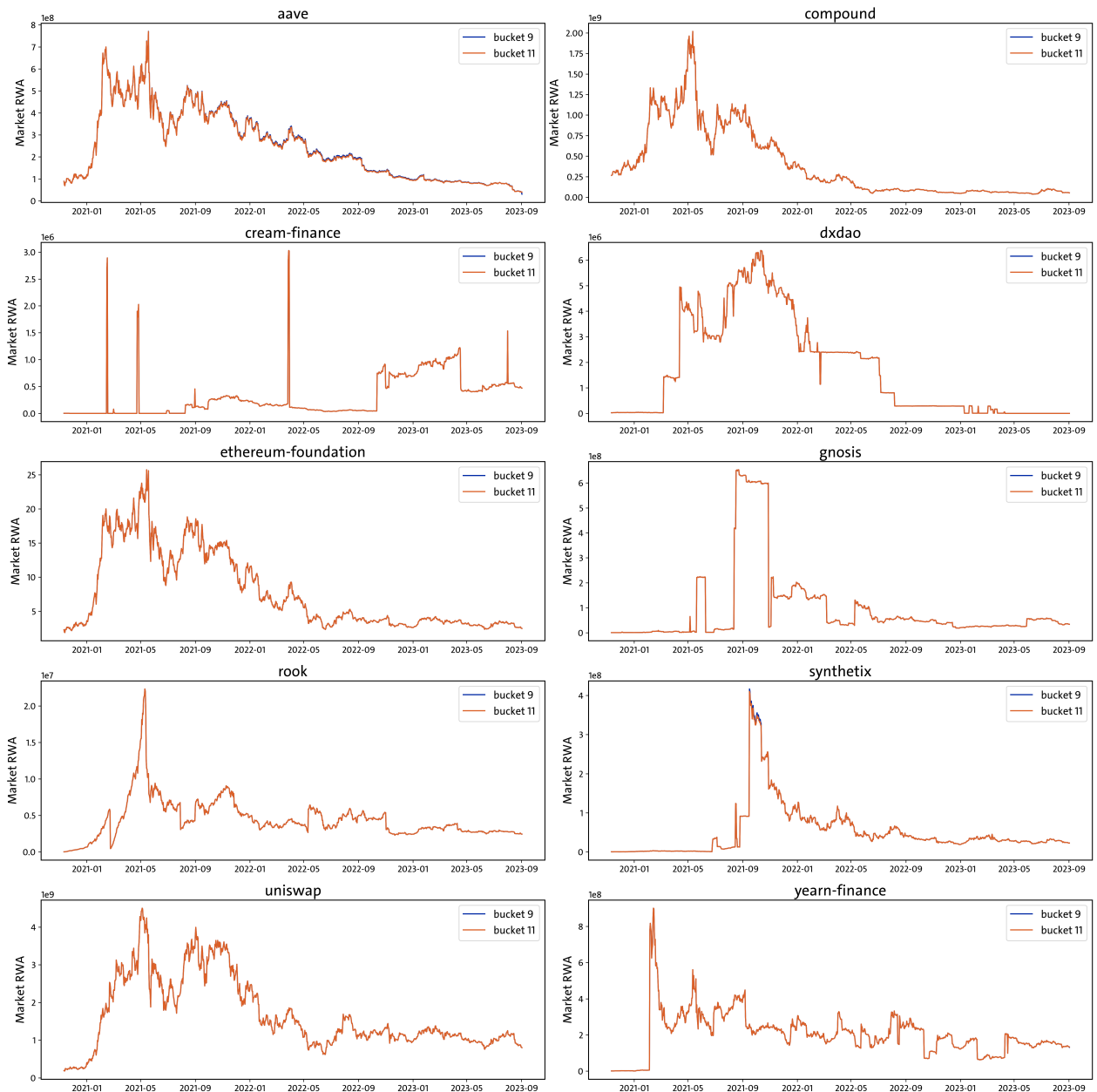
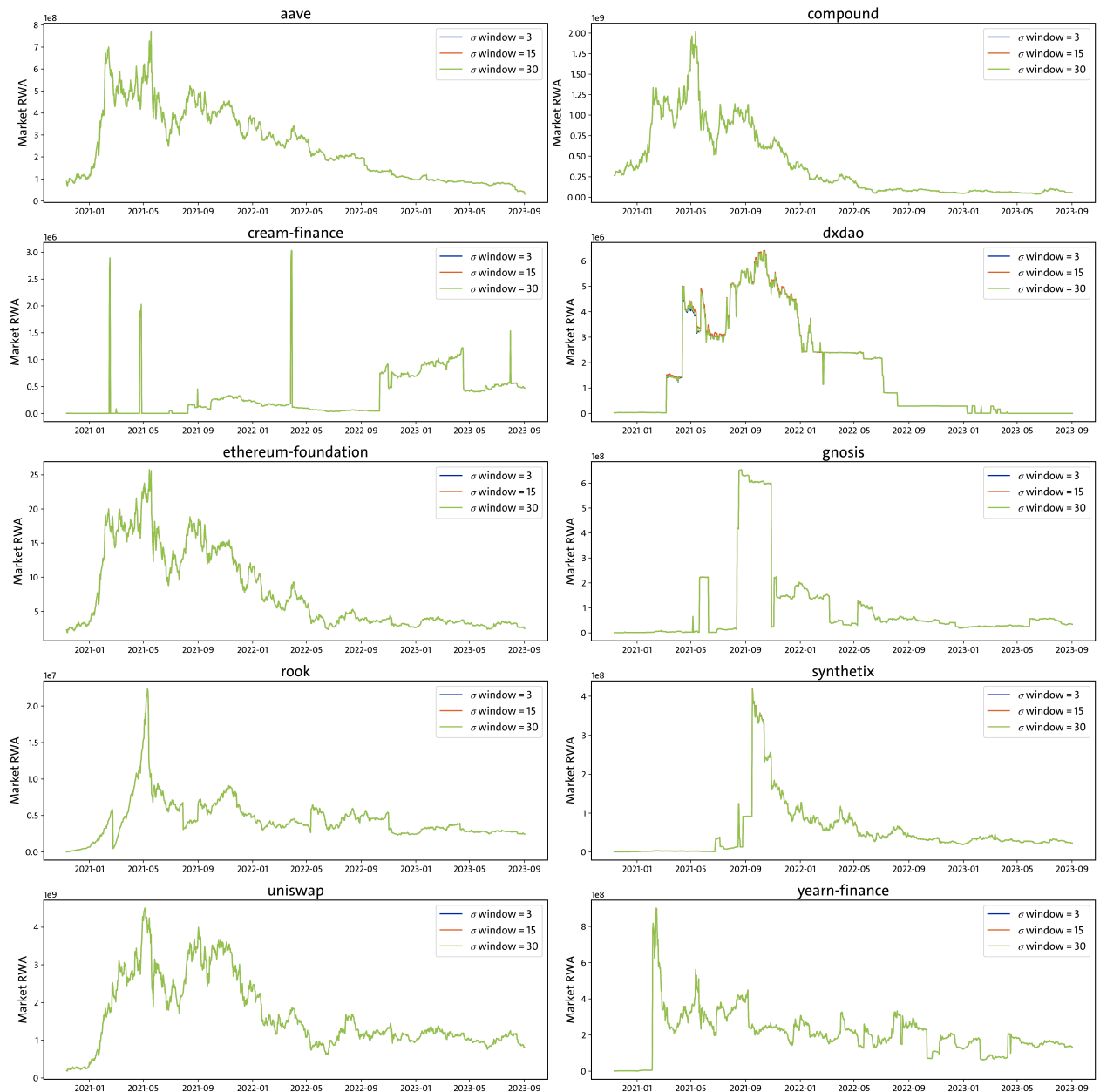
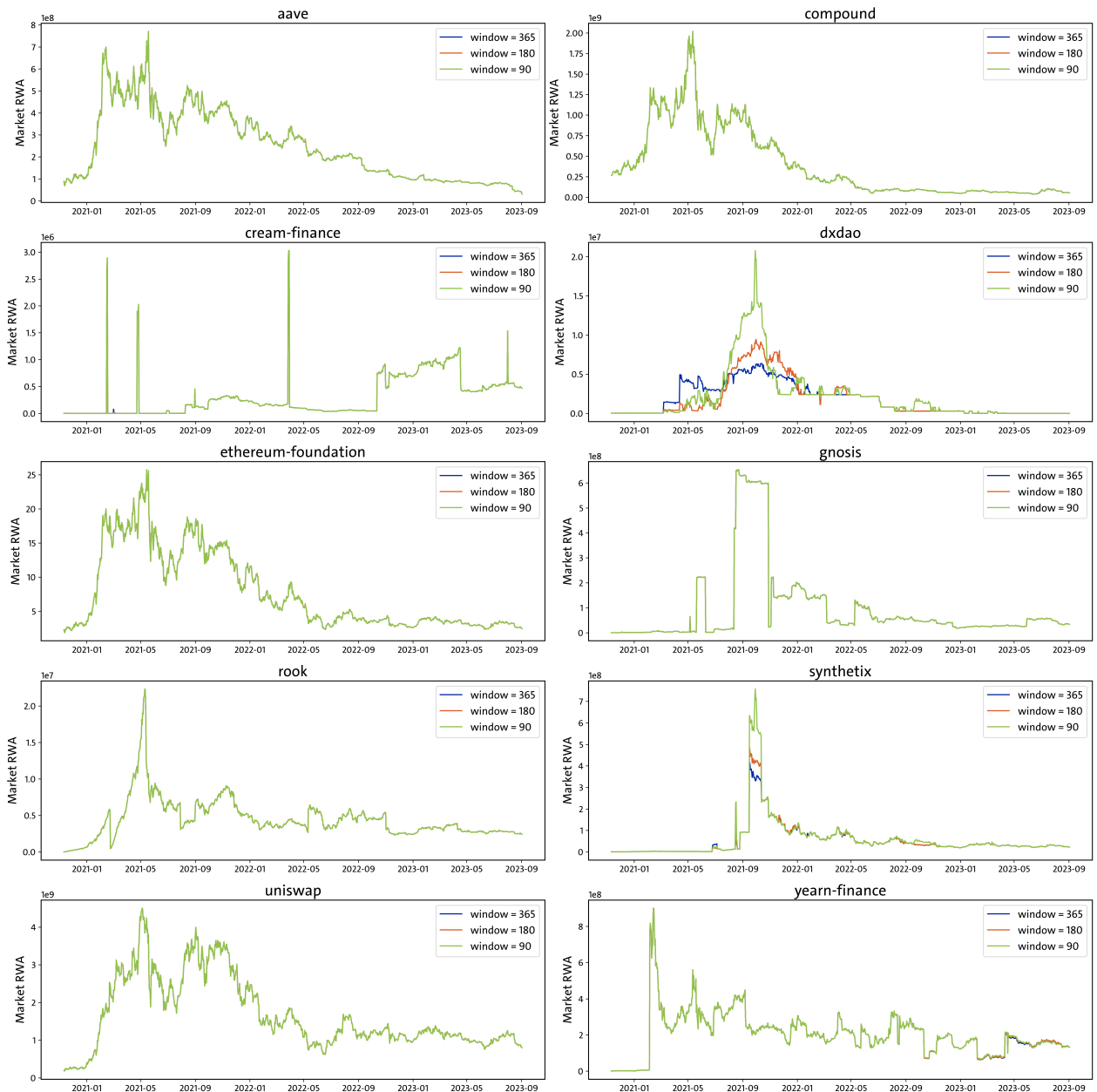


Figure B.3 – RWA for market risk, changing the industry bucket



**Figure B.4 – RWA for market risk, changing the window for  $\sigma$**



**Figure B.5 – RWA for market risk, changing the window for delta and vega**

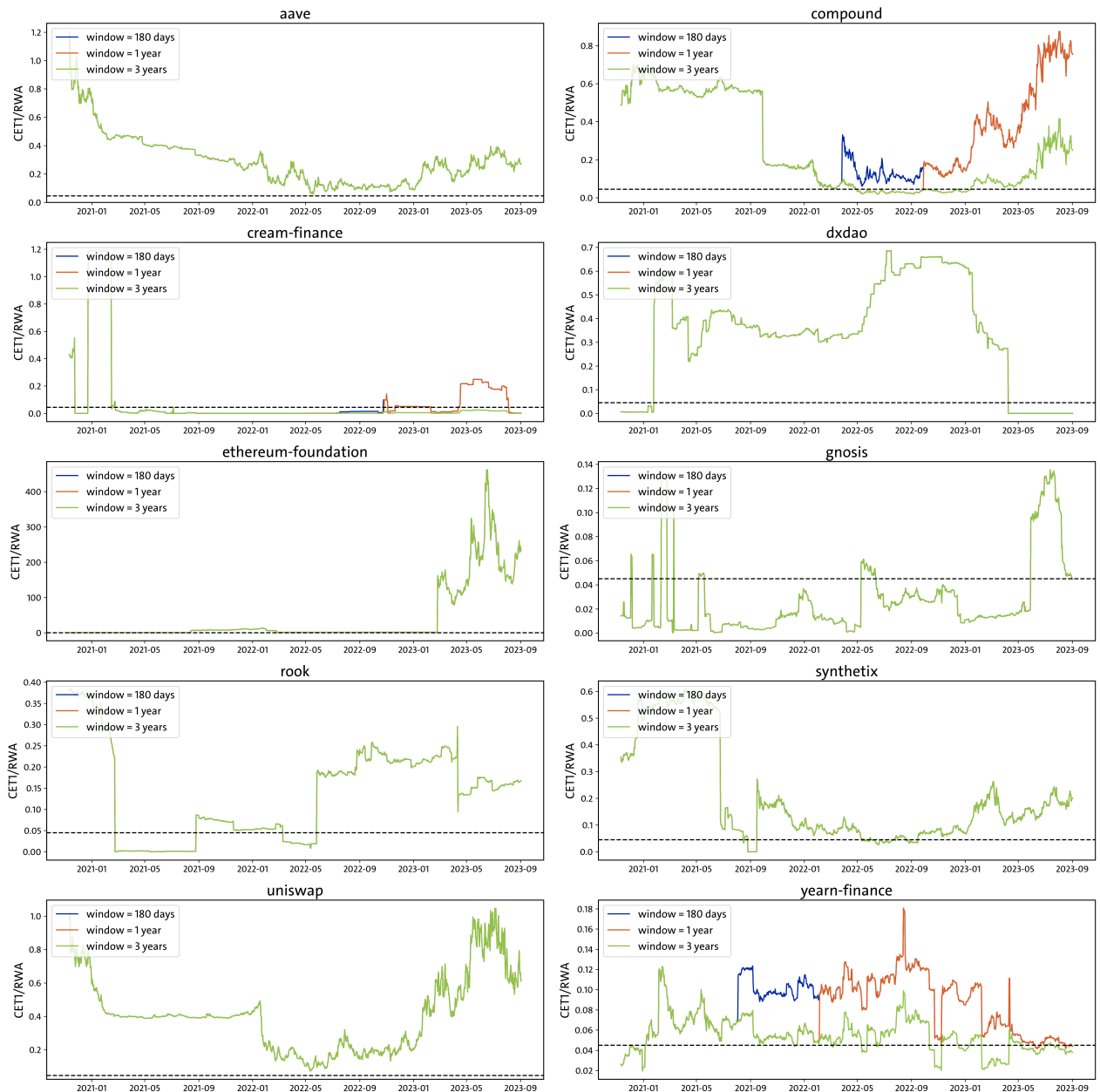


**Figure B.6 – CET1/RWA of 10 protocols, changing the window for hacks**

# Bibliography

- Acemoglu, Daron, Asuman E. Ozdaglar, and Alireza Tahbaz-Salehi (2013). “Systemic Risk and Stability in Financial Networks”. In: *Financial Crises eJournal*.
- Aigner, Andreas A and Gurvinder Dhaliwal (2021). “Uniswap: Impermanent loss and risk profile of a liquidity provider”. In: *arXiv preprint arXiv:2106.14404*.
- Alonso, Mikel, Raphael A. Auer, Marcel Bluhm, Claudio Borio, Stijn Claessens, Sebastian Doerr, Jon Frost, Anneke Kosse, Asad Khan, Ulf Lewrick, Benoît Mojon, Benedicte Nolens, Tara Rice, Hyun Song Shin, Vladyslav Sushko, Sirio Aramonte, Wenqian Huang, and Andreas Schrimpf (2021). “DeFi risks and the decentralisation illusion”. In.
- Antonakakis, Nikolaos, Ioannis Chatziantoniou, and David Gabauer (2020). “Refined measures of dynamic connectedness based on time-varying parameter vector autoregressions”. In: *Journal of Risk and Financial Management* 13.4, p. 84.
- Auer, Raphael, Bernhard Haslhofer, Stefan Kitzler, Pietro Saggese, and Friedhelm Victor (Aug. 2023). “The technology of decentralized finance (DeFi)”. In: *Digital Finance*, pp. 1–41. DOI: [10.1007/s42521-023-00088-8](https://doi.org/10.1007/s42521-023-00088-8).
- Bartoletti, Massimo, James Hsin-yu Chiang, and Alberto Lluch-Lafuente (2020). “SoK: Lending Pools in Decentralized Finance”. In: *Financial Cryptography Workshops*.
- Baruniák, Jozef and Tomáš Křehlík (2018). “Measuring the frequency dynamics of financial connectedness and systemic risk”. In: *Journal of Financial Econometrics* 16.2, pp. 271–296.
- Battiston, Stefano, Domenico Delli Gatti, Mauro Gallegati, Bruce C. N. Greenwald, and J. E. Stiglitz (2012). “Liaisons dangereuses: Increasing connectivity, risk sharing, and systemic risk”. In: *Journal of Economic Dynamics and Control* 36, pp. 1121–1141.
- Bayer, Michael (2012). “SQLAlchemy”. In: *The Architecture of Open Source Applications Volume II: Structure, Scale, and a Few More Fearless Hacks*. Ed. by Amy Brown and Greg Wilson. [aosabook.org](http://aosabook.org).
- BCBS et al. (2021). “Prudential treatment of cryptoasset exposures”. In: *Basel Committee on Banking Supervision, BIS Consultative Document*.
- Beck, Roman, Christoph Müller-Bloch, and John Leslie King (2018). “Governance in the blockchain economy: A framework and research agenda”. In: *Journal of the association for information systems* 19.10, p. 1.

- Borri, Nicola (2018). "Conditional Tail-Risk in Cryptocurrency Markets". In: *Innovation Finance & Accounting eJournal*.
- Boss, Michael, Helmut Elsinger, Martin Summer, and Stefan Thurner 4 (2003). "Network topology of the interbank market". In: *Quantitative Finance* 4, pp. 677–684.
- Chen, Ting, Zihao Li, Yuxiao Zhu, Jiachi Chen, Xiapu Luo, John Chi-Shing Lui, Xiaodong Lin, and Xiaosong Zhang (2020). "Understanding ethereum via graph analysis". In: *ACM Transactions on Internet Technology (TOIT)* 20.2, pp. 1–32.
- Cong, Lin William, Ye Li, and Neng Wang (2020). "Tokenomics: Dynamic Adoption and Valuation". In: *NBER Working Paper Series*.
- Corbet, Shaen, Andrew Meegan, Charles Larkin, Brian M. Lucey, and Larisa Yarovaya (2017). "Exploring the Dynamic Relationships between Cryptocurrencies and Other Financial Assets". In: *Econometric Modeling: Capital Markets - Asset Pricing eJournal*.
- Cousaert, Simon, Jiahua Xu, and Toshiko Matsui (2021). "SoK: Yield Aggregators in DeFi". In: *2022 IEEE International Conference on Blockchain and Cryptocurrency (ICBC)*, pp. 1–14.
- Demirer, Mert, Francis X. Diebold, Laura Xiaolei Liu, and Kamil Yilmaz (2015). "Estimating Global Bank Network Connectedness". In: *ERN: Financial Crises (Econometric) (Topic)*.
- Demirgüç-Kunt, Asli and Harry Huizinga (2009). "Bank Activity and Funding Strategies: The Impact on Risk and Return". In: *Banking & Financial Institutions*.
- DeYoung, Robert and Karin Pafford Roland (2001). "Product Mix and Earnings Volatility at Commercial Banks: Evidence from a Degree of Leverage Model". In: *Journal of Financial Abstracts eJournal*.
- Dickey, D. and Wayne Fuller (June 1979). "Distribution of the Estimators for Autoregressive Time Series With a Unit Root". In: *JASA. Journal of the American Statistical Association* 74. DOI: [10.2307/2286348](https://doi.org/10.2307/2286348).
- Diebold, Francis X and Kamil Yilmaz (2012). "Better to give than to receive: Predictive directional measurement of volatility spillovers". In: *International Journal of forecasting* 28.1, pp. 57–66.
- Diebold, Francis X and Kamil Yilmaz (2015). *Financial and macroeconomic connectedness: A network approach to measurement and monitoring*. Oxford University Press, USA.
- Diebold, Francis X. and Kamil Yilmaz (2008). "Measuring Financial Asset Return and Volatility Spillovers, with Application to Global Equity Markets". In: *Wiley-Blackwell: Economic Journal*.
- (2011). "On the Network Topology of Variance Decompositions: Measuring the Connectedness of Financial Firms". In: *Econometrics: Mathematical Methods & Programming eJournal*.
- Foglia, Antonella (2008). "Stress Testing Credit Risk: A Survey of Authorities' Approaches". In: *Monetary Economics eJournal*.
- Gabauer, David (2020). "Volatility impulse response analysis for DCC-GARCH models: The role of volatility transmission mechanisms". In: *Journal of Forecasting*.

- Gabauer, David (2021). "Dynamic measures of asymmetric & pairwise connectedness within an optimal currency area: Evidence from the ERM I system". In: *Journal of Multinational Financial Management* 60, p. 100680.
- (2022). "Package ‘ConnectednessApproach’". In:
- Gai, Prasanna and Sujit Kapadia (2010). "Contagion in financial networks". In: *Proceedings of the Royal Society A: Mathematical, Physical and Engineering Sciences* 466, pp. 2401–2423.
- Granger, Clive WJ (1969). "Investigating causal relations by econometric models and cross-spectral methods". In: *Econometrica: journal of the Econometric Society*, pp. 424–438.
- Grönholm, Alex (2009). *Advanced Python Scheduler (APScheduler): Task scheduling library for Python*.
- Gudgeon, Lewis, Daniel Perez, Dominik Harz, Benjamin Livshits, and Arthur Gervais (2020). "The Decentralized Financial Crisis". In: *2020 Crypto Valley Conference on Blockchain Technology (CVCBT)*, pp. 1–15.
- Heimbach, Lioba, Eric Schertenleib, and Roger Wattenhofer (2022). "Risks and returns of uniswap v3 liquidity providers". In: *arXiv preprint arXiv:2205.08904*.
- Khan, Arijit (2022). "Graph Analysis of the Ethereum Blockchain Data: A Survey of Datasets, Methods, and Future Work". In: *2022 IEEE International Conference on Blockchain (Blockchain)*, pp. 250–257.
- Klages-Mundt, Ariah, Dominik Harz, Lewis Gudgeon, Jun-You Liu, and Andreea Minca (2020). "Stablecoins 2.0: Economic Foundations and Risk-based Models". In: *Proceedings of the 2nd ACM Conference on Advances in Financial Technologies*.
- Kolb, Robert (2011). "What is Financial Contagion?" In: *Microeconomics: General Equilibrium & Disequilibrium Models of Financial Markets eJournal*.
- Korobilis, Dimitris and Kamil Yilmaz (2018). "Measuring Dynamic Connectedness with Large Bayesian VAR Models". In: *Banking & Insurance eJournal*.
- Lepetit, Laetitia, Emmanuelle Nys, Philippe Rous, and Amine Tarazi (2008). "Bank Income Structure and Risk: An Empirical Analysis of European Banks". In: *Journal of Banking and Finance* 32, pp. 1452–1467.
- Li, Yitao, Umar Islambekov, Cuneyt Akcora, Ekaterina Smirnova, Yulia R Gel, and Murat Kantarcioglu (2020). "Dissecting ethereum blockchain analytics: What we learn from topology and geometry of the ethereum graph?" In: *Proceedings of the 2020 SIAM international conference on data mining*. SIAM, pp. 523–531.
- Liu, Yukun and Aleh Tsyvinski (2018). "Risks and Returns of Cryptocurrency". In: *Global Business Issues eJournal*.
- Lütkepohl, Helmut (2005). *New introduction to multiple time series analysis*. Springer Science & Business Media.
- Merkel, Dirk (2014). "Docker: lightweight linux containers for consistent development and deployment". In: *Linux journal* 2014.239, p. 2.

- Naeem, Muhammad Abubakr, Saba Qureshi, Mobeen Ur Rehman, and Faruk Balli (2021). "COVID-19 and cryptocurrency market: Evidence from quantile connectedness". In: *Applied Economics* 54, pp. 280–306.
- Nier, Erlend W., J. Yang, Tanju Yorulmazer, and Amadeo Alentorn (2007). "Network Models and Financial Stability". In: *Economics of Networks*.
- Perez, Daniel, Sam M. Werner, Jiahua Xu, and Benjamin Livshits (2020). "Liquidations: DeFi on a Knife-Edge". In: *Financial Cryptography*.
- Qin, Kaihua, Liyi Zhou, Yaroslav Afonin, Ludovico Lazzaretti, and Arthur Gervais (2021). "CeFi vs. DeFi - Comparing Centralized to Decentralized Finance". In: *ArXiv* abs/2106.08157.
- Qin, Kaihua, Liyi Zhou, Benjamin Livshits, and Arthur Gervais (2020). "Attacking the DeFi Ecosystem with Flash Loans for Fun and Profit". In: *ArXiv* abs/2003.03810.
- Ramírez, Sebastián (2018). *FastAPI framework, high performance, easy to learn, fast to code, ready for production*.
- Seabold, Skipper and Josef Perktold (2010). "statsmodels: Econometric and statistical modeling with python". In: *9th Python in Science Conference*.
- Somin, Shahar, Yaniv Altshuler, Goren Gordon, Alex'Sandy' Pentland, and Erez Shmueli (2020). "Network dynamics of a financial ecosystem". In: *Scientific reports* 10.1, p. 4587.
- Somin, Shahar, Goren Gordon, and Yaniv Altshuler (2018). "Network analysis of erc20 tokens trading on ethereum blockchain". In: *Unifying Themes in Complex Systems IX: Proceedings of the Ninth International Conference on Complex Systems 9*. Springer, pp. 439–450.
- Stiroh, Kevin J. (2002). "Diversification in Banking: Is Noninterest Income the Answer?" In: *Journal of Money, Credit, and Banking* 36, pp. 853–882.
- Tolmach, Palina, Yi Li, Shang-Wei Lin, and Yang Liu (2021). "Formal Analysis of Composable DeFi Protocols". In: *Financial Cryptography Workshops*.
- Victor, Friedhelm and Bianca Katharina Lüders (2019). "Measuring ethereum-based erc20 token networks". In: *Financial Cryptography and Data Security: 23rd International Conference, FC 2019, Frigate Bay, St. Kitts and Nevis, February 18–22, 2019, Revised Selected Papers 23*. Springer, pp. 113–129.
- Werner, Sam M., Daniel Perez, Lewis Gudgeon, Ariah Klages-Mundt, Dominik Harz, and William John Knottenbelt (2021). "SoK: Decentralized Finance (DeFi)". In: *Proceedings of the 4th ACM Conference on Advances in Financial Technologies*.
- Wu, Siwei, Dabao Wang, Jianting He, Yajin Zhou, L. Wu, Xingliang Yuan, Qinming He, and Kui Ren (2021). "DeFiRanger: Detecting Price Manipulation Attacks on DeFi Applications". In: *ArXiv* abs/2104.15068.
- Xu, Jiahua and Yebo Feng (2022). "Reap the Harvest on Blockchain: A Survey of Yield Farming Protocols". In: *IEEE Transactions on Network and Service Management* 20, pp. 858–869.
- Yi, Shuyue, Zishuang Xu, and Gangjin Wang (2018). "Volatility connectedness in the cryptocurrency market: Is Bitcoin a dominant cryptocurrency?" In: *International Review of Financial Analysis*.

## Eidesstattliche Erklärung

Der/Die Verfasser/in erklärt an Eides statt, dass er/sie die vorliegende Arbeit selbstständig, ohne fremde Hilfe und ohne Benutzung anderer als die angegebenen Hilfsmittel angefertigt hat. Die aus fremden Quellen (einschliesslich elektronischer Quellen) direkt oder indirekt übernommenen Gedanken sind ausnahmslos als solche kenntlich gemacht. Die Arbeit ist in gleicher oder ähnlicher Form oder auszugsweise im Rahmen einer anderen Prüfung noch nicht vorgelegt worden.

Zürich, 21.09.2023

.....  
Ort, Datum



.....  
Unterschrift des/der Verfassers/in